Politecnico di Torino

Politecnico di Torino

FACOLTÀ DI INGEGNERIA CIVILE
Corso di Laurea Magistrale in Ingegneria Civile

FACTORS AFFECTING THE MECHANICAL RESPONSE UNDER LOADING OF UNBOUND GRANULAR MATERIALS

Candidato:
Paolo Chianella

Relatore:
Prof. Ezio Santagata

Correlatori:
Prof.ssa Lucia Tsantilis
Prof. Pier Paolo Riviera

Anno Accademico 2020-2021

Contents

List of Figures

List of Tables

Chapter 1

Abstract

Several studies are devoted to the calculation of serviceability life and design of foundation layers of road pavements, which are the main concerns of pavement engineering. For comprehension it is fundamental to have a knowledge of the mechanical behaviour of granular materials to reach a satisfactory pavement structural analysis and design. One of the most used parameters is the resilient modulus.

The structural analysis starts with the assumption of constant elastic modulus used as an input for the calculation of the internal tensions in order to obtain resilient modulus using regression parameters k_1, k_2 and k_3. By the use of constant Young modulus, the first problem was to verify if such approximation generates valid results. The behaviour of granular materials depends on stresses and moreover it changes properties with the variation of the environmental conditions. Through the analysis of the obtained results, a second problem emerged: the choice of representative points where tensions could be calculated. Indeed, stresses are strictly dependant on the point of calculation and tension results.

Instead, with the experimental analysis the resilient modulus was obtained by tests on specimens in which it was tried to reproduce "in situ" conditions. Indeed, specimens were realized with different combinations of density and water content. Supposing to create a representative condition of land, the variations of moisture content, compaction density and loads applied are the main three characteristics that allow identifying six different specimen configurations. Thanks to this, it was possible to understand how to change material behaviour in different conditions. Density effect and influence of water content were analysed for this purpose.

Chapter 2

Introduction

The successful design and operating life of new road infrastructure depend on the characteristics and composition of construction materials. One of the most critical problems for pavement layers is represented by the correct value ables to describe the material's stiffness. It is suggested to choose a constant parameter that is iterated until the value's convergence. After choosing constant parameters, the first consideration is regarding the reliability of that assumption and if it is possible to approximate these values. The material properties depend on several parameters, like stress, density, water content, loads applied and position of evaluation points. Still, it is essential to check the errors by studying different material configurations. The configurations studied can be regarding environmental effects, as the content of water and deficiency in the construction processes, like reducing the density of the material layer. Furthermore, two approaches are considered to study how much the position of the points in which stresses are evaluated affects the final results.
Finally, due to the degradation of the pavement caused by traffic actions and environmental effects, the pavement's design life is studied to quantify the time in which infrastructure can satisfy functional and structural requisites. The pavement's design life is analysed with varying resilient modulus to understand how it changes with the stiffness of layers. The study of the design life is performed, integrating the regression parameters obtained by the experimental tests with the structural analysis process.

Experimental tests are made upon a specimen in which it was tried to reproduce "in situ" conditions of land to have a reliable response in terms of data. Characteristics varied are:

- **Moissture Content**
- **Density of Compaction**
- **Loads Applied**;

They are the factors that more influence the mechanical behaviour of the material. After preliminary testing, the first set of samples is realised with an optimal condition: optimum water content and maximum compaction density. Instead, the other specimens are made as the optimum case, but before testing, they are left to dry and wet for different periods:

- **Dry for 60 hours**
- **Dry for 96 hours**
- **Wet for 96 hours**.

The last factor that varied is the density of compaction: 90% of the maximum density. It represents a decrement of stiffness properties of the material due, in general, to construction issues.

Two protocols are considered: Sub-Base and Subgrade protocol. Each protocol takes the name from the pavement layer where generally it is used. The experimental tests made it possible to extract regression parameters, different for each protocol, used to manipulate the structural analysis results. Naturally, the regression parameters are dependant on the models chosen. Hicks-Monismith, Uzan and MEPDG models are considered more representative for the analysis.

After the experimental analysis, the study moves to the design process of the pavement. The design process is performed using two different software: ALVA-master and KENLAYER. With ALVA-master are analysed, the sub-base layer zones subjected to more significant stresses. Using KENLAYER, the procedure is more conservative, indeed are taken into account different points in which the loads are lower than the previous case and, consequently, the resilient modulus computed are lesser. In addition, the use of KENLAYER allowed considering the layer's non-linearity behaviour and the ground's weight.

Chapter 3

Background

Introduction: This chapter consists of a literature review conducted on the behaviour of granular materials under repeated loading in different conditions. First, resilient modulus and permanent deformation properties are discussed. Moreover, models used to compare stiffness results are explained. Finally, the factors that affect the behaviour of material are analyzed.

Resilient Modulus is the most important parameter that represents the structural response and performance of the flexible pavement. This factor is analyzed considering results obtained by linear regressions in form of k_1, k_2 and k_3.

Resilient Modulus: Resilient modulus characterizes the behaviour of granular materials. In energetical terms, "resilient" corresponds to the portion of energy during the loaded phase, which is recovered when the material is unloaded. The rest of the energy that is not recovered produces an accumulation of permanent strain on the material. The resilient module's parameters are determined using a repeated load triaxial test (explained next chapter). More simply, the resilient modulus is defined as the ratio between deviatoric stress and axial strain as expressed below:

$$M_r = \frac{\sigma_1 - \sigma_3}{\epsilon_1}$$

where:

M_r = resilient modulus,
σ_1 = major principal or axial stress,
σ_3 = minor principal or confining stress,
ϵ_1 = major principal or axial resilient strain.

3.1 Models

A great majority of models found in the literature research are based on simple curve fitting procedures, using data obtained from laboratory triaxial testing. Therefore, the analysis of results are performed considering three main models: Hiks-Monismith, Uzan and Mechanistic-Empirical Pavement Design Guide (MEPDG), because considered more reliable.

3.1.1 Hicks-Monismith Model

It is one of the "simplified models", and for many years, it has been employed to characterise granular material [3]. In this model, the resilient modulus is associated with the first invariant of stress, as shown in the followed formula:

$$M_r = k_1 p_a (\frac{\theta}{p_a})^{k_2}$$

where:

M_r = resilient modulus,
θ = Bulk stress = σ_1+σ_2+σ_3,
k_1 = constant of material,
k_2 = constant of material,
p_a = atmospheric pressure.

From experience, it was possible to ascertain that in the granular material with higher performance, k_1 increases and k_2 decreases [4]. Roles of regression parameter k_1 and k_2 will be explained in the following Chapters. The model is reliable for interpreting triaxial tests performed on coarse-grained soil (mixed granular or earth). However, the limits of this model are that are not take into account stresses and deformations due to shear and volumetric deformation. With the Uzan model, it was possible to overpass these limitations.

3.1.2 Uzan Model

Uzan model is one of the advanced models, and it represents an evolution of the "Bulk Stress Model" or "Hicks-Monismith Model" because they are considered the shear effects in this model. Uzan ascertained that Hicks-Monismith Model was reliable only for small vertical deformation (ϵ_z)and for the high value of confining pressure. In all other cases, the model was far from the practical reality because it is not considered dilatancy produced by tangential tensions, dependent on deviatoric tension.

$$M_r = k_1 \theta^{k_2} \sigma_d^{k_3}$$

where:

M_r = resilient modulus,
θ = Bulk stress = σ_1+σ_2+σ_3,
k_1 = constant of material,
k_2 = constant of material,
k_3 = constant of material,
$sigma_d$ = deviatoric stress.

Normalizing the resilient modulus and the state of stress:

$$M_r = k_1 p_a (\frac{\theta}{p_a})^{k_2} (\frac{\sigma_d}{p_a})^{k_3}$$

where:

p_a = atmosferic pressure.

Roles of regression parameter k_1, k_2 and k_3 will be explained in the following Chapter.

3.1.3 MEPDG (Mechanistic-Empirical Pavement Design Guide)

The Mechanistic-Empirical Pavement Design Guide (MEPDG) is the latest pavement design method that was developed using data from the Strategic Highway Research Program (SHRP) Long-Term Pavement Performance (LTPP) study [5]. The MEPDG predicts multiple performance indicators, and it provides a direct tie between materials, structural design, climate, construction, traffic and pavement management system.
The general constitutive equation for resilient modulus selected for implementation in MEPDG was developed through the National Cooperative Highway Research Program (NCHRP) project 1-28A as follow:

$$M_r = k_1 p_a (\frac{\theta}{p_a})^{k_2} (\frac{\tau_{oct}}{p_a} + 1)^{k_3}$$

where:

M_r = resilient modulus,
p_a = atmospheric pressure,
k_1 = constant of material,
k_2 = constant of material,
k_3 = constant of material,
θ = Bulk stress = $\sigma_1+\sigma_2+\sigma_3$,
τ_{oct} = octahedral shear stress.

Roles of regression parameter k_1, k_2 and k_3 will be explained in the Chapter 4.1.
The main difference between this model and the other two is that this approach considers octahedral tensions. Octahedral planes are defined as the four planes with normal lines parallel to the trisection of the principal axis.

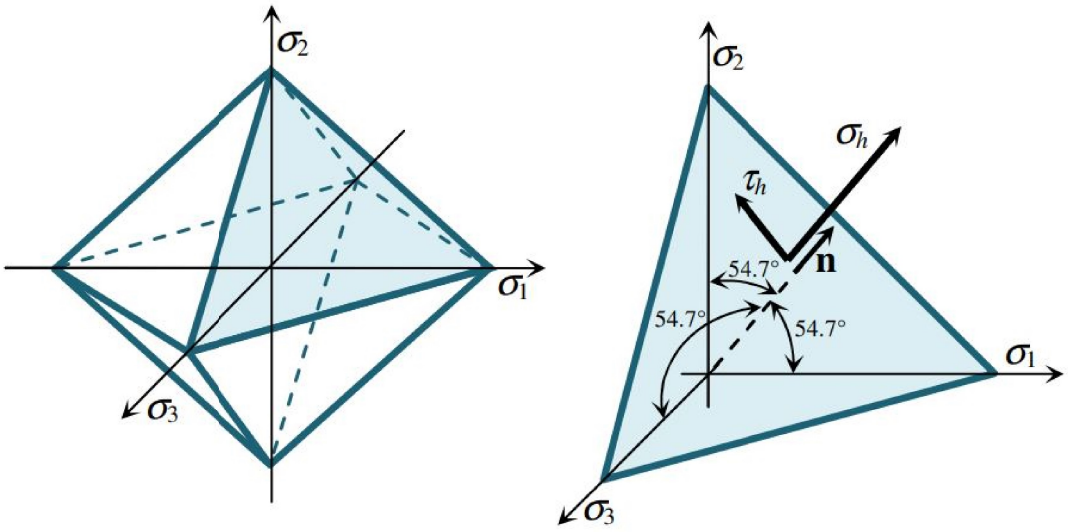

Figure 3.1: Octahedron and Octahedral Plane of First Quadrant

Normal and tangential tensions act on a octahedra planes, are defined as "octahedral tensions", they are given by the followed equations:

$$\sigma_h = \frac{\sigma_1 + \sigma_2 + \sigma_3}{3} \; ; \; \tau_{oct} = \frac{1}{3}\sqrt{(\sigma_1 - \sigma_2)^2 + (\sigma_2 - \sigma_3)^2 + (\sigma_1 - \sigma_3)^2}$$

This type of solicitation is essential because, in terms of materials' resistance, they can resist hydrostatic tensions bigger than uniaxial tensions.
This model can be used for any soil.

3.2 Factors Affecting Resilient Response

Since 1960, many research efforts have been devoted to characterizing the resilient behaviour of granular materials. Granular pavement layers have a non-linear and time-dependent elastoplastic response under traffic loading. For this reason, the resilient response of granular material is usually defined by resilient modulus and Poisson's ratio or by using shear and bulk moduli. Therefore, it is essential to consider how resilient behaviour varies with changes in different influencing factors. Many factors simultaneously affect both the resilient modulus and permanent deformation properties of granular materials. However, the factors influence resilient modulus and permanent deformation differently.

3.2.1 Effect of Stress

Stress level is the factor that has the most significant impact on the resilient properties of granular materials [6]. Many studies have shown a very high degree of dependence from the sum of principal stresses and confining pressure for resilient modulus of untreated granular materials [7]-[12]. Resilient modulus increases considerably with an increase of confining pressure and the sum of principal stresses. Resilient modulus increases are as significant as 500% changing confining pressure from 20 to 200 kPa [8]. An increment of 50% of resilient modulus increased principal stress from 70 to 1140 kPa [10]. Instead, it decreases slightly with an increment of repeated deviator stress under constant confinement [13]. Hicks and Monismith [9] reported a slight stiffening at low deviatoric stress levels and a slight stiffening at higher stress levels. Brown and Hyde [14] suggest that variable confining pressure and constant confining pressure

tests yield the same resilient modulus values. It provided that the confining pressure in the constant confining pressure test is equal to the mean value of the pressure used in the variable confining pressure test. The failure in granular materials under repeated loading is a gradual process and not a sudden collapse [15].

3.2.2 Effect of Density

It has been known that the increasing density of a granular material alters its characteristics, causing both stiffer and more robust. However, the literature is not clear regarding the impact of density on the resilient response of granular materials. Several studies confirmed that resilient modulus increases with an increment of density [16]-[19][6]. Trollope et al. [16], after a slow repeated load test on uniform sand, found an increment of resilient modulus of 50% between loose and dense specimens. Similar results were obtained by Robinson [18]; he also tested uniform sand. The number of particle contacts per particle increases significantly with increased density. Its, in turn, decreases the average contact stress corresponding to a particular external load. Decreasing deformation in particle contacts, resilient modulus increase [6]. Other results obtained Thom and Brown [20] and Brown and Selig [21]: the state of compaction and density are insignificant. Comparing tests for partially crushed and fully crushed aggregates: the resilient modulus was reported to increase relative density for the partially crushed aggregate tested, but it remained almost unchanged when the aggregate was fully crushed [9]. Hicks and Monismith further reported that the significance of changes in density decreased as the fines content of the granular material increased. For Barksdale and Itani [22], they were increasing density the resilient modulus increases only at low mean stress values. At density above the optimum value, the resilient modulus is not very density-sensitive [23].

3.2.3 Effect of Grading, Fine Content and Maximum grain size

Granular materials are composed of particles of different sizes; particle size and distribution affect material stiffness. However, the literature is not entirely clear about the influence of fines content on the material's stiffness. Some researchers have reported a decrement of resilient modulus with an increment of fine contents [24][25]. A resilient modulus decreased with an increment of fines for partially crushed aggregate tested; instead, the behaviour of material was the opposite for thoroughly crushed aggregates

[9]. Other research showed increasing stiffness and a considerable reduction as clayey fines were added to a crushed aggregate [26]. The initial improvement in stiffness is attributed to increased contacts as pore space is filled. Gradually, excess fines displace the coarse particles so that the mechanical performance relies only on the fines, and stiffness decreases. In the material with the same amount of fines and similar shape of grain size distribution, modulus increases with increasing maximum particle size [6][27][28]. According to Kolisoja, this response explains that the loads act not in a toral area of pavement but on a granular assembly, transmitted by particle queues [6]. When coarser particles transmit the load, a reduction of contact points results in minor total deformation and, consequently, higher stiffness. Heydinger et al. compared the effect of grading on resilient modulus for limestone, gravel, and slag [29]. Limestone showed a higher resilient modulus when open-graded, whereas no trend could be noted for the modulus variation in gravel. For slag, however, the results were the opposite, and the denser gradation tended to give higher stiffness. Van Niekerk et al. investigated the behaviour of specimens of sands, crushed masonry, and crushed concrete [30]. The results showed higher stiffness for well-graded than for uniformly graded specimens. This conflict with previous results can be explained that, due to a more significant number of contact areas at equal confinement, a well-graded material can take up sizeable deviatoric stress for equal deformation, thus resulting in higher stiffness.

3.2.4 Effect of Moisture Content

One of the most critical elements that affect material performance is the degree of saturation or moisture content. Resilient response of dry or partially saturated granular materials is similar, but it is not the same when materials are complete saturated: resilient behaviour may be affected significantly [10][23]. After some studies about the behaviour of granular materials at the high degree of saturation, it was discovered a dependence of resilient modulus on moisture content, modulus decreasing with growing saturation level [9][22][31][32]. Passing from 70% to 97% of saturation degree, resilient modulus in gravel decreases 50% [31]. Other research showed as resilient modulus has a constant decrement when moisture content increases above its optimum value [9]. Decrement of resilient modulus due to saturation was observed only when the analysis was based on total stress [7][17][33]. Instead, analyzing effective stress, resilient modulus remains approximately unchanged [34]. Thom and Brown argued that moisture in an aggregate assembly has some lubricating effect on

particles. It would increase the deformation in the aggregate assembly with a consequent reduction of the resilient modulus, even without generating any pore-water pressure. Thom and Brown confirmed this hypothesis with repeated load triaxial tests on a crushed rock, where the moisture content was one of the parameters changed. Despite the lack of pore pressure, the test results showed a reduction to the resilient modulus with increasing moisture content, which was related to water's lubricating effect [24]. The effect of moisture on resilient behaviour is most significant in well-graded material with a high portion of fines: water is more readily held in the pores of that materials. Instead, a material with uniformly graded materials allows better drainage [35]. Dawson et al. tested a range of well-graded unbound aggregates. They argued that the stiffness tends to increase below the optimum moisture content, increasing moisture level due to the suction effect. Then as the material becomes more saturated and excess pore water pressure is developed, the effect changes to the opposite, and stiffness rapidly decrease [32].

3.2.5 Effect of Stress History and Number of Load Cycles

Stress history effects occur due to repeated application of stress, which involves progressive densification [36]. Load triaxial tests performed on well-graded limestone showed that the material was subjected to stress history effects. Still, these could be reduced by preloading the material and avoiding high-stress ratios in the triaxial test [37]. Hicks reported a stable and steady resilient response of material after applying 100 cycles of the same stress amplitude [17]; Allen, instead, suggested conditioning of a sample of 1000 cycles [38]. Some studies have also concerned the number of load applications. Following the experience of Moore et al., resilient modulus increase as the load repetitions increase, partially due to the loss of water during testing [39]. Hicks, Allen and Thompson, reported the same result about the resilient response, with a repetition load of 50-100 and 2500 [17][41].

3.2.6 Effect of Aggregate Type and Particle Shape

Crushed aggregate with angular to subangular shaped particles provides better load spreading properties and a higher resilient modulus than uncrushed gravel with subrounded or rounded particles. A rough particle surface is also said to result in a higher resilient modulus [9][17][22][28][40][42]. Investigating several types of aggregate, Barksdale

and Itani reported that angular crushed materials were higher than rounded gravel by a factor of about 50% at low mean normal stress and about 25% at high mean normal stress [22].

3.2.7 Effect of Load Duration, Frequency and Load Sequence

The studies made showed that load sequence didn't affect resilient performance [17][40]. The results are the same regarding load duration and frequency: they didn't affect or have a small influence on resilient material response. Seed et al. reported a small increment of resilient modulus of sand samples (from 160 to 190 MPa) as the duration load passed from 20 minutes to 0.3 seconds [43]. Hicks found no change in resilient modulus and Poisson's ratio, conducting tests at stress duration of 0.1, 0.15 and 0.25 seconds [17]. Although it could be possible a reduction of resilient modulus with increasing load frequency when the moisture content is close to saturation, this effect is due to the formation of transient pore pressure, than causing a reduction of effective stress.

Chapter 4

Structural Analysis

This chapter shows the results obtained by the design analysis and verifies flexible pavements. Based on advanced international methodologies, this study must consider the future scientific and technological evolutions regarding the type of material, mechanical characteristics of the vehicle, and construction techniques. The design approach is based on the analytical manipulation of data, considering a road pavement as a multi-layer system. The movement of the vehicles and environmental effects produce solicitations in the layers and variation of the characteristic properties of the material. From the tensional point of view, it is possible to consider an analytical approach and a rational theory for analysing road pavements considering loads applied. The road pavement is treated as a beam structure in the analytical process. Its mechanical behaviour can be regarded as dependent on the same parameters used for concrete and steelwork. However, following a more rational theory to establish pavement design and construction criteria, it is essential to understand the layers' response under traffic action. Indeed, on the surface, they act different loads: vertical (deadweight, dynamic effect), longitudinal (traction, breaking, the horizontal force due to friction), and transversal (centrifugal effects, vehicle instability, contact angle between pavement and wheel); the stress path induced in a pavement is quite complex due to a movement of wheel: each element is subjected to stress pulses, vertical, horizontal and shear component. Vertical stress and horizontal stress are both always positive. Instead, shear stress becomes negative as the load passes; this last configuration causes a rotation of principal stress axes.

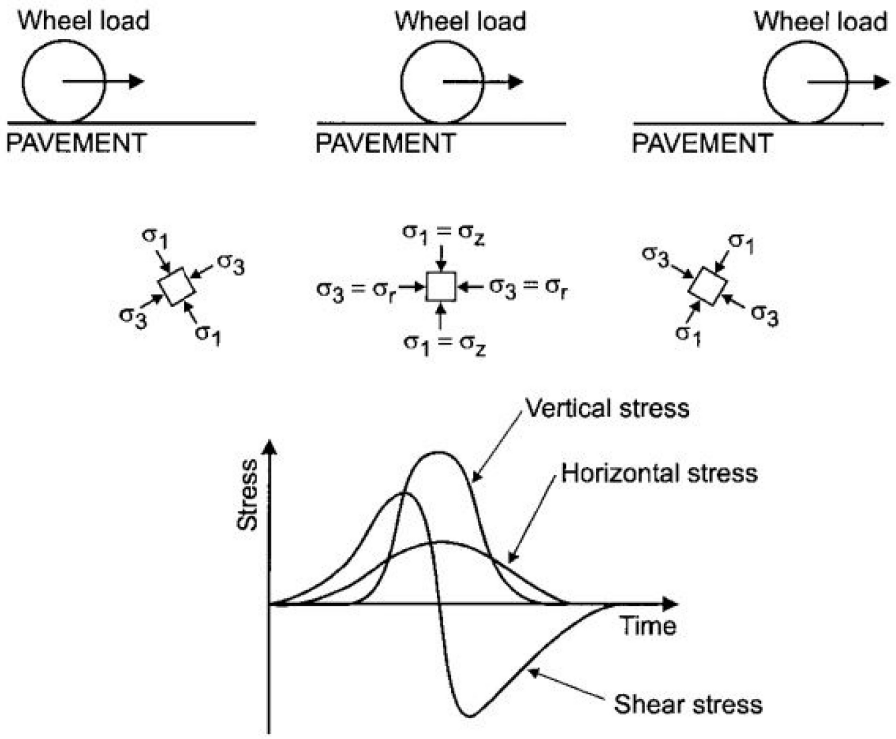

Figure 4.1: Stresses Under Rolling Wheel Load

Based on the parameter obtained with experimental tests, two software are used to retrieve data: ALVA-master and KENLAYER. Moreover, three analytical models are employed to manipulate the data and simulate the materials' "in situ" condition.

The analysis is regarding an existing road infrastructure. Although the pavement characteristics are the same for both software, the use of two tools is because they work using two different approaches. Moreover, the points in which stresses are computed, the input data, and the load applied on the pavement are other.

ALVA-master

The first study is regarding the structural analysis of the pavement's layer using ALVA-master. It is a MATLAB package for pavement modelling. The aim of the software is an advanced pavement modelling tool capable of supporting current and future pavement evaluation needs. Thanks to this tool, it is possible to obtain the internal tensions of the soil to obtain data about the stiffness of the layer.

The pavement analysed comprises five layers: the HMA layer formed by wear, binder and base, sub-base and subgrade layers. In addition, the proposed analysis considers the pavement component's natural characteristics of Poisson ratio, thickness, and elastic modulus with a seasonal variation.

Layer	**Thickness**	**Poisson Ratio**	**El. Module S.**	**El. Module W.**
[-]	[**mm**]	[**-**]	[**MPa**]	[**MPa**]
Wear	400	0.35	2641	5304
Binder	900	0.35	6084	10680
Base	600	0.35	6605	11380
Sub-Base	100; 200; 300	0.40	100	100
Subgrade	inf.	0.45	98	98

Table 4.1: ALVA-master Layer's Characteristics

It is considered a load area with a constant pressure of 800 MPa. Two loads are chosen for the "dual tires" axle: the standard case (80 kN) and 120 kN. Moreover, the critical points chosen are nine, and each of these nine points is in the sub-base layer but have different depth and radial positions concerning the centre of the external wheel. The image below shows that the critical points are aligned, forming a regular mesh in the sub-base layer. The first two columns of points correspond to the wheel's centre and edge, and the third is between the two wheels. Furthermore, in terms of depth, at a difference of the second row (placed in the centre of the layer), the first and third rows of points have a distance of 0.01 m, respectively, from the upper and lower surface separation layers. Therefore, it is supposed that the geometry of the axle is symmetric, and the weight is uniformly distributed; indeed, the half configuration of loads is taken into account.

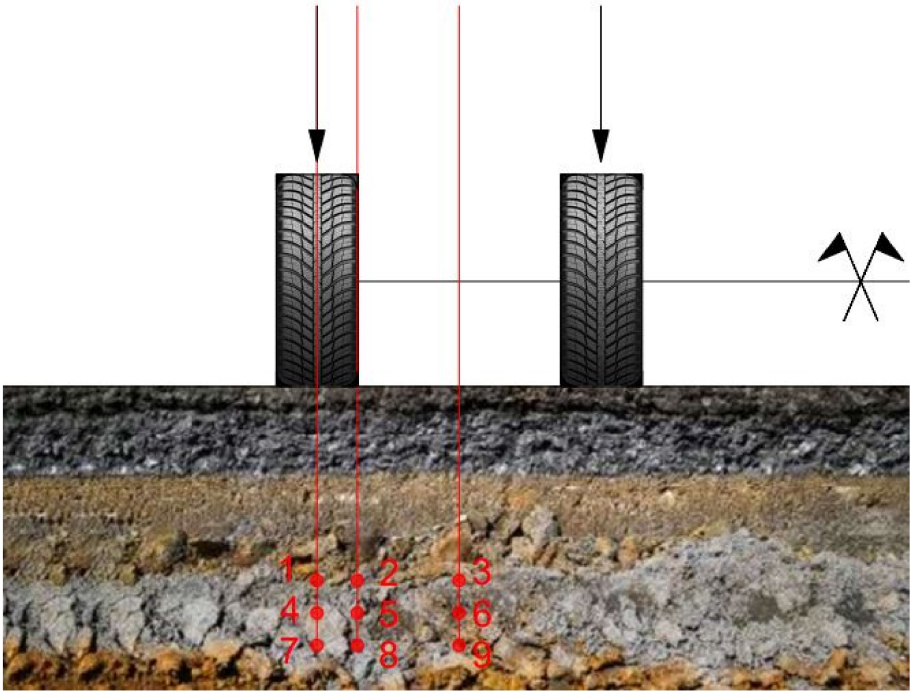

Figure 4.2: ALVA-master Geometry of Points Configuration

Once to obtain the stresses, it was fundamental to pass from cartesian coordinates (σ_x, σ_y and σ_z) to principal stresses (σ_1, σ_2 and σ_3), following equations.

$$\sigma_1 = (\frac{\sigma_y + \sigma_z}{2})^2 - \sqrt{(\frac{\sigma_y - \sigma_z}{2})^2 + (\tau_{yz})^2}$$

$$\sigma_2 = (\frac{\sigma_z + \sigma_x}{2})^2 + \sqrt{(\frac{\sigma_z - \sigma_x}{2})^2 + (\tau_{zx})^2}$$

$$\sigma_3 = (\frac{\sigma_x + \sigma_y}{2})^2 + \sqrt{(\frac{\sigma_x - \sigma_y}{2})^2 + (\tau_{xy})^2}$$

Then, the deformation tensor is computed by the principal stresses.

$$\theta = \sigma_1 + \sigma_2 + \sigma_3$$

It is studied the differences of the behaviour of the pavement layers, with different thicknesses and seasonal variations (summer and winter), in which the air temperature, and consequently also layers, are much different. Moreover, a parallel study was conducted on the stiffness increment of the sub-base layer with the addition of cement layer paced upper that sub-base layer. At the end of the procedure, the resilient modulus results are iterated till the final convergence of the values.
The essential scope of this study is to know the state of stress in the pavement layers.

KENLAYER

The methodology employed for the design and verification is based on the approximation of the road pavement to a multi-layer system in which the monthly traffic represents the load's action. As in the previous case, for each layer is defined thickness, elastic module and Poisson ratio; moreover, the adhesion conditions offered to the interfaces that separate the various layers are also defined within the layer: they can correspond, depending on the case, to total adhesion, total slippage or intermediate conditions between these extremes. This type of schematisation allows the evaluation of the stressed deformation state induced at any system point. Based on the accumulated traffic over the useful life of the superstructure and the related traffic spectrum, deriving from specific specialist studies, the total number of standard axle applications that have an effect equivalent to that of the expected loads is then evaluated. For evaluating the useful life of the

pavement, reference is made to limit criteria that define the achievement of the ultimate conditions in terms of various instabilities characteristic of the pavement. These criteria, which must necessarily consider the specific characteristics of the materials used, are expressed as functions that link the number of permissible applications of the load with the extent of the induced deformation, evaluated in characteristic points of the superstructure. The calculation method considers that the

stress-deformation state induced in the pavement depends on the upper layers bound to the bitumen, the temperature, which varies over the year, and the number of vehicles. About temperature dependence, the generic year of useful life is divided into periods, generally made to coincide with the 12 months of the year, in correspondence with which the characteristic temperatures of each layer can be defined. Moreover, for each period of the year, the damage induced by the load application is considered, and the pavement's design life is computed.

The multi-layer system analysed comprises five layers: the HMA layer formed by wear, binder and base, sub-base and subgrade layers. In addition, the proposed analysis considers the pavement component's natural characteristics of Poisson ratio, thickness, and elastic modulus with a seasonal variation.
It is supposed to divide the attributes of the layers in the base of the different year phases: optimum, dry and wet conditions; moreover, the situation with a loss of density is studied.

Layer	**Thickness**	**Poisson Ratio**	**El. Module**
[-]	[**mm**]	[-]	[**MPa**]
Wear	400	0.35	5304
Binder	900	0.35	10680
Base	600	0.35	11380
Sub-Base	100	0.40	454
Subgrade	inf.	0.45	98

Table 4.2: KENLAYER January, February, November and December Periods

Layer	**Thickness**	**Poisson Ratio**	**El. Module**
[-]	[mm]	[-]	[MPa]
Wear	400	0.35	3458
Binder	900	0.35	7594
Base	600	0.35	8180
Sub-Base	100	0.40	454
Subgrade	inf.	0.45	98

Table 4.3: KENLAYER March, April, May, September and October Periods

Layer	**Thickness**	**Poisson Ratio**	**El. Module**
[-]	[mm]	[-]	[MPa]
Wear	400	0.35	2641
Binder	900	0.35	6084
Base	600	0.35	6605
Sub-Base	100	0.40	454
Subgrade	inf.	0.45	98

Table 4.4: KENLAYER June, July and August Periods

Month	TNRL
Jan	162703
Feb	162054
Mar	180360
Apr	160968
May	166007
Jun	149503
Jul	156966
Ago	125751
Sep	161364
Oct	166840
Nov	152487
Dec	130459

Table 4.5: KENLAYER Load Repetition (TNLR)

After defining the material's properties, the analysis selects the critical points in which stresses-strains are computed. Huang theory suggests three methods for the choice of that points:

- **Method 1:** In this method, the non-linear layer is subdivided into several layers, and the stresses at the mid-depth of each layer are considered to determine the modulus. If the horizontal pressure, including the geostatic stress, is negative or in tension, it is set to 0. This stress modification is necessary to avoid negative θ. With the two horizontal stresses equal to 0, the elastic modulus is dependent on the vertical stress only, with no contributions from the horizontal stresses. The vertical stress at a stress point near the load is always positive, so the modulus will also be positive, and no minimum modulus needs to be specified;

- **Method 2:** In this method, the granular layer is considered as a single layer, and an approximate stress point, usually between the upper quarter and the upper third of the layer, is selected to compute the modulus. Because the stress point is near the load at the upper part of the layer, there is no chance that the stress invariant, θ, will become negative, so no stress modification is needed. In other words, the negative horizontal stresses are used to compute θ. To avoid using

an unreasonably low modulus, a minimum modulus, indicated by the value of ϕ, must be specified. If the computed modulus is smaller than ϕ, ϕ will be used as the modulus of the layer. It is suggested that k_1 of the granular material be used as ϕ so that the computed modulus will never be smaller than k_1; this relationship is always true unless θ is smaller than 1 psi (6.9kPa);

- **Method 3**: In this method, the granular layer is considered as a single layer with the stress point at the midheight of the layer. The negative or small horizontal stresses are modified according to the Mohr-Coulomb theory of failure so that the strength of the materials will not exceed. This method was initially proposed by Raad and Figueroa and was later incorporated in the ILLI-PAVE and MICH-PAVE computer programs. The case to be considered in KENLAYER is much simpler than that in those finite-element programs. It is simpler because the stress points are located under or near the load; the vertical stress can be considered the major principal stress and the horizontal stress as the minor principal stress. No adjustments for fine-grained soils are needed because the horizontal stresses at the stress point in the subgrade are always positive and satisfy the Mohr-Coulomb failure criterion. The Mohr's circle based on the major and minor principal stresses must be tangent to the failure envelope when a failure occurs. The geometry can easily prove that

$$\sigma_h = \sigma_v tan^2(45 - \frac{\phi}{2})$$

No circle should cut and lie outside the envelope, so no horizontal stress should be smaller than σ_h. When ϕ is assigned 0, $\sigma_h = \sigma_v$; when ϕ is assigned 90° $\sigma_h = 0$. It is suggested that the ϕ value of 40 be used for a weak subgrade with a modulus less than 10000 psi (69 MPa). Larger ϕ values up to 60, be used for a stiff subgrade. The case of $\phi = 90$ is the same as method 1, with the implication that $\sigma_h = 0$. Instead of using an awkward ϕ value (90) to indicate method 1, the value zero may be used for simplicity. When ϕ is inputted as 0, KENLAYER will automatically change it to 90°.

Several tries are made to choose the method used; after that, method 1 is selected because it is more conservative between the three ways than the others. So, the points considered are chosen at a depth of 21,5 cm and 26,5

cm. The radial coordinate depends on the inclination of the projection line that starts by the wheel's external edge, as shown in the picture below: the slope of that line, as suggested by Huang theory, is equal to 0,5. Moreover, the division of the sublayer is chosen similar to two because to obtain the best results, Huang recommended subdividing the granular layer into a number of 2 in. (50-mm). Finally, the axle configuration is chosen "dual" due to the several tries made with different cases.

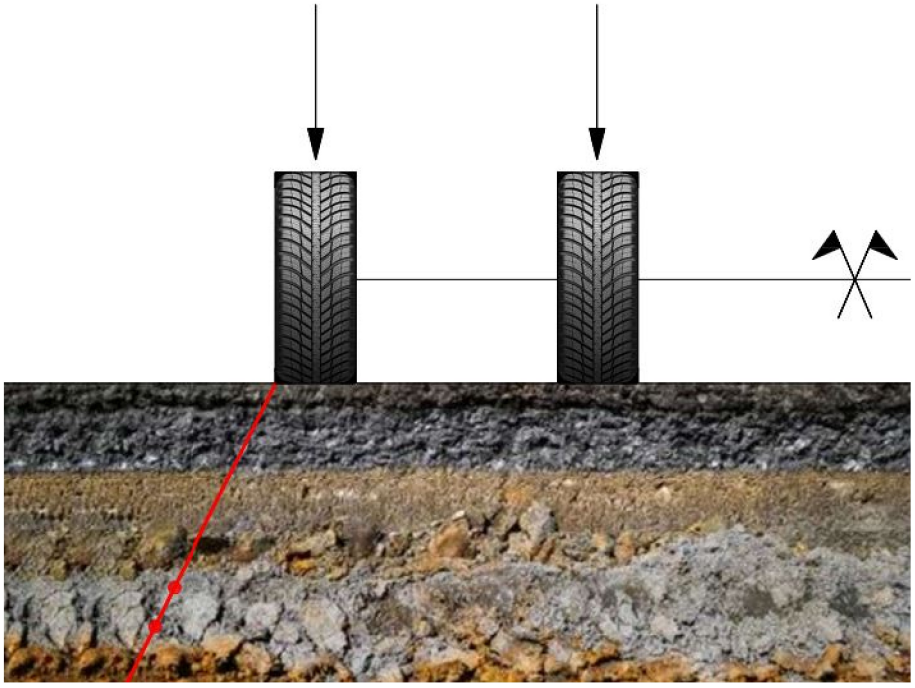

Figure 4.3: KENLAYER Geometry of Points Configuration

As in the previous structural analysis, software results of stresses are in cartesian type, and it is fundamental to pass in principal stresses.

$$\sigma_1 = (\frac{\sigma_y + \sigma_z}{2})^2 - \sqrt{(\frac{\sigma_y - \sigma_z}{2})^2 + (\tau_{yz})^2}$$

$$\sigma_2 = (\frac{\sigma_z + \sigma_x}{2})^2 + \sqrt{(\frac{\sigma_z - \sigma_x}{2})^2 + (\tau_{zx})^2}$$

$$\sigma_3 = (\frac{\sigma_x + \sigma_y}{2})^2 + \sqrt{(\frac{\sigma_x - \sigma_y}{2})^2 + (\tau_{xy})^2}$$

Moreover, the deformation tensor is computed by the principal stresses.

$$\theta = \sigma_1 + \sigma_2 + \sigma_3$$

This study evaluates the damage and computes the pavement's design life in different conditions. Three failure criteria are considered for thorough research: fatigue failure for binder and base layer and rutting failure for subgrade layer. Furthermore, the variations of characteristics can be environmental and factorial type: interpretation of moisture content, the density of compaction, and protocols used to manipulate the data.

In addition to the temperature variation that influences the entity of the elastic modulus of the pavement layers, it is essential to proceed with the experimental analysis to simulate the different conditions during the year. Thanks to these tests, also considering the three models explained before, it is possible to obtain regression parameters k_1, k_2 and k_3. These factors are used to model the results obtained from the structural analysis for both software. Each combination of values of k_1, and k_2, or k_1, and $k_2$and k_3 corresponds to a different period of the year in which the pavement can be found.

4.1 Experimental Analysis

This section consists of an explanation and results analysis obtained from triaxial tests done directly on the material. Tests are devoted to studying the material's behaviour in different environmental conditions. The resilient modulus and maximum shear tension results are presented, and a study on the influence parameters is conducted.

4.1.1 Triaxial Test

The triaxial test is the previous study performed on the material after the preliminary tests and Proctor and CBR tests in which the main characteristic of the material are obtained.
Resilient modulus (M_R) is a parameter able to evaluate the elastic behaviour of unbound aggregates under the effect of dynamic loads. As said in the previous chapter, Resilient Modulus is defined as the ratio between deviatoric tension (σ_d) and resilient deformation (ϵ_r).

$$M_r = \frac{\sigma_1 - \sigma_3}{\epsilon_1}$$

Resilient modulus's determination is generally accomplished through the "Triaxial Test" (picture of the machinery is shown below).

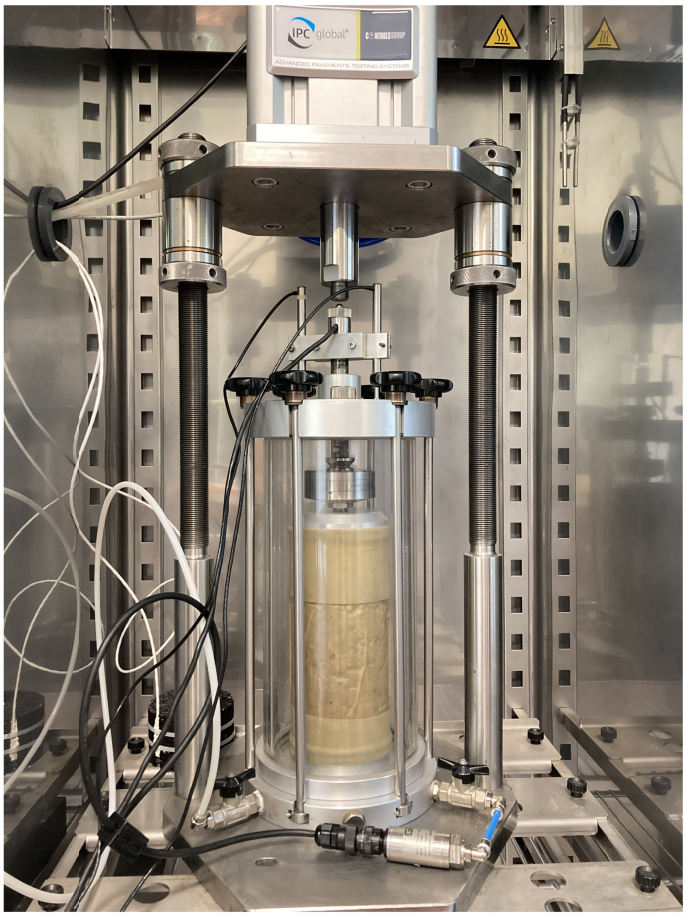

Figure 4.4: Triaxial Test

Triaxial Test allows a good simulation of tension and deformation regime when vehicles move on pavement layer. During the passage of vehicles, the base layer is suggested to a triaxial effort that changes in time. On the other hand, the resilient modulus is an elastic and dynamic modulus that considers the plastic deformation component; it is possible to observe that resilient deformation remains constant during load action; instead, plastic deformation decreases with the increment of loads.
Specimens are prepared to simulate the entire year periods in which water content, density, and loads act on the pavement are different. During the useful life of the soil, soil changes are due to temperature, seasons, weather, and other environmental factors. Knowing how to aggregate blend behaves is helpful to understand how material works. Changing characteristics cause altering of the response of the material layer; it can improve or decrease performance. Moisture content and density variation are two of the most critical factors that affect performance material. Therefore, at least two samples with the same characteristics are studied for each test. Six typologies of configuration are chosen to simulate the in situ conditions:

- **Combination 1:** the specimens are realized with optimum water content at a maximum density and tested following sub-base combination loads;
- **Combination 2:** the specimens are realized with optimum water content at 90% of maximum density and tested following sub-base combination loads;
- **Combination 3:** the specimens are realized with a water content obtained after drying of 72 hours, maximum density and tested following sub-base combination loads;
- **Combination 4:** the specimens are realized with a water content obtained after drying of 96 hours (it is supposed that specimens are dehydrated), maximum density and tested following sub-base combination loads;
- **Combination 5:** the specimens are realized with a water content obtained after wetting of 96 hours (it is supposed that specimens are saturated), maximum density and tested following sub-base combination loads;
- **Combination 6:** the specimens are realized with optimum water content at a maximum density and tested following subgrades combination loads.

The first combination is tested following two protocols: Sub-Base and Subgrade. Their differences are regarding the vertical load and confining pressure; two different solicitation values are used to understand how the effect of other loads influences the stiffness behaviour of the foundation layer. Instead, the tests on specimens realized following combination 2 characterize a condition in which soil is less compacted. Furthermore, the goal of the other configurations is to study the effect of the water on the ground.

Results obtained by triaxial tests are compared with resilient modulus computed using models of Hicks-Monismith, Uzan and MEPDG as described in Chapter 3. Models use regression parameters k_1, k_2 and k_3 for determination of resilient modulus, they depend by materials characteristics.

4.1.2 Influence Of Moisture Content On Test Results

The results indicate that resilient modulus tends to increase with a decrement of water content, and contemporaneously, it decreases with high saturation material values. Furthermore, the material has a stiffer performance with a dry material than wet aggregates.

Specimen	$M_{R_{min}}$	$M_{R_{max}}$
[-]	**[MPa]**	**[MPa]**
Optimum	118.5	410.7
Dry 2,5gg	258.7	455.6
Dry 4gg	319	603.2
Wet 4gg	56.3	283

Table 4.6: Resilient Modulus Results With a Variation of Moisture Content

Another study was conducted using the adimensional parameters obtained by manipulating the data using different models. As it said, regression parameters depend on the characteristics of each material. For example, in graphical terms, k_1 and k_2 correspond, respectively, y-intercept and slope of a regression line on a log-log plot of resilient modulus versus Bulk stress (as showed in the figure below).

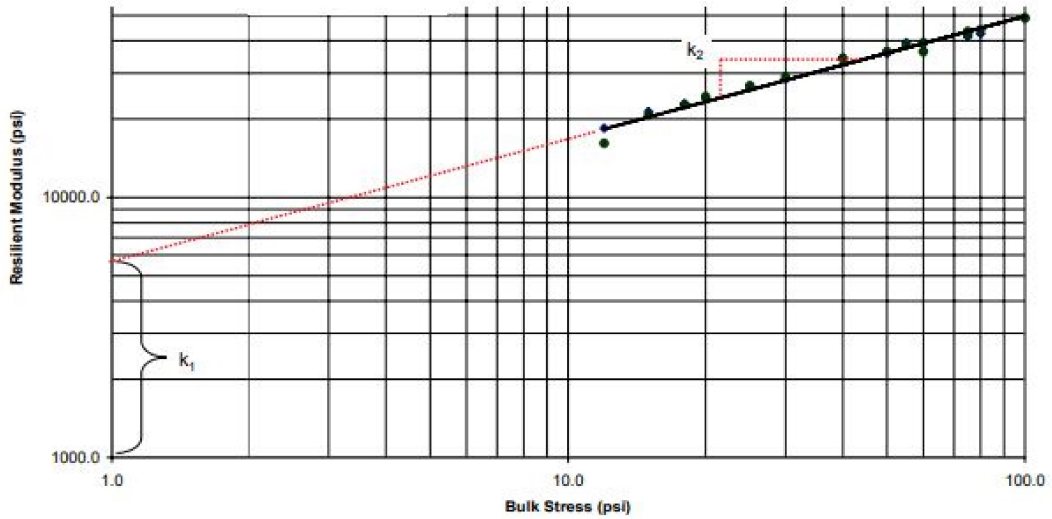

Figure 4.5: Resilient Modulus Versus Bulk Stress

From the behavioural point of view: k_1 is proportional to the elastic modulus of the material, and it is always positive. High values of k_1 means the high performance of material [4]. k_2 is an exponent of the Bulk stress term, and it is positive since increasing bulk stress results in a higher modulus. Instead, k_3 is the shear stress exponent, and it is typically negative since increasing shear stress will likely weaken the material resulting in a lower modulus.

This section distinguishes "measured" and "computed" resilient modulus: the first is referred to as values obtained by the triaxial test; instead, seconds indicate values computed using calculus models. Results are compared and plotted on a graphs; it is important evaluate amount of measured resilient modulus ($M_{R_{measured}}$) with: Bulk stresses (θ), cycle tensions (σ_d) and resilient modulus computed ($M_{R_{computed}}$) referred to each model.
The tables below represent regression parameters for each model for the different water content conditions.

Specimen	k_1	k_2
Optimum	1178	0.69
Dry 2.5gg	2543	0.30
Dry 4gg	3060.5	0.38
Wet 4gg	635.2	0.81

Table 4.7: Regression Parameters of Hiks-Monismith Models

Specimen	k_1	k_2	k_3
Optimum	973	0.84	-0.15
Dry 2.5gg	2392	0.35	-0.05
Dry 4gg	2538	0.52	-0.15
Wet 4gg	525	0.95	-0.14

Table 4.8: Regression Parameters of Uzan Models

Specimen	k_1	k_2	k_3
Optimum	630	0.84	-0.15
Dry 2.5gg	2067	0.35	-0.05
Dry 4gg	1590	0.52	-0.15
Wet 4gg	336	0.95	-0.14

Table 4.9: Regression Parameters of MEPDG Models

As in the considerations made before, also analyzing results using the models, the material's tendency to be stiffer for lower water content is respected for the first two models (Hiks-Monismith and Uzan). Instead, for the MEPDG model, the same tendency is repeated until the drying of 2.5 days; however, granular material tends to lose stiffness after this condition.

4.1.3 Influence Of Density On Test Results

The variation of the density in the unbound granular material of the pavements field occurs, in general, for a deficiency in human work or due to other environmental special conditions.
Test realized to check what happens when the density of the layer is lower than optimal condition is performed on samples with the same water content but with different percentages of density. Results showed a slight variation of resilient modulus between samples compacted from a range belonging to 90% and 100% of maximum density:29.4 MPa. Samples with a compaction percentage between grains lower than the above said can not be tested.

Specimen	$M_{R_{min}}$	$M_{R_{max}}$
[-]	**[MPa]**	**[MPa]**
Maximum Density	118.5	410.7
90% of Maximum Density	140.1	381.6

Table 4.10: Resilient Modulus Results With a Variation of Density

Also, in this case, a study with the three different models is performed. After manipulation, the parameters k_2 and k_3 between models doesn't change a lot. Instead, k_1 has a more significant value for the first model (Hiks-Monismith) and a decrement amount for the last two models (Uzan and MEPDG). Therefore, studies with the MEPDG model are more conservative because results following the first two approaches return a stiffer layer.

Specimen	k_1	k_2
Maximum Density	1178	0.69
90% of Maximum Density	1364	0.55

Table 4.11: Regression Parameters of Hiks-Monismith Models

Specimen	k_1	k_2	k_3
Maximum Density	973	0.84	-0.15
90% of Maximum Density	1183	0.66	-0.11

Table 4.12: Regression Parameters of Uzan Models

Specimen	k_1	k_2	k_3
Maximum Density	630	0.84	-0.15
90% of Maximum Density	839	0.66	-0.11

Table 4.13: Regression Parameters of MEPDG Models

4.1.4 Influence Of Load On Test Results

Following the same guideline, the material is tested applying different protocols. First, as explained in Chapter 2, the material tested is employed for the foundation layer of road pavements. The Italian rule [44] provides two types of combination of load: one for the foundation materials and the other for the subgrade layer. The previous tests consider the right couple of vertical loads and confining pressure. With this type of test, two kinds of combination loads are applied: Sub-Base and Subgrade protocols. The difference between the two combinations is the entities of loads. The pictures below show the two protocols. In the sub-base case, piston action and lateral pressure's are more significant because the vehicles' movement on the pavement is transmitted from the pavement to the depth layers, decreasing downward.

Table 1—Testing Sequence for Subgrade Soil

Sequence No.	Confining Pressure, S_3		Max. Axial Stress, S_{max}		Cyclic Stress, S_{cyclic}		Constant Stress, $0.1S_{max}$		No. of Load Applications
	kPa	psi	kPa	psi	kPa	psi	kPa	psi	
0	41.4	6	27.6	4	24.8	3.6	2.8	0.4	500–1000
1	41.4	6	13.8	2	12.4	1.8	1.4	0.2	100
2	41.4	6	27.6	4	24.8	3.6	2.8	0.4	100
3	41.4	6	41.4	6	37.3	5.4	4.1	0.6	100
4	41.4	6	55.2	8	49.7	7.2	5.5	0.8	100
5	41.4	6	68.9	10	62.0	9.0	6.9	1.0	100
6	27.6	4	13.8	2	12.4	1.8	1.4	0.2	100
7	27.6	4	27.6	4	24.8	3.6	2.8	0.4	100
8	27.6	4	41.4	6	37.3	5.4	4.1	0.6	100
9	27.6	4	55.2	8	49.7	7.2	5.5	0.8	100
10	27.6	4	68.9	10	62.0	9.0	6.9	1.0	100
11	13.8	2	13.8	2	12.4	1.8	1.4	0.2	100
12	13.8	2	27.6	4	24.8	3.6	2.8	0.4	100
13	13.8	2	41.4	6	37.3	5.4	4.1	0.6	100
14	13.8	2	55.2	8	49.7	7.2	5.5	0.8	100
15	13.8	2	68.9	10	62.0	9.0	6.9	1.0	100

Note: Load sequences 14 and 15 are not to be used for materials designed as Type 1.

Figure 4.6: Sub-Base Protocol Combination Loads

Table 2—Testing Sequences for Base/Subbase Materials

Sequence No.	Confining Pressure, S_3		Max. Axial Stress, S_{max}		Cyclic Stress, S_{cyclic}		Constant Stress, $0.1S_{max}$		No. of Load Applications
	kPa	psi	kPa	psi	kPa	psi	kPa	psi	
0	103.4	15	103.4	15	93.1	13.5	10.3	1.5	500–1000
1	20.7	3	20.7	3	18.6	2.7	2.1	0.3	100
2	20.7	3	41.4	6	37.3	5.4	4.1	0.6	100
3	20.7	3	62.1	9	55.9	8.1	6.2	0.9	100
4	34.5	5	34.5	5	31.0	4.5	3.5	0.5	100
5	34.5	5	68.9	10	62.0	9.0	6.9	1.0	100
6	34.5	5	103.4	15	93.1	13.5	10.3	1.5	100
7	68.9	10	68.9	10	62.0	9.0	6.9	1.0	100
8	68.9	10	137.9	20	124.1	18.0	13.8	2.0	100
9	68.9	10	206.8	30	186.1	27.0	20.7	3.0	100
10	103.4	15	68.9	10	62.0	9.0	6.9	1.0	100
11	103.4	15	103.4	15	93.1	13.5	10.3	1.5	100
12	103.4	15	206.8	30	186.1	27.0	20.7	3.0	100
13	137.9	20	103.4	15	93.1	13.5	10.3	1.5	100
14	137.9	20	137.9	20	124.1	18.0	13.8	2.0	100
15	137.9	20	275.8	40	248.2	36.0	27.6	4.0	100

Figure 4.7: Subgrade Protocol Combination Loads

As expected, the results in terms of resilient modulus are more significant in the first case, with a gap between them equal to 233.8 MAp, as shown in the table and histogram below.

Specimen	$M_{R_{min}}$	$M_{R_{max}}$
[-]	**[MPa]**	**[MPa]**
Sub-Base Protocol	118.5	410.7
Subgrade Protocol	104.7	176.9

Table 4.14: Resilient Modulus Results With a Variation of Loads

On the same line as the previous studies, regression parameters obtained with data manipulation are considered. Again, values of k_1 are decrescent from the simple (Hiks-Monismith) to the complex (MEPG) model, and the tendency to be more conservative of the last model is respected.

Specimen	k_1	k_2
Sub-Base Protocol	1178	0.69
Subgrade Protocol	1364	0.47

Table 4.15: Regression Parameters of Hiks-Monismith Models

Specimen	k_1	k_2	k_3
Sub-Base Protocol	973	0.84	-0.15
Subgrade Protocol	1116	0.56	-0.13

Table 4.16: Regression Parameters of Uzan Models

The utility of this type of test also consists of verifying if the choice to use two different models is justified or if it is superfluous. The chek can plot a couple of values of the Bulk stress (θ) and resilient modulus M_R obtained by the experimental test. Red and blue points correspond to subgrade and subbase results: red points correspond to a "queue" of blue points. Integrating these tendencies and the previous structural tests results (analyzed in Chapter 4) makes it possible to consider the better protocol to use.

Specimen	k_1	k_2	k_3
Sub-Base Protocol	630	0.84	-0.15
Subgrade Protocol	743	0.56	-0.13

Table 4.17: Regression Parameters of MEPDG Models

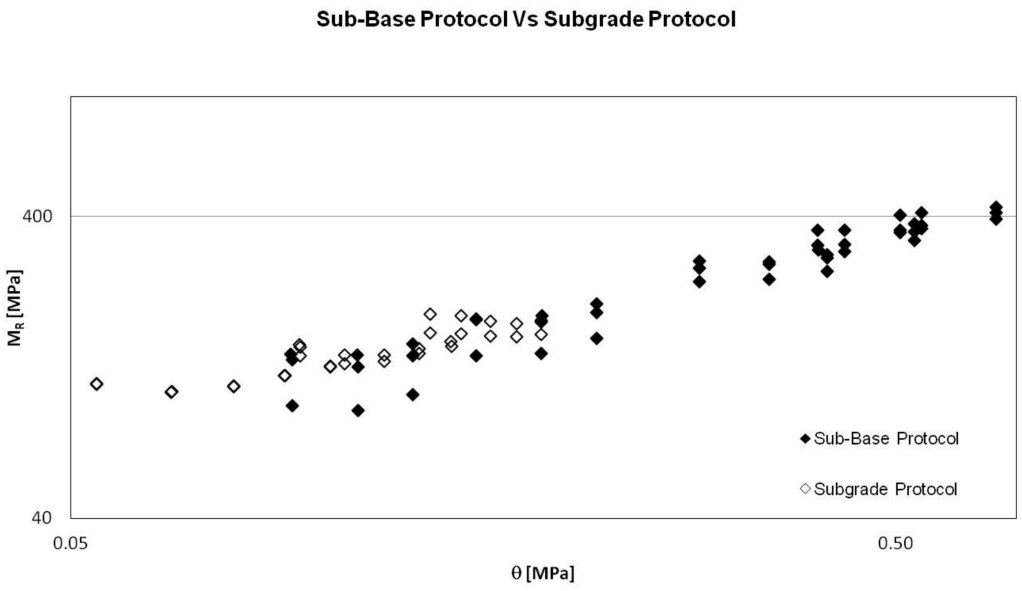

Figure 4.8: Sub-Base Protocol Vs Subgrade Protocol

4.1.5 Quick Shear Test

After completing the resilient modulus test procedure, if the total vertical strain exceeds 5%, it can be possible to test the same specimen to a Quick Shear Test; otherwise, the test is completed. This test is performed to compute maximum axial tension before the failure of the specimen. Test procedure provides to impose a constant confining pressure, generally are tested three samples formed with the same blend of aggregate and water, for each specimen constant confining pressure changes to check how material changes behaviour. Three confining pressures chosen are $0kPa$, $35kPa$ and $69kPa$. The test ends in three ways: when load values decrease with increasing strain if 5% strain is reached or capacity of the load cell is reached. The more important obtained parameters of the test are deformation, vertical tension, and maximum vertical tension (in the table

below); the first two can be plotted on a graph to show how deformation increases increasing vertical load.
In the graph below, tension and deformation in which specimen reach break (peak of the curve) can be seen, the peak of the curve also corresponds, in terms of pressure, to maximum vertical stress that material can resist. Therefore, Quick shear is a destructive test after the solicitation sample is broken (as shown in the picture below).

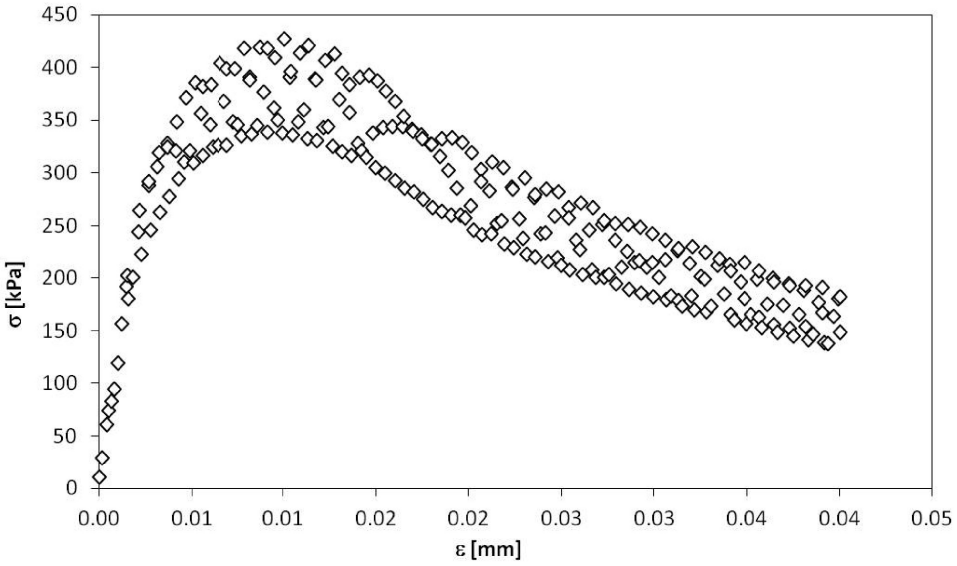

Figure 4.9: Stress Strain Curve

Figure 4.10: Specimen After Quick Shear Test

Specimen	σ_3	**UCS**
[-]	[MPa]	[MPa]
Optimum Condition	0	0.27
Optimum Condition	34.5	0.53
90% of Max Density	0	0.12
90% of Max Density	34.5	0.35
Dry 2.5gg	0	0.43
Dry 2.5gg	69	0.69
Subgrade Protocol	34.5	0.37
Subgrade Protocol	69	0.63

Table 4.18: Maximum Vertical Tensions

Mohr's Circles

Thanks to the quick shear test, it is possible to draw also Mohr's circles. Mohr's circles are a graphical representation of the internal state of stress in a material's point. Circles are drawn in a two-dimensional plane in which are reported standard components (σ_n) and tangential components (τ) of stress in a point. Varying plain's lying points describe a circle in the same plane. Thus, Mohr's circles allow locating central tensions and the main direction of the tension problem. Generally, Mohr's circles are represented by semicircles in the first and fourth quadrant. First, tensional states about specimens with similar characteristics are reported in the same plane. Then, it is drawn line with equation dependant by three circles. Other essential parameters representing the material's breaking criteria are cohesion (c') and the internal friction angle (ϕ). The cohesion represents the intercept of the tangent line to the circles with the vertical axis. Instead, the internal friction angle indicates the slope of the tangent line to the circles. Following Mohr's theory, all tensional states below the line are in safety conditions; above that line, the tensions bring the layer to the failure. The picture below represents the two Mohr's circles relative to the specimens realized with the optimum water content and compacted at the maximum density. In the Appendix, there are the remaining graphs of Mohr's results. Instead, the tables below show the amount of cohesion and internal friction angle.

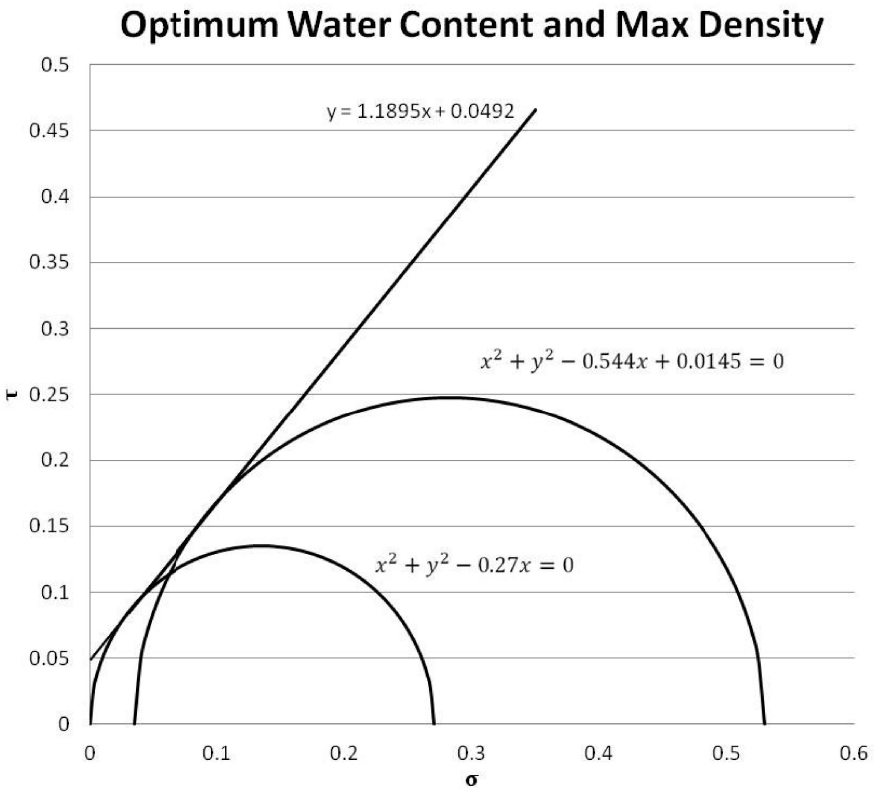

Figure 4.11: Mohr's Circles Sub-Base Protocol

Specimen	**c'**	ϕ
[-]	[-]	[°]
Optimum Condition	0.0491	50
90% of Max Density	0.0234	47
Dry 2.5gg	0.196	36
Subgrade Protocol	0.021	50

Table 4.19: Mohr's Parameters

4.2 ALVA-master Results

Based on experimental test results, the structural analysis is done. The study is performed using all constants; this means having k_1, k_2 and k_3 for each soil condition and model used. The tables below represent the amount for the different states.

Cases	k_1	k_2
1	1178	0.69
2	1364	0.55
3	2543	0.30
4	3060.5	0.38
5	635.2	0.81
6	1364	0.47

Table 4.20: Regression Parameters of Hiks-Monismith Models

Cases	k_1	k_2	k_3
1	973	0.84	-0.15
2	1183	0.66	-0.11
3	2392	0.35	-0.05
4	2538	0.52	-0.15
5	525	0.95	-0.14
6	1116	0.56	-0.13

Table 4.21: Regression Parameters of Uzan Models

Cases	k_1	k_2	k_3
1	630	0.84	-0.15
2	839	0.66	-0.11
3	2067	0.35	-0.05
4	1590	0.52	-0.15
5	336	0.95	-0.14
6	743	0.56	-0.13

Table 4.22: Regression Parameters of MEPDG Models

From the representation point of view, the structural analysis using ALVA-master is compared with the results obtained by the experimental tests for both protocols. The results are plotted below; the blue, red and black indicators are referred, respectively, to as sub-base and subgrade protocols and ALVA-master results. For a more straightforward explanation, the graphs plotted below are referred to a sub-base thickness layer of 10 cm. Moreover, the same charts are obtained with manipulation data using the MEPDG model; it is chosen for better modulus results between the three approaches. The other diagrams, in which sub-base thickness is increased, and the manipulation of the results is made using the other two models, can be seen in the Appendix chapter.

4.2.1 Dual Axle; 80 kN of Load; Sub-Base 10cm Thick

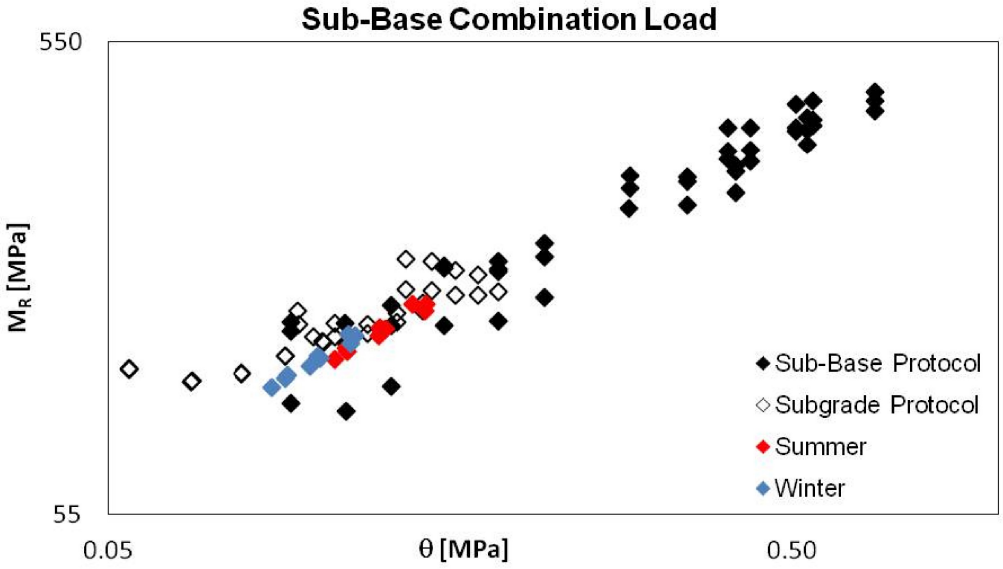

Figure 4.12: ALVA-master Results, 80kN, 10cm, Sub-Base Protocol

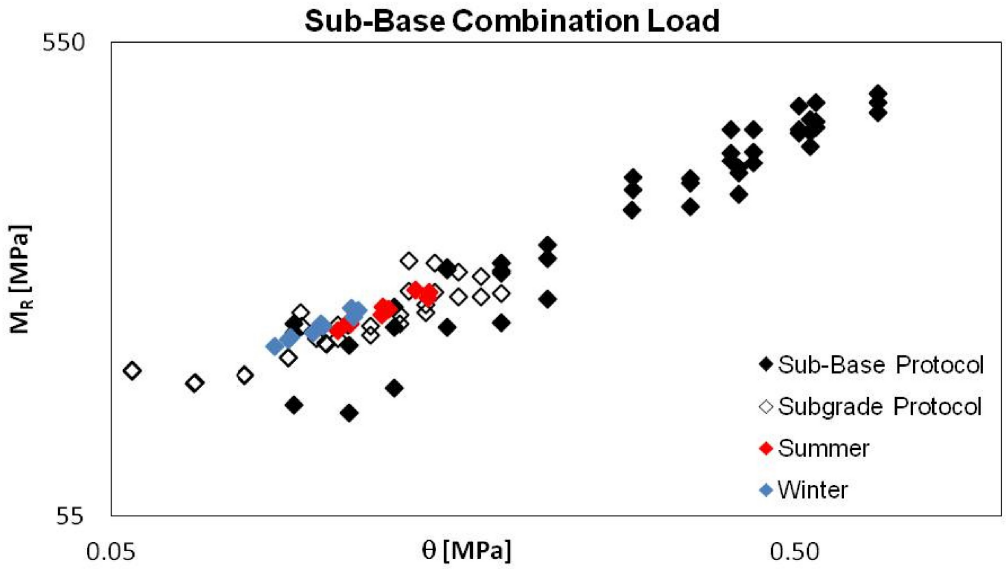

Figure 4.13: ALVA-master Results, 80kN, 10cm, Subgrade Protocol

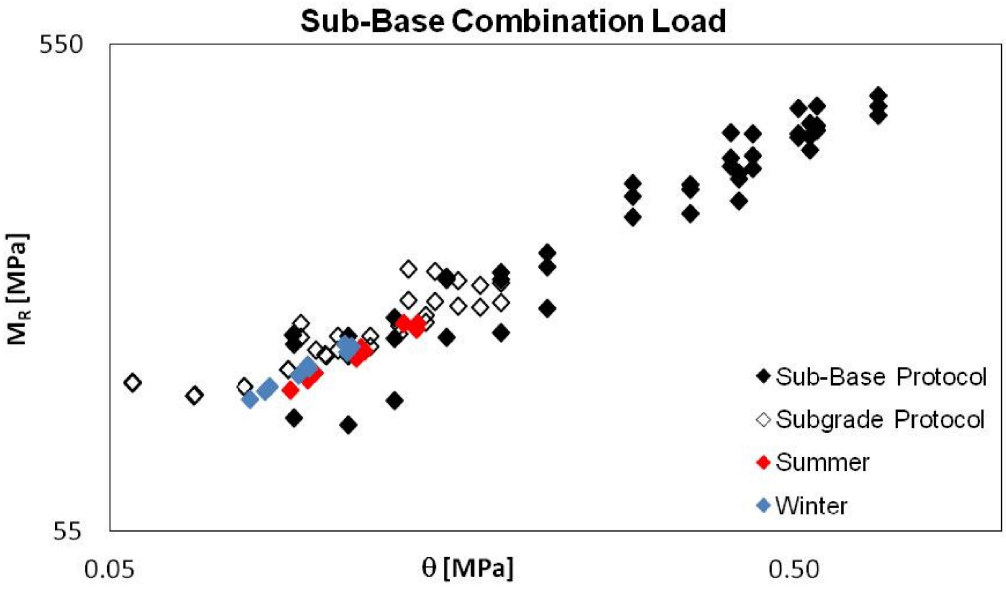

Figure 4.14: ALVA-master Results, 80kN, 10cm, Mix Protocol, After Second Iteration

4.2.2 Dual Axle; 120 kN of Load; Sub-Base 10cm Thick

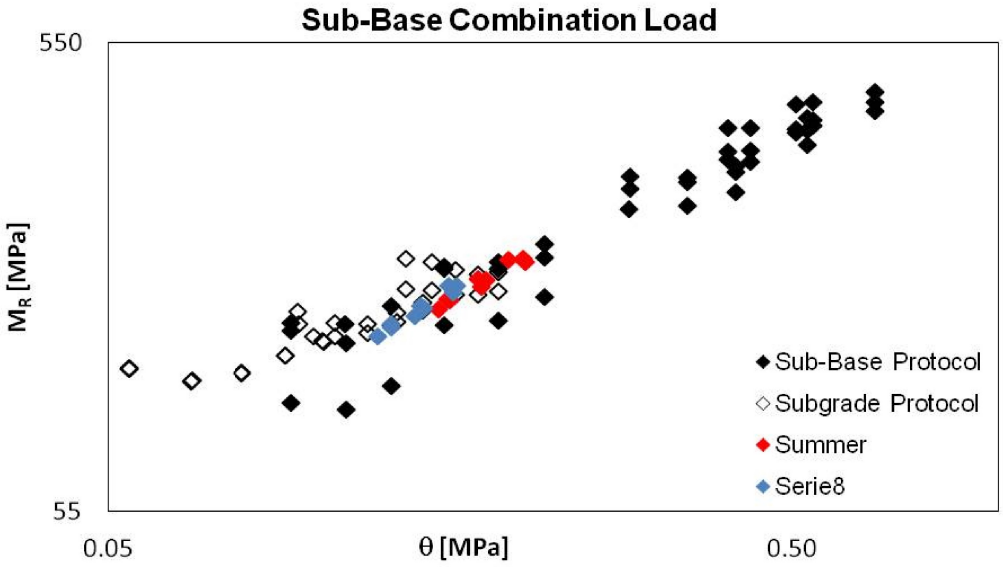

Figure 4.15: ALVA-master Results, 120kN, 10cm, Sub-Base Protocol

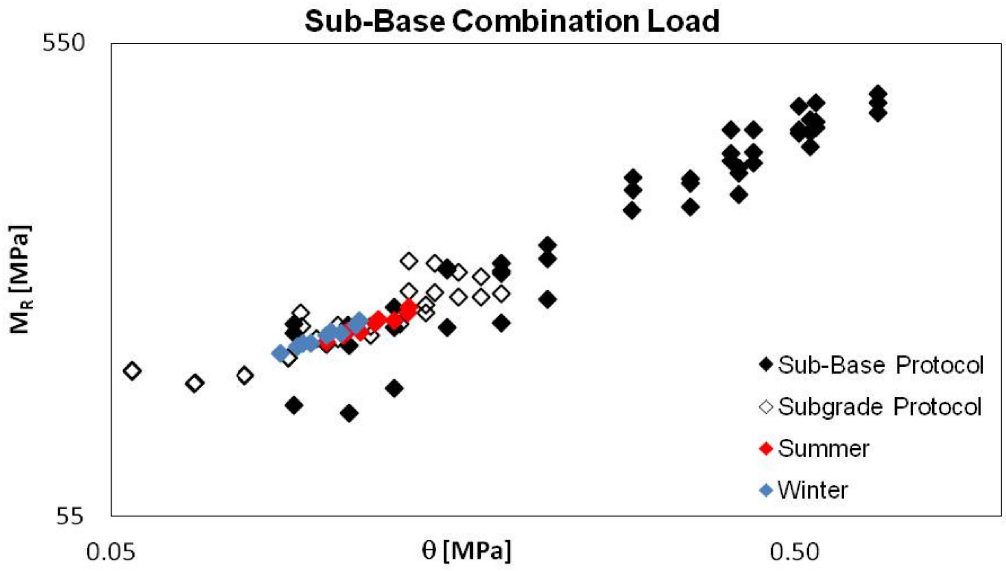

Figure 4.16: ALVA-master Results, 120kN, 10cm, Subgrade Protocol

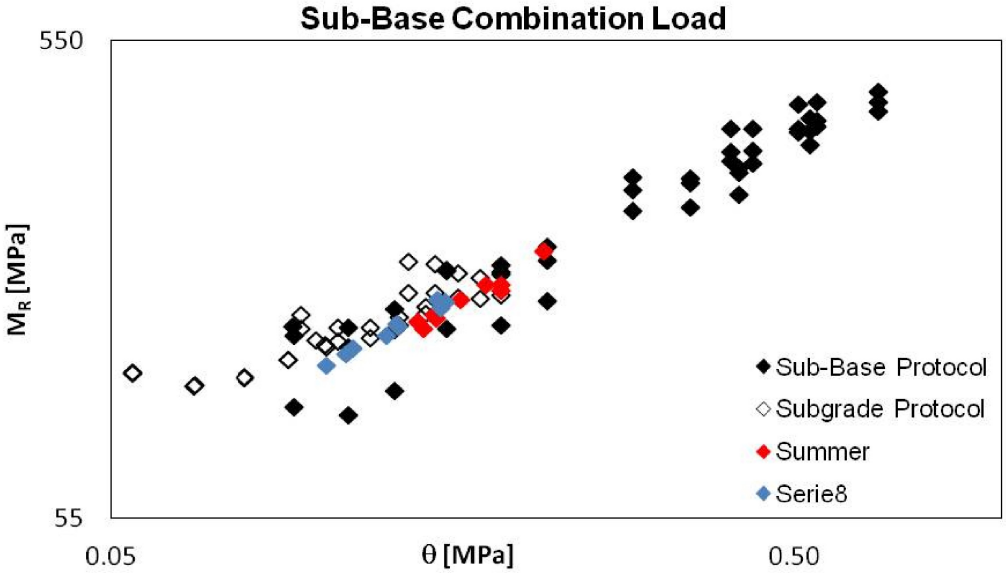

Figure 4.17: ALVA-master Results, 120kN, 10cm, Mix Protocol, After Second Iteration

As aspected, the amount of resilient modulus computed for a dual tire of 120 kN is greater than the resilient modulus obtained with a load of 80 kN. As seen in the picture, the results are in the plan where there is a superposition of protocols values for both solicitations (80 and 120 kN). It means that for a test of unbound granular material, it is mandatory to use two different protocols based on the type of layer and the performance that must be satisfied. However, increasing the thickness of the sub-base layer is witnessing a behaviour in which the stresses are slightly reduced. In the case in which the thickness layer is 20cm, the results fall in the superposition zone; instead, in the case with sub-base layer thickness is 30 cm, the values aren't belonging to all in that area of the plan.

An additional study was conducted considering an addiction to a stiff layer in concrete between the base layer of pavement and the sub-base. The scope of this analysis is to verify what changes in the state of stress of the sub-base layer. Moreover, as in the previous case, it is possible to confirm which type of protocol is better to use or if it is mandatory to use both protocols: one for the subgrade and the other for the sub-base layers.
The characteristics of this layer are reported below.

Layer	**Thickness**	**Poisson Ratio**	**El. Module S.**	**El. Module W.**
[-]	[mm]	[-]	[MPa]	[MPa]
Concrete	100	0.40	454	454

Table 4.23: ALVA-master Concrete Layer's Characteristics

4.2.3 Dual Axle; 80 kN of Load; Sub-Base 10cm Thick; With Concrete Layer

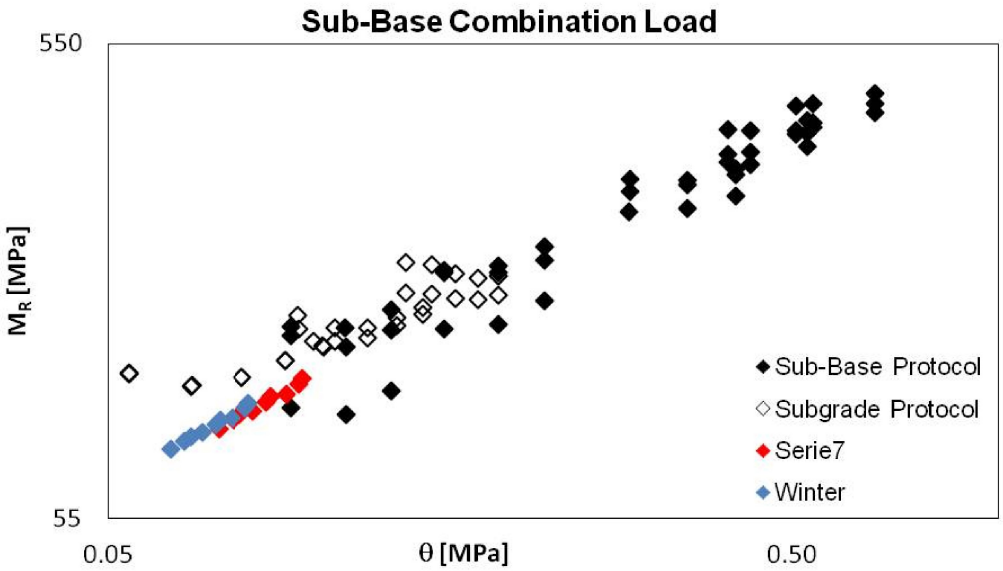

Figure 4.18: ALVA-master Results, 80kN, 10cm, With Concrete Layer, Sub-Base Protocol

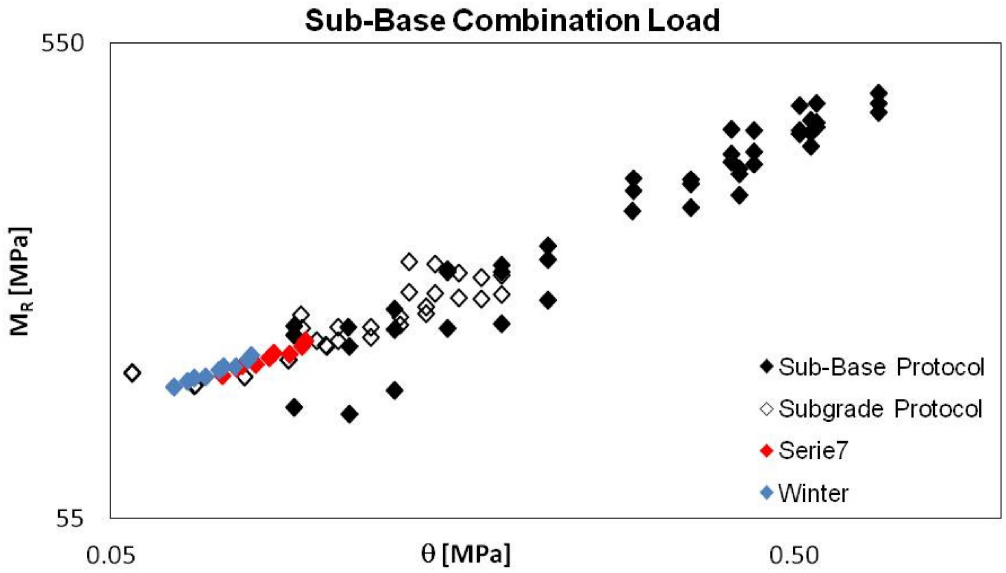

Figure 4.19: ALVA-master Results, 80kN, 10cm, With Concrete Layer, Subgrade Protocol

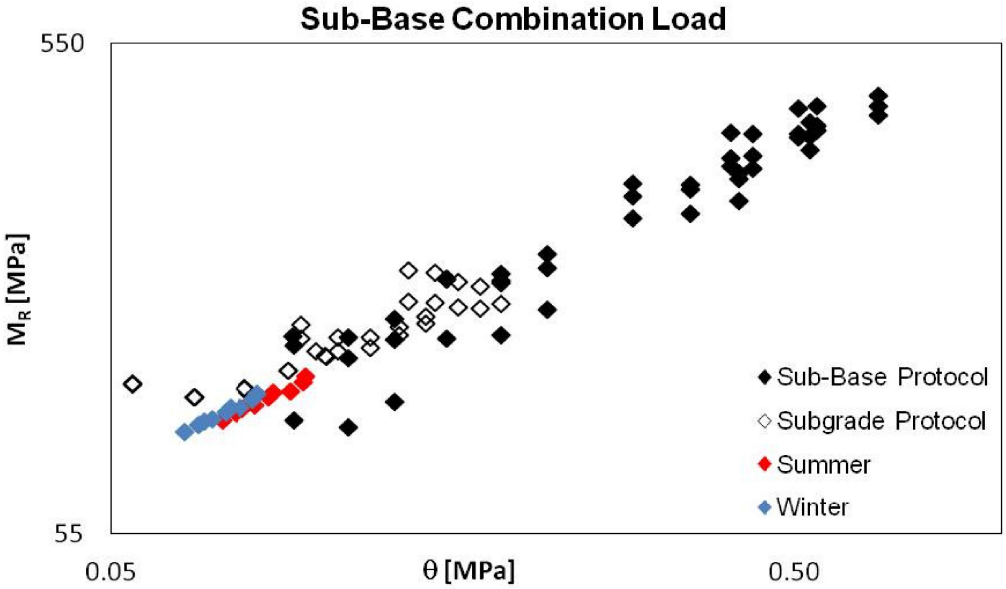

Figure 4.20: ALVA-master Results, 80kN, 10cm, With Concrete Layer, Mix Protocol, After Second Iteration

4.2.4 Dual Axle; 120 kN of Load; Sub-Base 10cm Thick

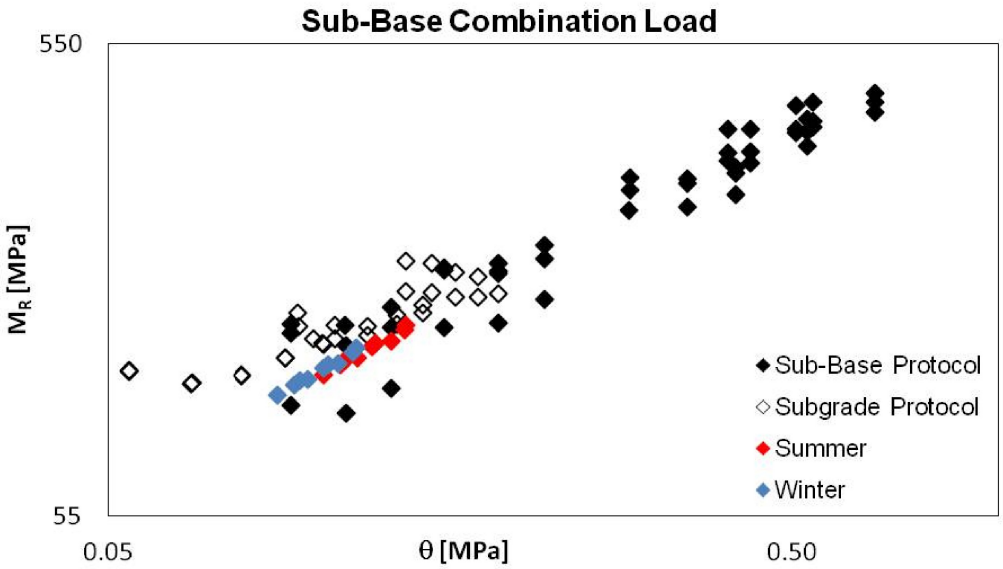

Figure 4.21: ALVA-master Results, 120kN, 10cm, With Concrete Layer, Sub-Base Protocol

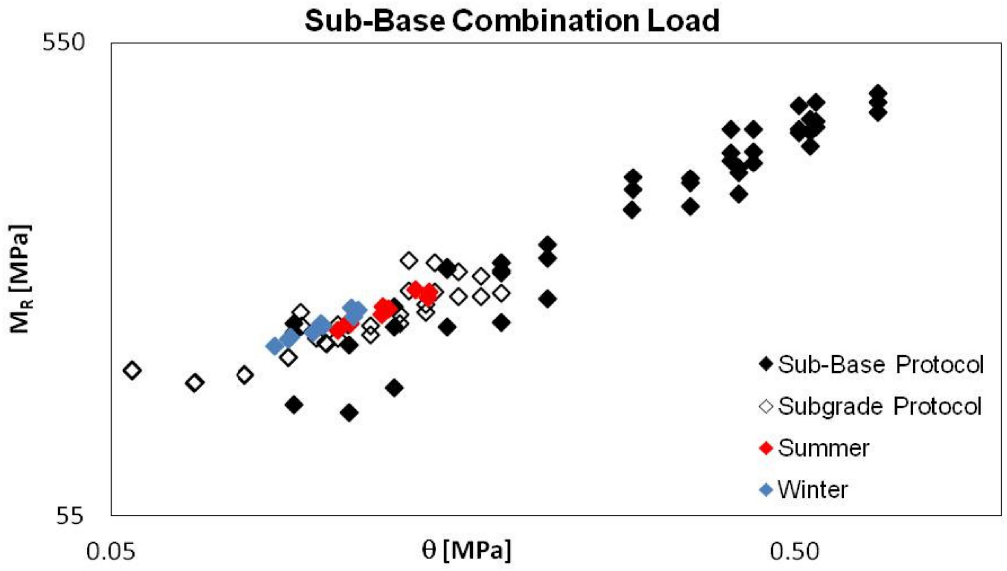

Figure 4.22: ALVA-master Results, 120kN, 10cm, With Concrete Layer, Subgrade Protocol

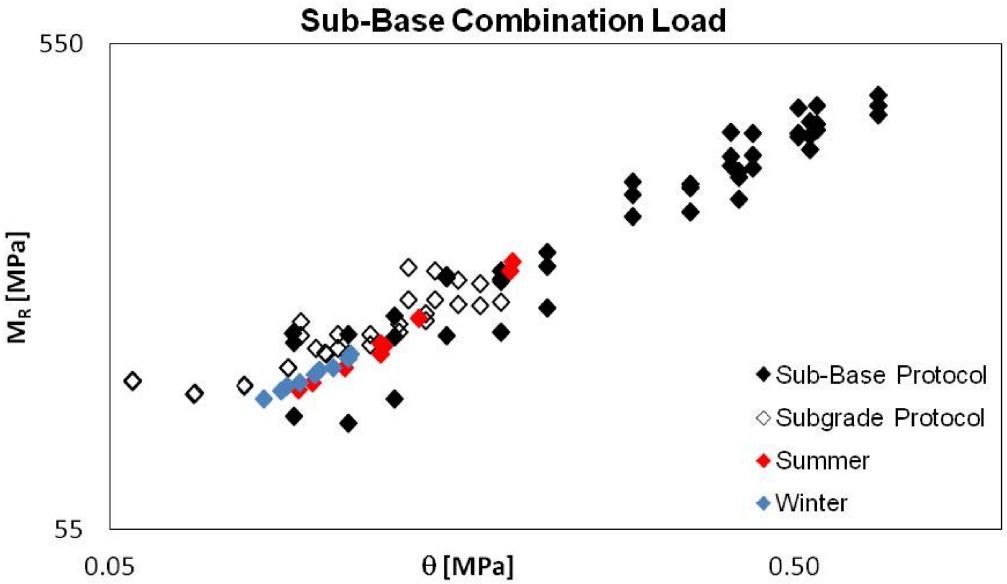

Figure 4.23: ALVA-master Results, 120kN, 10cm, With Concrete Layer, Mix Protocol, After Second Iteration

With the addition of the concrete layer, the software returns values of stresses in the layer studied slightly lower than the other case. Therefore, it is justified that this stiff layer dissipates part of the solicitation. Moreover, for a dual axle of 120 kN, as in the previous case, the results are in the superposition zone of protocols yet; however, this is not the same when the load considered is 80 kN. Therefore, in this last analysis, part of the results occur not more in the same zone but between the superposition and the subgrade protocol results; in a particular case for the winter periods in which behaviour of the shallow layer is stiffer than the summer case.

In the structural analysis using ALVA-master are analyzed the more critical conditions, in terms of stresses, that can occur in road pavement. The second study using KENLAYER software seeks to understand how to change the stresses outside the critical zone considering points of interest in a different position than the previous case; moreover, this analysis favours safety.

4.3 KENLAYER Results

As in the previous case, the study is performed using the regression parameters obtained by the experimental tests; however, in this case, the same parameters are purified by the atmospheric pressure p_a.

The actual formulations of the resilient modulus comprise the amount of atmospheric pressure, but the KENLAYER software works with regression parameters without that amount. So it is fundamental to remove the atmospheric pressure before working with the software as in the old formulation.

$$M_R = k_1 \theta^{k_2}$$

Another "limit" of the software is regarding the model used. With the experimental analysis are studied three models: Hicks-Monismith, Uzan and MEPDG and for each of them are computed regression parameters for each condition of the soil. However, the input values used are the regression parameter only for the Hicks-Monismith model in addition to the material characteristics.

Cases	k_1	k_2
Sub-Base Protocol	4855	0.68
Subgrade Protocol	22297	0.39
Mix Protocols	5667	0.66
90% of Maximum Density	10603	0.56
Dry Condition	7647	0.70
Wet Condition	1559	0.81

Table 4.24: KENLAYER, Regression Parameters of Hiks-Monismith Model

It was tried to consider different axles of the vehicle to obtain a more convenient solution in terms of safety. Single and dual axles are compared, and results decreed the dual axle is a more conservative configuration. So, the following analysis reproduces the dual axle results.

Starting from the general solution, in which the data are modelled with regression parameters obtained by the sub-base protocol for a standard material for all 12 months of the years (optimum content of water and a maximum density of compaction), the failure occurs for rutting of the subgrade with a design life of 17 years. The graph below shows the modelled results in resilient modulus and first invariant of tensions (red) compared with experimental results modelled with both protocols (black and white).

Conditions	**Breaking Criterion**	**Damage**	**Design Life**
Standard	Rutting of Subgrade	0.0588	17 years

Table 4.25: KENLAYER, Damage and Design Life of Material in Standard Conditions, Sub-Base Protocol

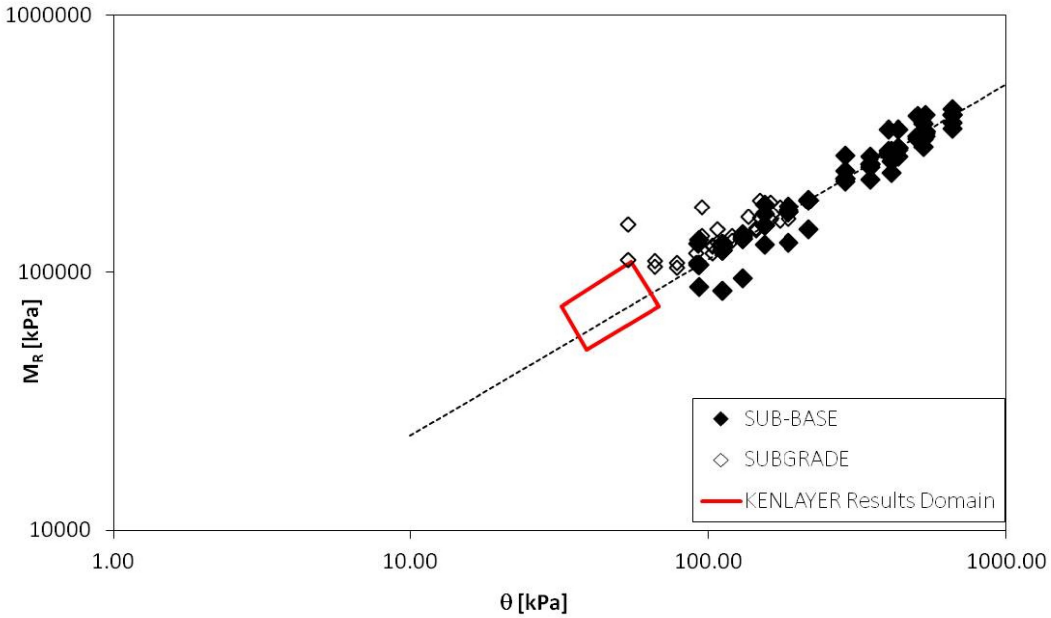

Figure 4.24: KENLAYER Results Modelled With Sub-Base Protocol For a Material In Standard Condition

4.3.1 Variation of Analysis Protocol

The first change analyzed is the factorial type. Results acquired by KENLAYER are manipulated at first using the parameter of subgrade protocol and later employing a parameter obtained by the combination of both protocols (sub-base and subgrade). The results can be seen in the followed graphs and tables.

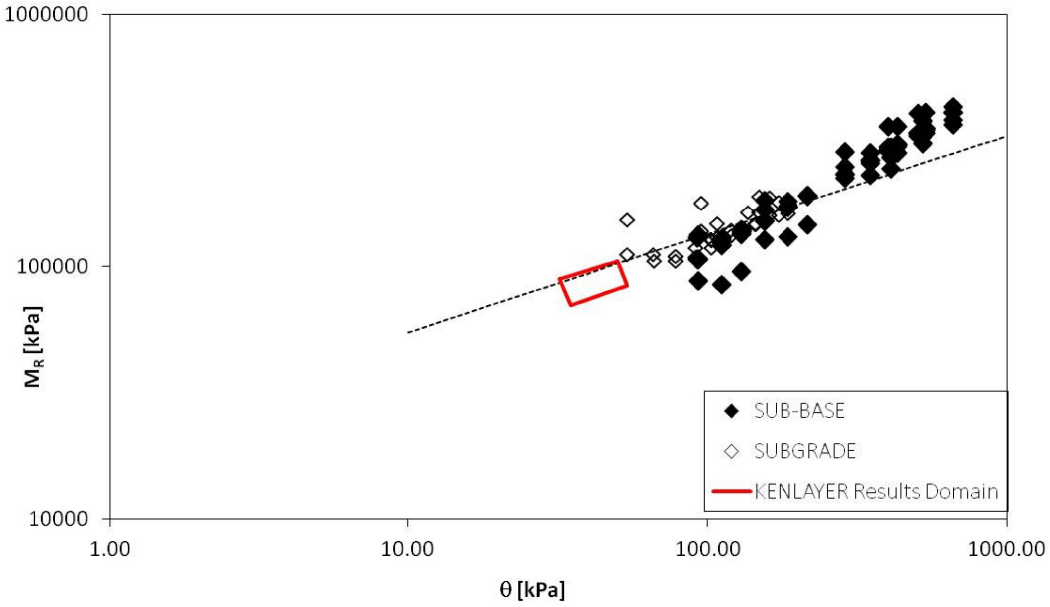

Figure 4.25: KENLAYER Results Modelled With Subgrade Protocol For a Material In Standard Condition

Conditions	**Breaking Criterion**	**Damage**	**Design Life**
Standard	Fatigue of Base	0.0532	18.8 years

Table 4.26: KENLAYER, Damage and Design Life of Material in Standard Conditions, Subgrade Protocol

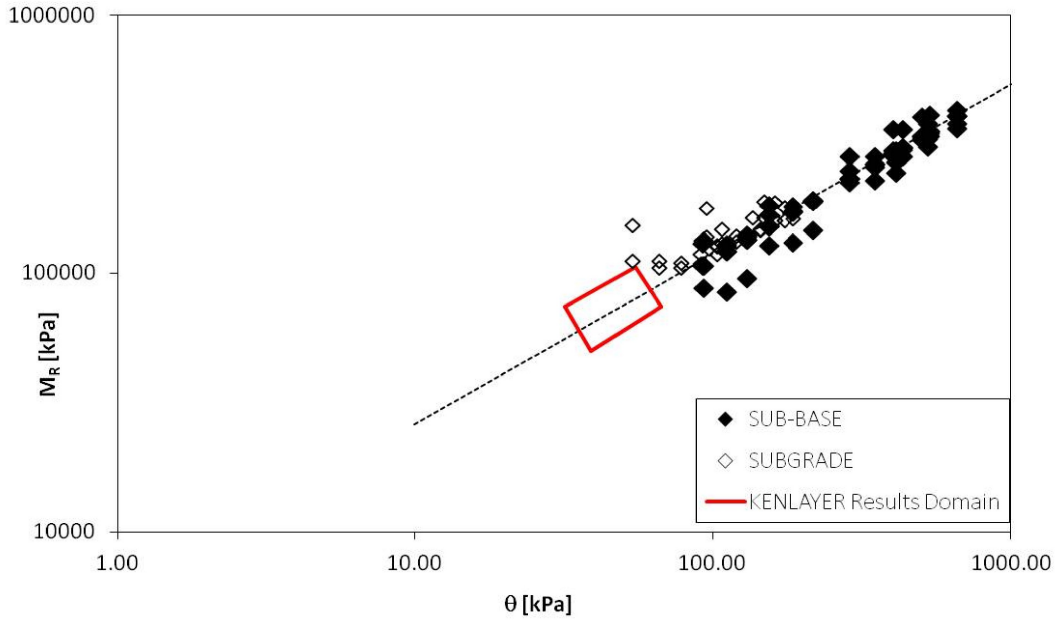

Figure 4.26: KENLAYER Results Modelled With Mix Protocol For a Material In Standard Condition

Conditions	**Breaking Criterion**	**Damage**	**Design Life**
Standard	Fatigue of Base	0.0566	17.7 years

Table 4.27: KENLAYER, Damage and Design Life of Material in Standard Conditions, Mix Protocol

The results modelled with sub-base protocol show a change in damage failure in the other two cases. Moreover, the damage is reduced with a consequent increment of the design life.

4.3.2 Variation of Density Compaction

Starting always by the general case, in which the soil characteristics have optimum water content and a maximum density of compaction, the influence of the density on the material's behaviour is studied. Indeed, always considering the sub-base protocol, a case where the soil has a compaction density equal to 90% of the maximum is investigated. Then, as shown in the graph and the table below, the effect of density is practically null for the material's behaviour except for the breaking criterion: it passes from rutting in the subgrade to fatigue in the base layer.

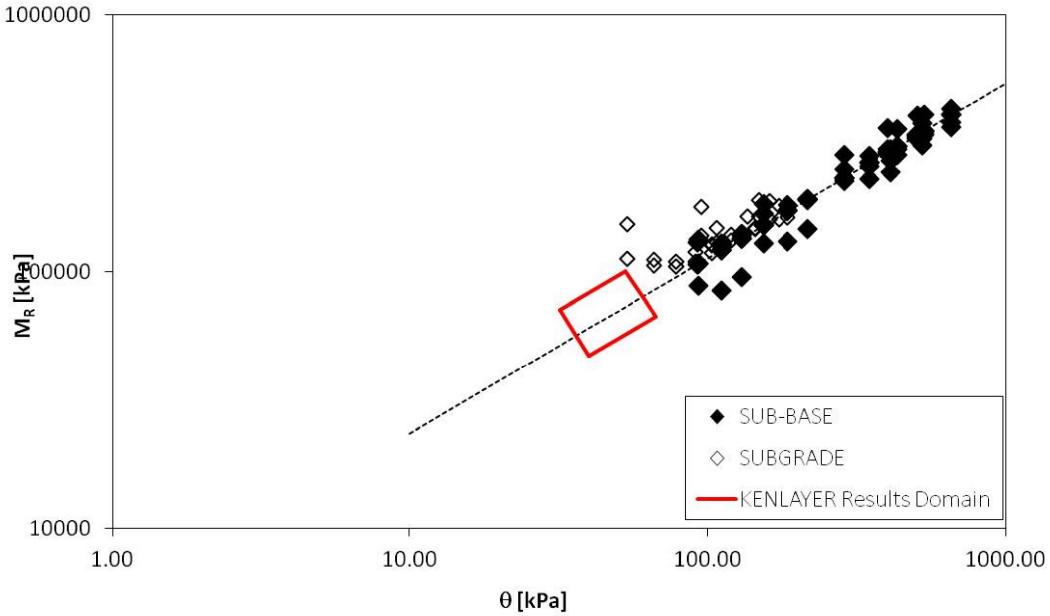

Figure 4.27: KENLAYER Results Modelled With Sub-Base Protocol For a Material With a Reduction Density

Conditions	Breaking Criterion	Damage	Design Life
90% of Max Density	Fatigue of Base	0.0591	17 years

Table 4.28: KENLAYER, Damage and Design Life of Material With a Reduction Density, Sub-Base Protocol

4.3.3 Variation of Moisture Content

The moisture content variation is the last parameter varied for the study of the material. It is supposed to consider dividing the year into three periods: normal, dry and wet.

- **Normal Period:** It is a period in which optimum conditions in terms of moisture content and density are considered;
- **Dry Period:** It a period that corresponds to a summer season in which temperature is high and with rarely rain events;
- **Wet Period:** It is a period that corresponds to a rained season in which there is a high content of water in the soil and freezing, and thawing events are frequently.

Different combinations are made to obtain the final comparisons. It is clear, seeing the results below, how the effect of water in a road pavement is critical. The design life decreases from 17 to 7,7 years, considering only one wet month, and the situation became more acute in the other two combinations studied. The wet case is a highly critical configuration that rarely occurs during the year. Therefore, the analysis is regarding "special events" in which there is always rain during the month.

Period 1: 8 Normal, 3 Dry and 1 Wet

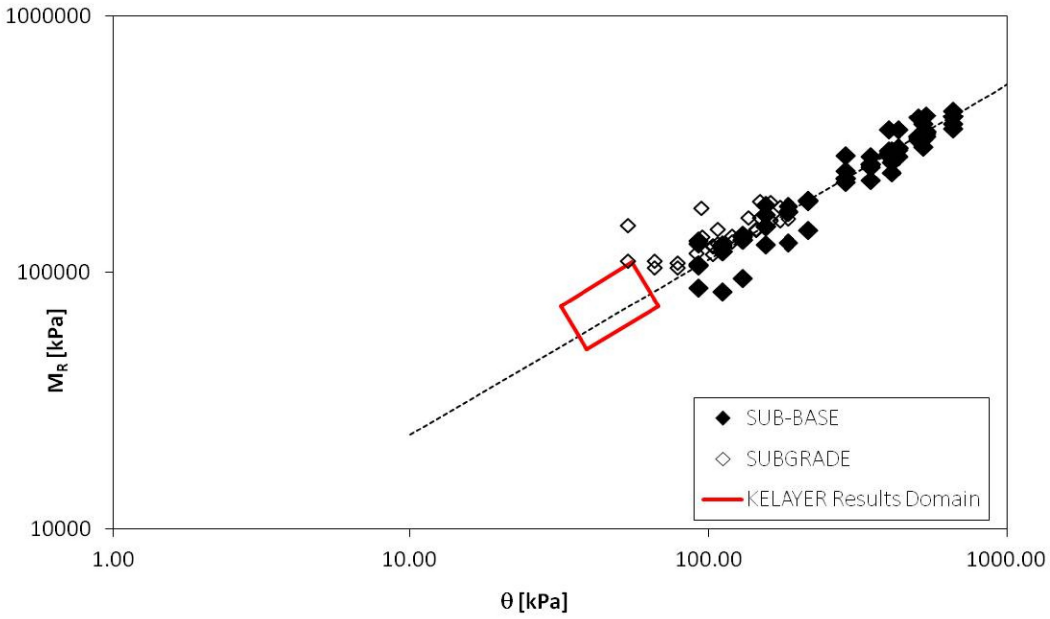

Figure 4.28: KENLAYER Results Modelled With Sub-Base Protocol For a Material During Period 1

Conditions	Breaking Criterion	Damage	Design Life
Period 1	Rutting of Subgrade	0.131	7.7 years

Table 4.29: KENLAYER, Damage and Design Life of Material During Period 1, Sub-Base Protocol

Period 2: 7 Normal, 3 Dry and 2 Wet

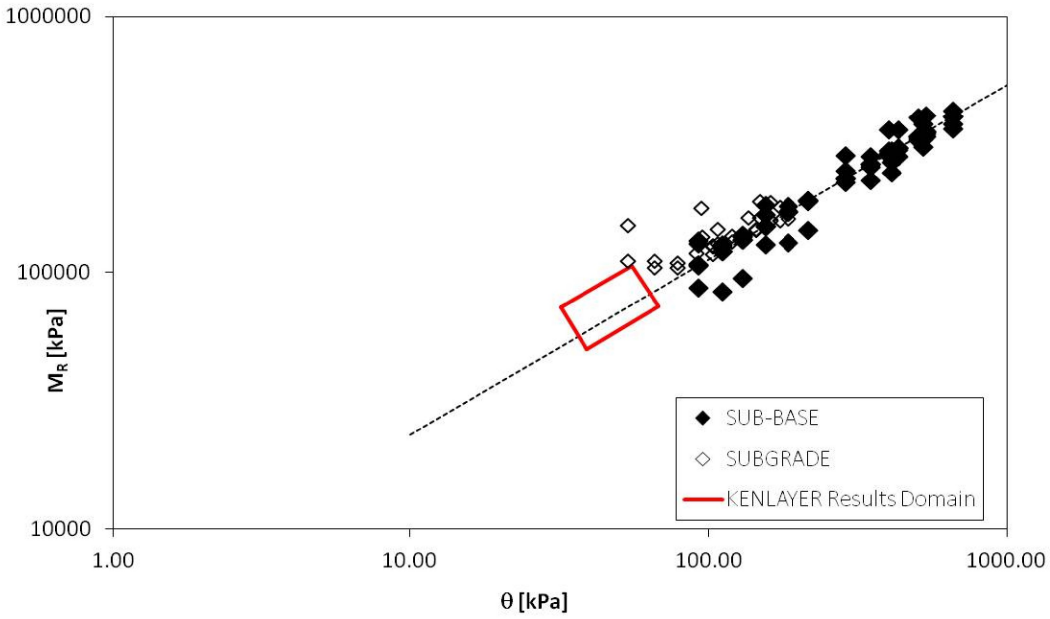

Figure 4.29: KENLAYER Results Modelled With Sub-Base Protocol For a Material During Period 2

Conditions	Breaking Criterion	Damage	Design Life
Period 2	Rutting of Subgrade	0.218	4.6 years

Table 4.30: KENLAYER, Damage and Design Life of Material During Period 2, Sub-Base Protocol

Period 3: 6 Normal, 3 Dry and 3 Wet

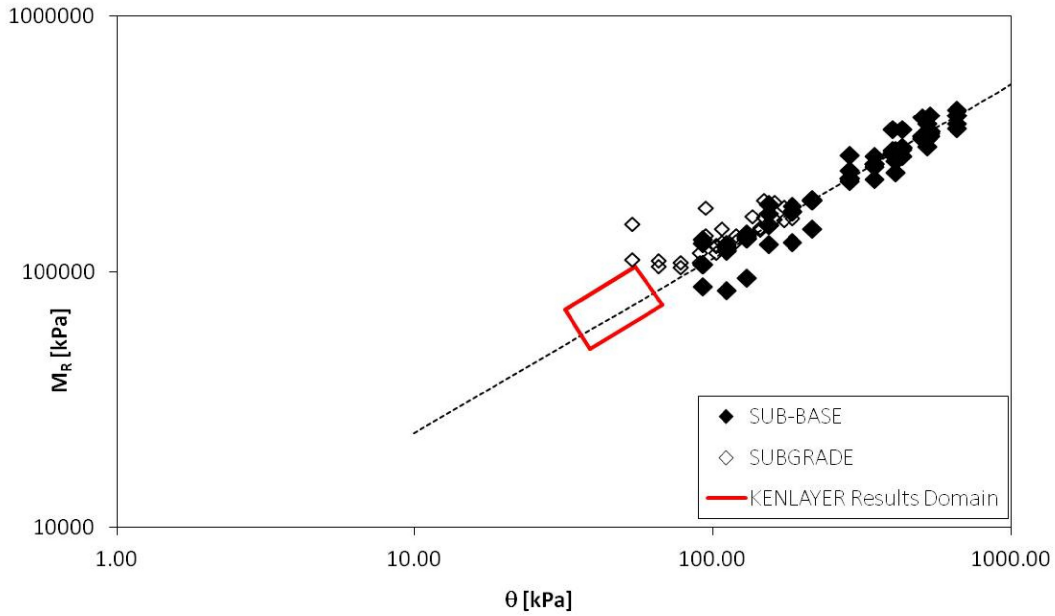

Figure 4.30: KENLAYER Results Modelled With Sub-Base Protocol For a Material During Period 3

Conditions	Breaking Criterion	Damage	Design Life
Period 3	Rutting of Subgrade	0.301	3.3 years

Table 4.31: KENLAYER, Damage and Design Life of Material During Period 3, Sub-Base Protocol

Chapter 5

Conclusions

Through bibliographic research, experimental analysis, and structural analysis, purpose this thesis is computing the design life of the road pavement. The analysis is based on the study of the mechanical behaviour of the sub-base foundation layer. The models used to manipulate the data are Hicks-Monismith, Uzan and MEPDG.

- The design life in the standard condition of the pavement is 17 years with a rutting subgrade failure criteria. The usual conditions are periods with moderate rain events, temperatures around 12°C and maximum compaction between grains.
- Differently from what was expected, a loss of density between grains of the sub-base layer, the design life changes of a negligible quantity. The failure criteria represent the only substantial difference: the failure occurs for fatigue in the base layer.
- The varied parameter that affects pavement design life more is the water content:
  - Simulating the dry extreme conditions period in which there aren't rain events and hot temperatures, the pavement's design life increase till 19 years.
  - Supposing to simulate the wet extreme condition period, in which there are only rainy periods and frequently freezing and thawing events, the design life of pavements is significantly reduced till one year.
  - It is tried to simulate real conditions during the year in terms of moisture content. Starting from 8 months natural, 3 months dry,

and 1 month wet, the pavement's design life of 8 years is computed. Moreover, decreasing normal conditions and increasing wet periods assist a decrement pavement's design life until 5 years. Further aggravating the states, the design life is 3 years.

Finally, for a good and reliable construction of road pavement, it is fundamental to realize an optimum drainage system of the water to avoid the soil's soaking effect that reduces the performance and design life of the road pavement.

Chapter 6

Appendix

6.1 Mohr's Circles

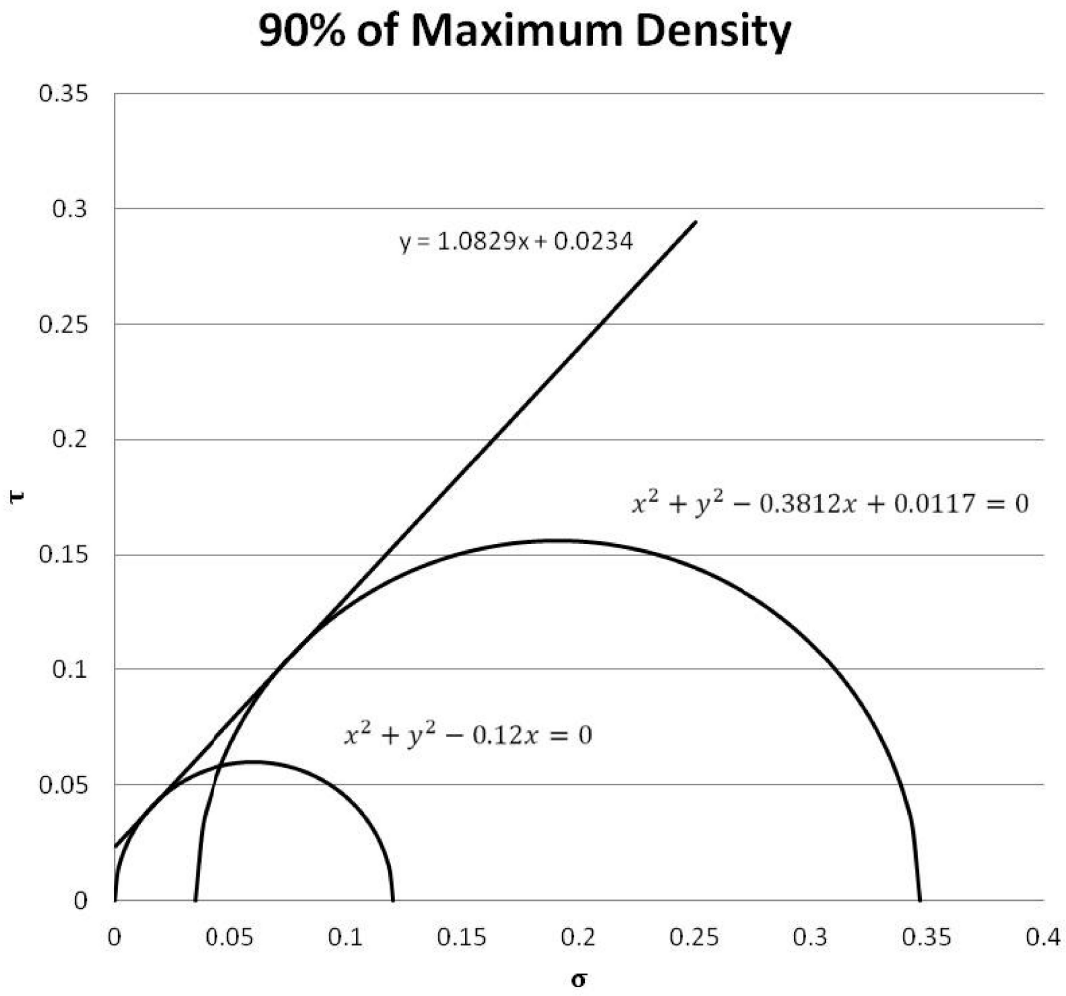

Figure 6.1: Mohr's Circles 90 perc. of Maximum Density

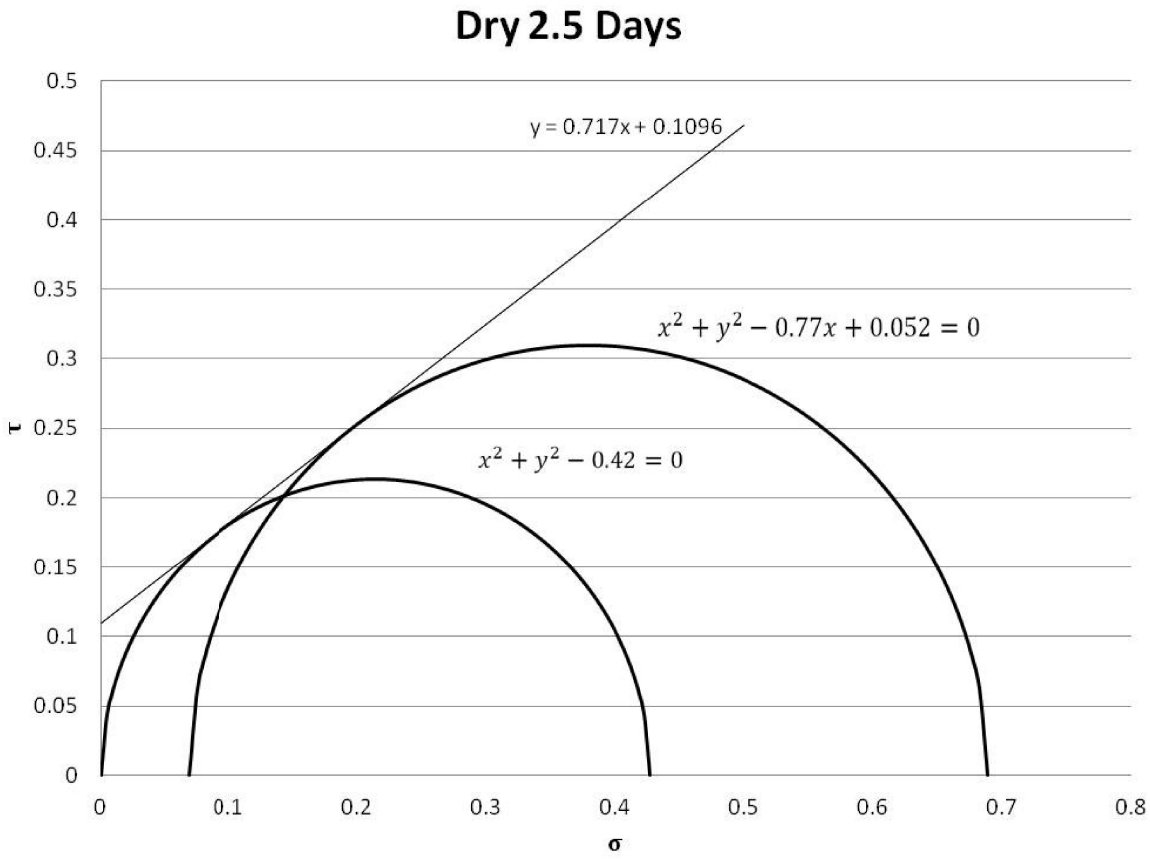

Figure 6.2: Mohr's Circles Dry 2.5 Days

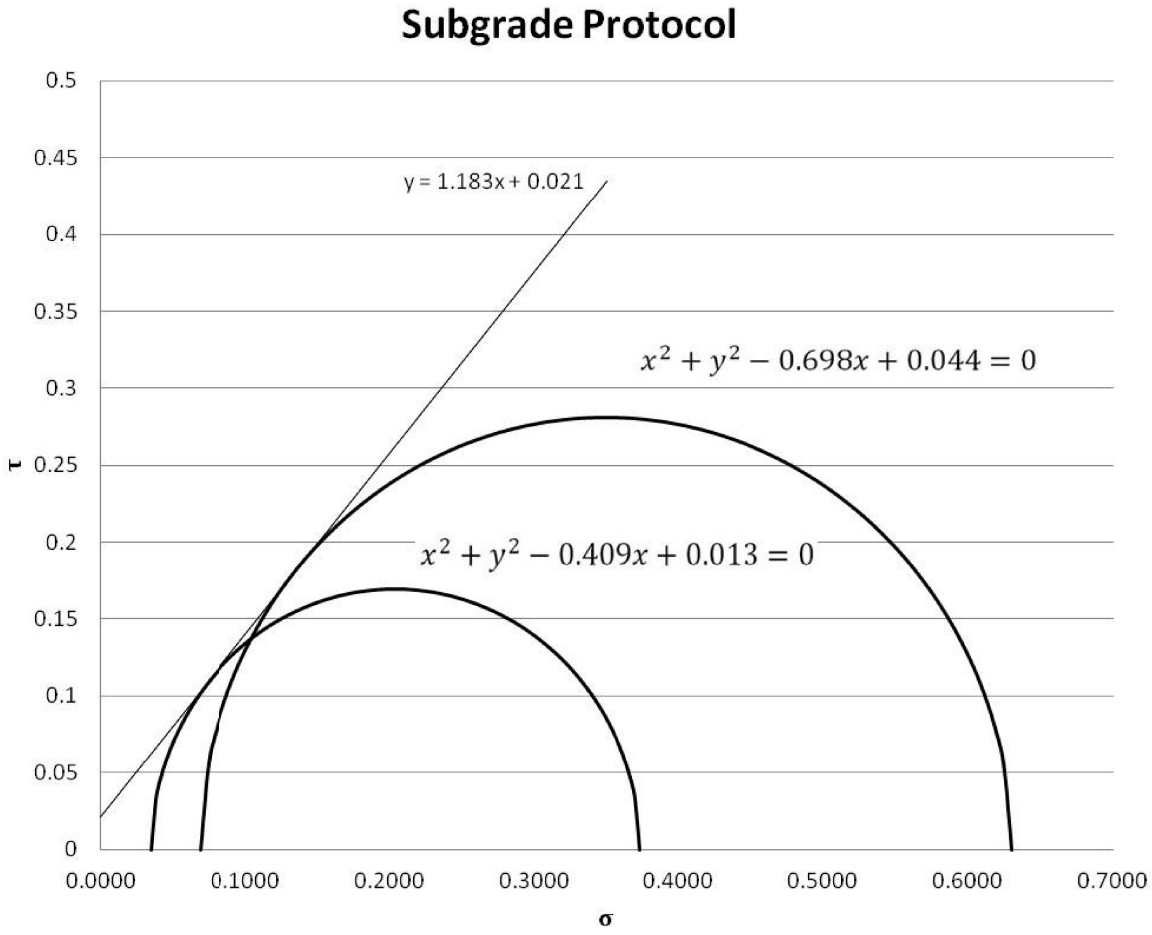

Figure 6.3: Mohr's Circles Subgrade Protocol

6.2 ALVA-master Graphs

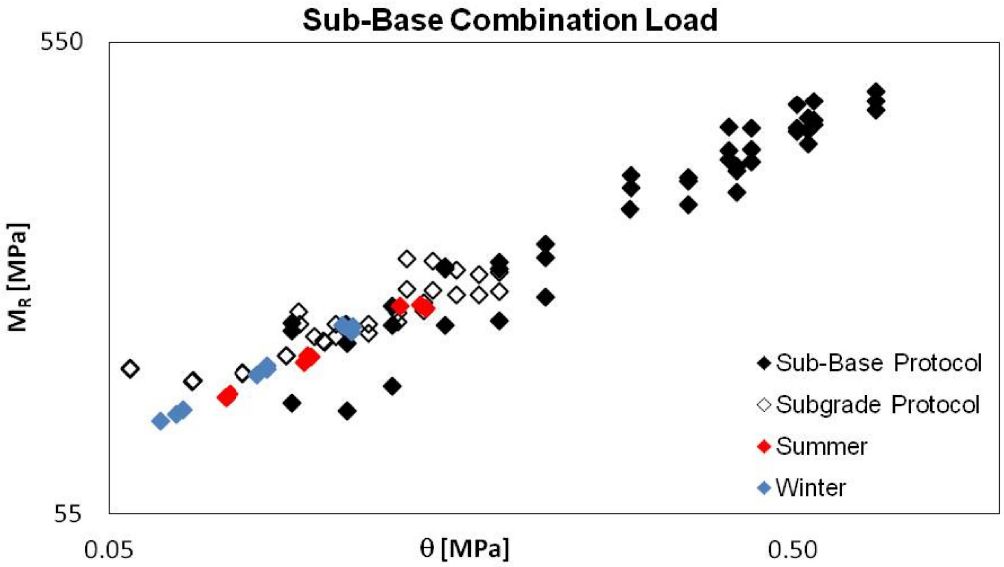

Figure 6.4: ALVA-master Results, 80kN, 20cm, Mix Protocol, After Second Iteration, MEPDG

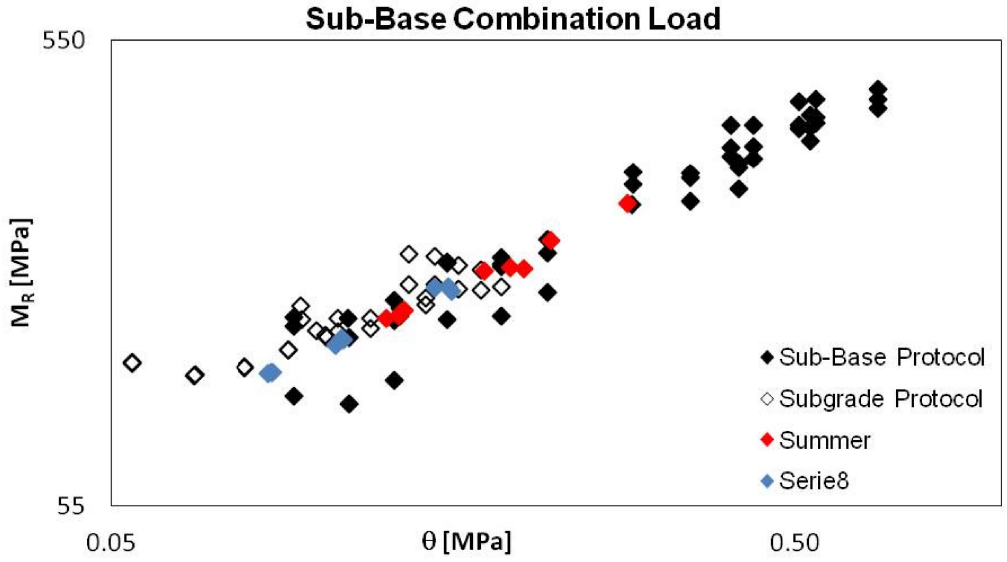

Figure 6.5: ALVA-master Results, 120kN, 20cm, Mix Protocol, After Second Iteration, MEPDG

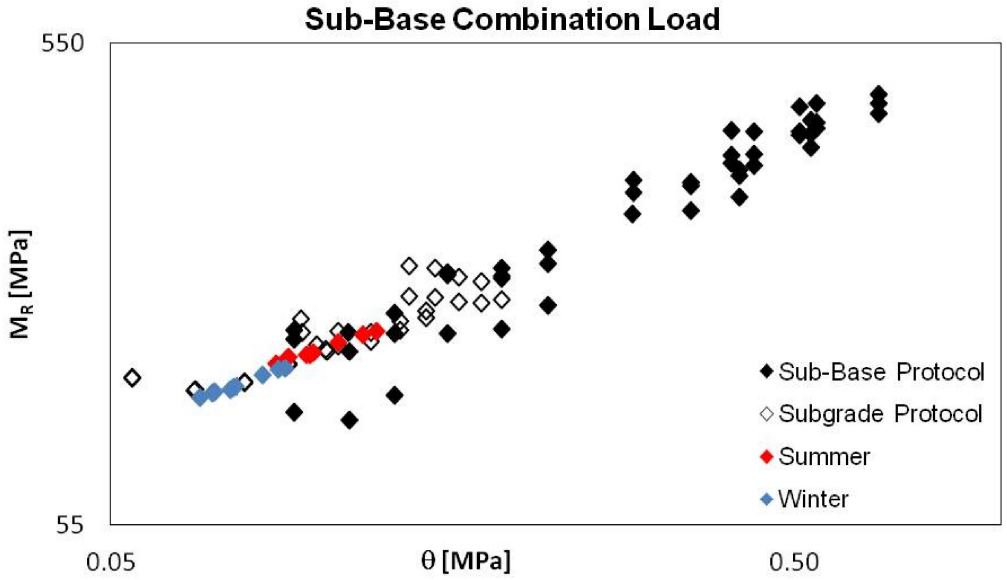

Figure 6.6: ALVA-master Results, 80kN, 20cm, With Concrete Layer, Mix Protocol, After Second Iteration, MEPDG

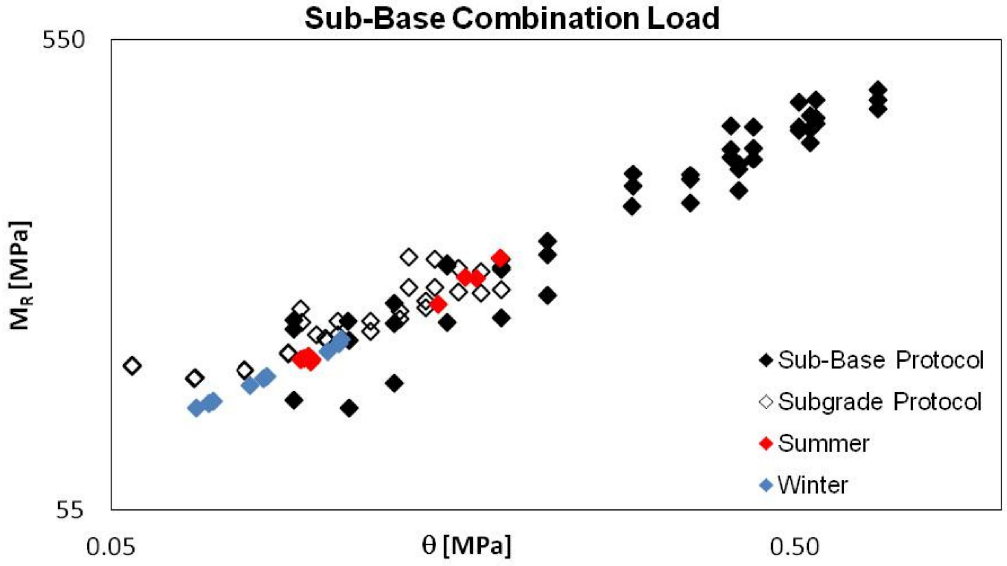

Figure 6.7: ALVA-master Results, 120kN, 20cm, With Concrete Layer, Mix Protocol, After Second Iteration, MEPDG

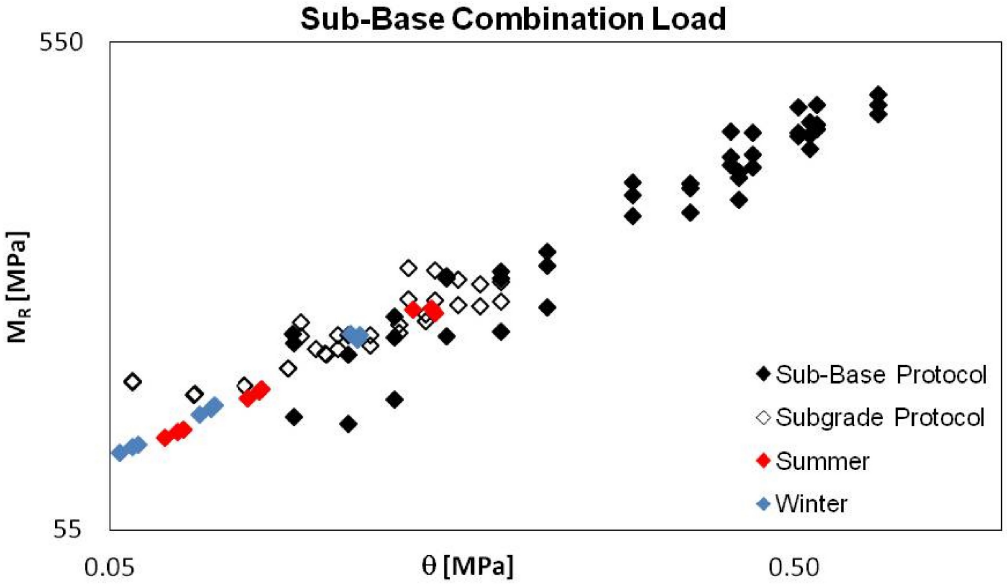

Figure 6.8: ALVA-master Results, 80kN, 30cm, Mix Protocol, After Second Iteration, MEPDG

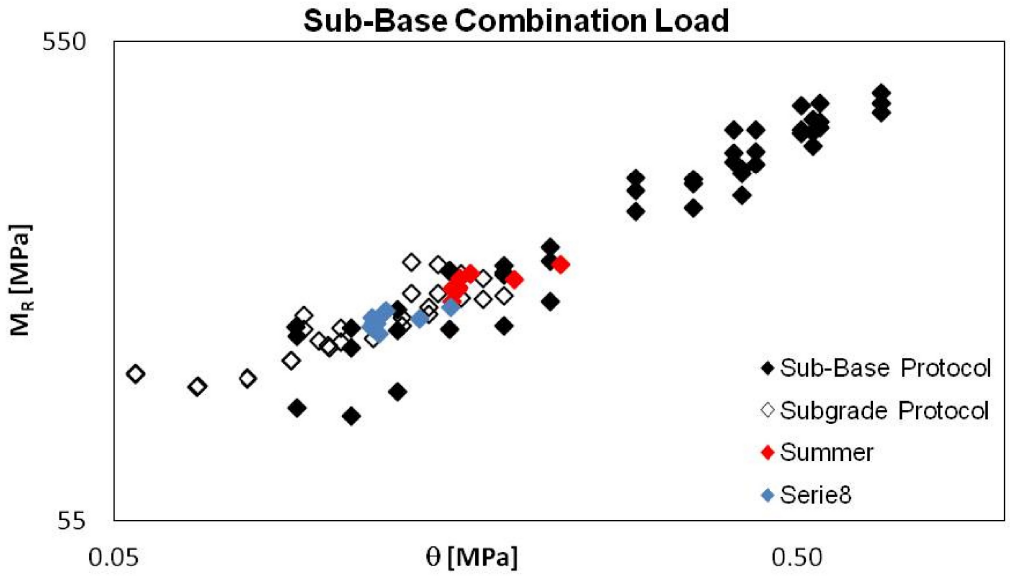

Figure 6.9: ALVA-master Results, 120kN, 30cm, Mix Protocol, After Second Iteration, MEPDG

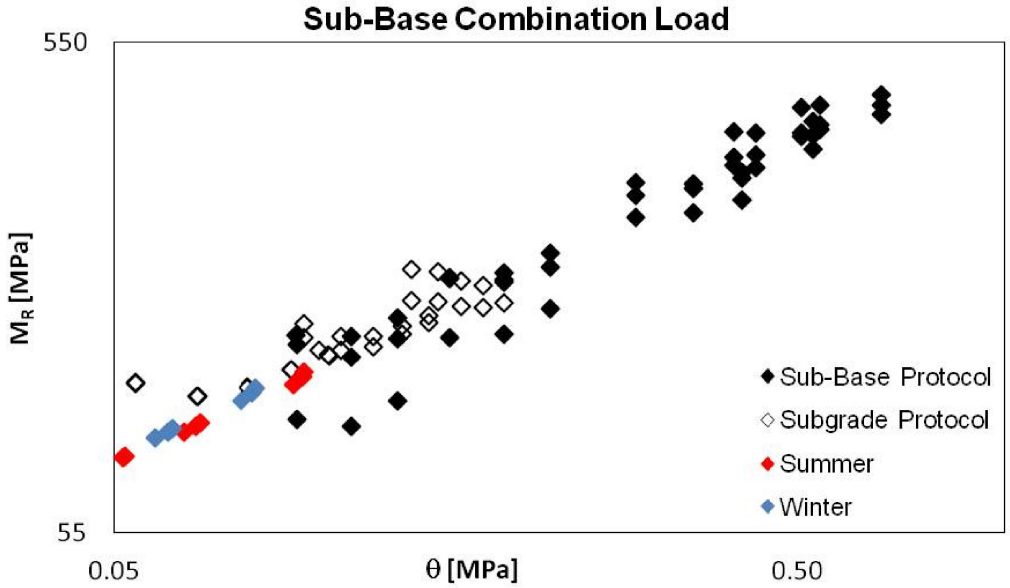

Figure 6.10: ALVA-master Results, 80kN, 30cm, With Concrete Layer, Mix Protocol, After Second Iteration, MEPDG

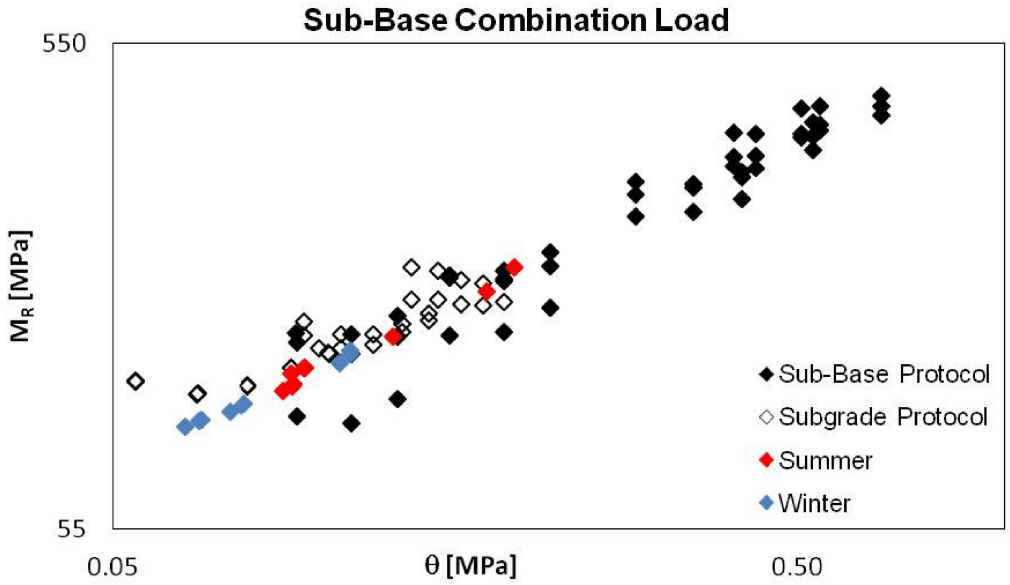

Figure 6.11: ALVA-master Results, 120kN, 30cm, With Concrete Layer, Mix Protocol, After Second Iteration, MEPDG

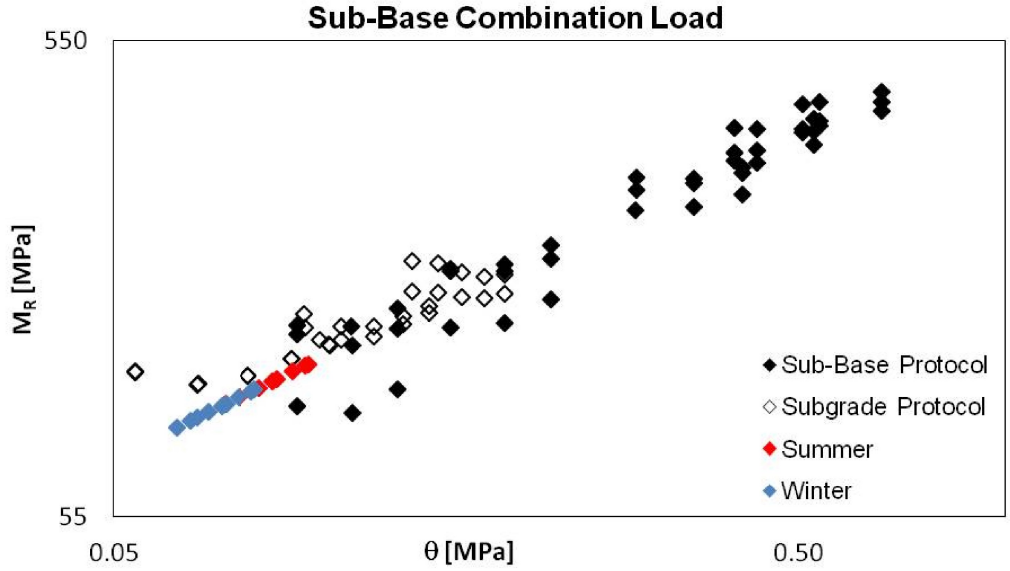

Figure 6.12: ALVA-master Results, 80kN, 10cm, Sub-Base, After Second Iteration, H-M

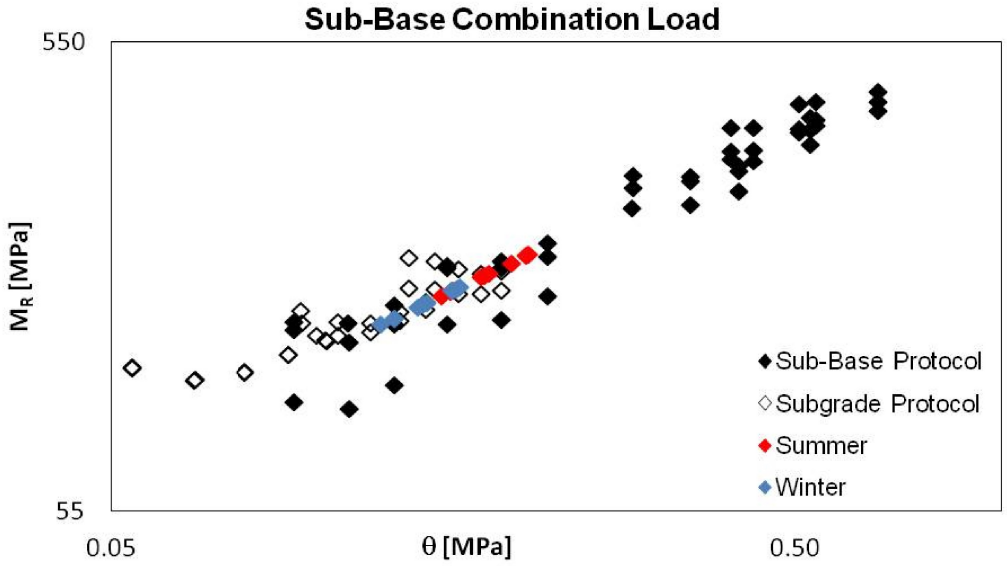

Figure 6.13: ALVA-master Results, 120kN, 10cm, Sub-Base, After Second Iteration, H-M

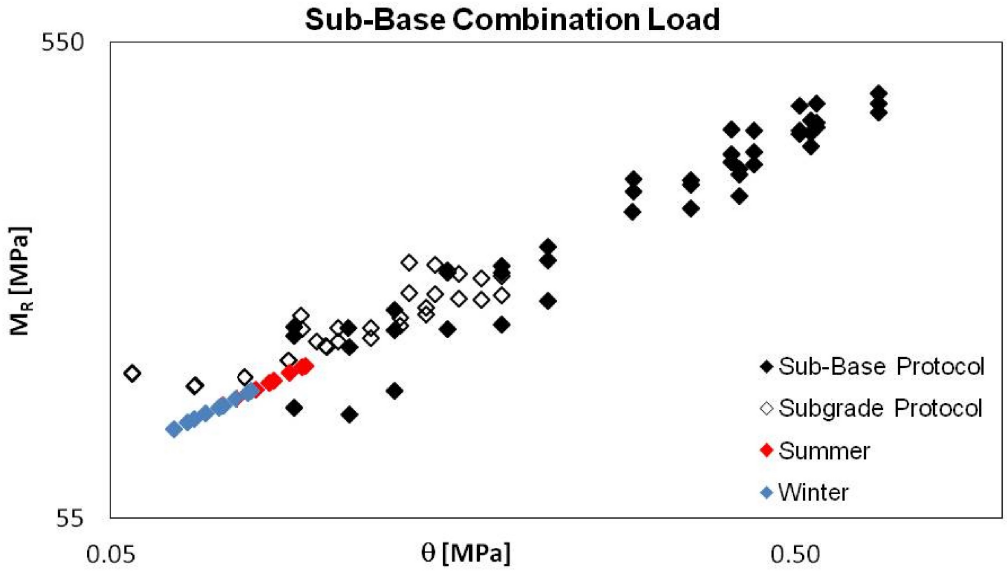

Figure 6.14: ALVA-master Results, 80kN, 10cm, With Concrete Layer, Sub-Base, After Second Iteration, H-M

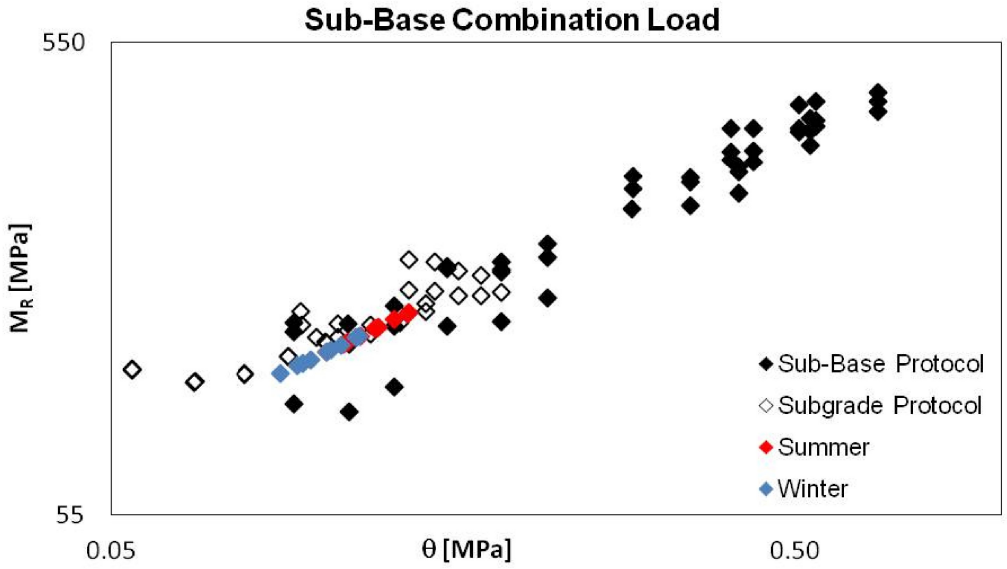

Figure 6.15: ALVA-master Results, 120kN, 10cm, With Concrete Layer, Sub-Base, After Second Iteration, H-M

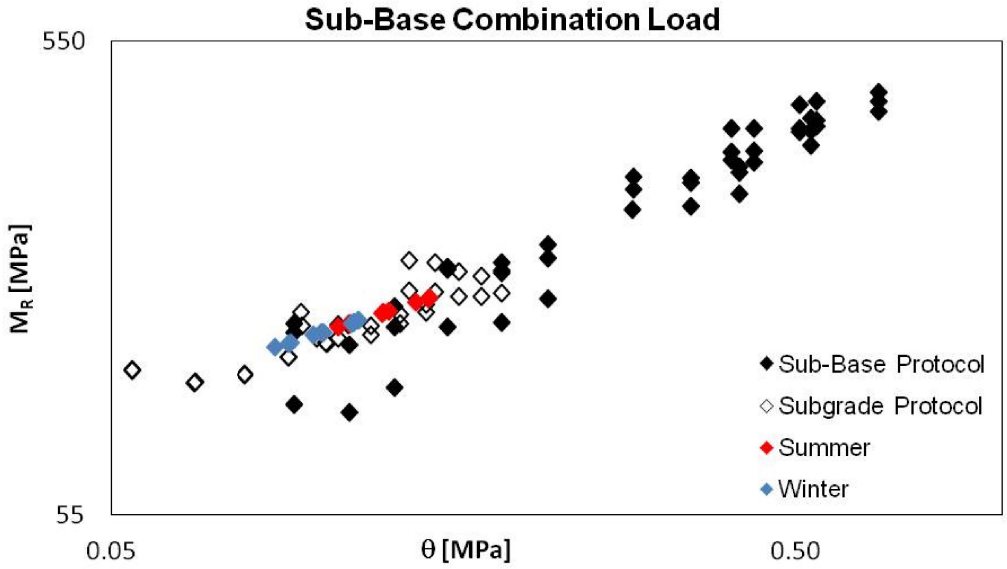

Figure 6.16: ALVA-master Results, 80kN, 10cm, Subgrade, After Second Iteration, H-M

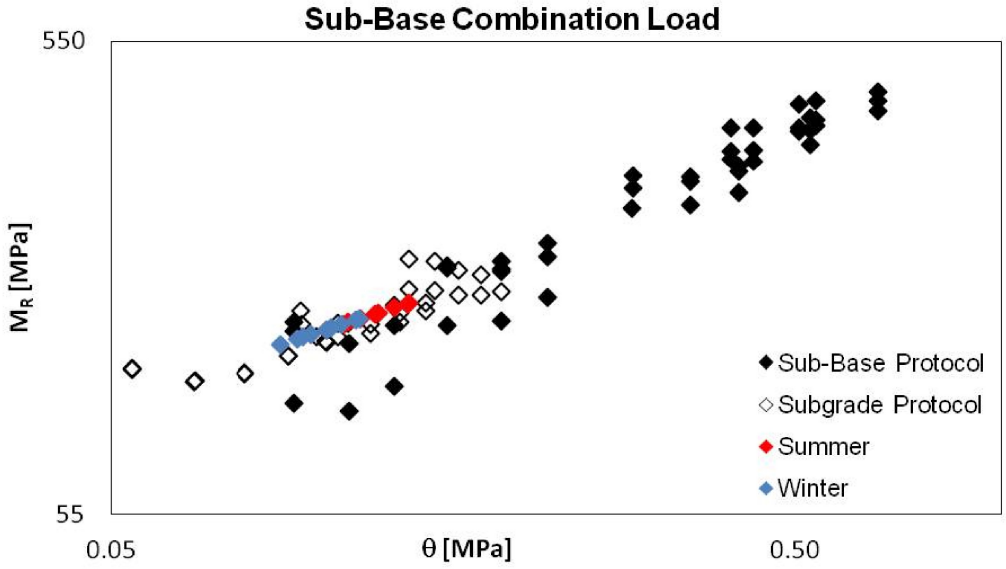

Figure 6.17: ALVA-master Results, 120kN, 10cm, Subgrade, After Second Iteration, H-M

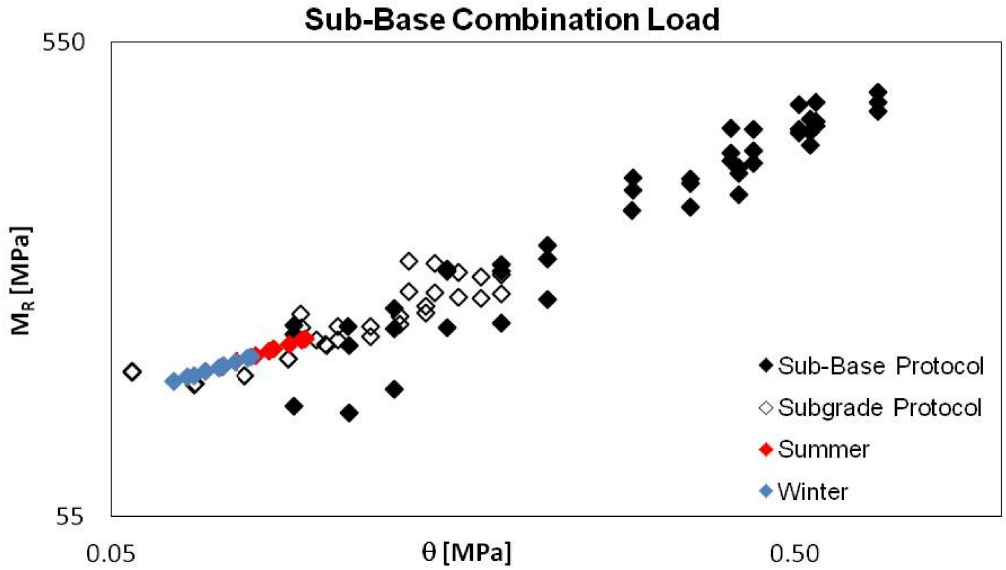

Figure 6.18: ALVA-master Results, 80kN, 10cm, With Concrete Layer, Subgrade, After Second Iteration, H-M

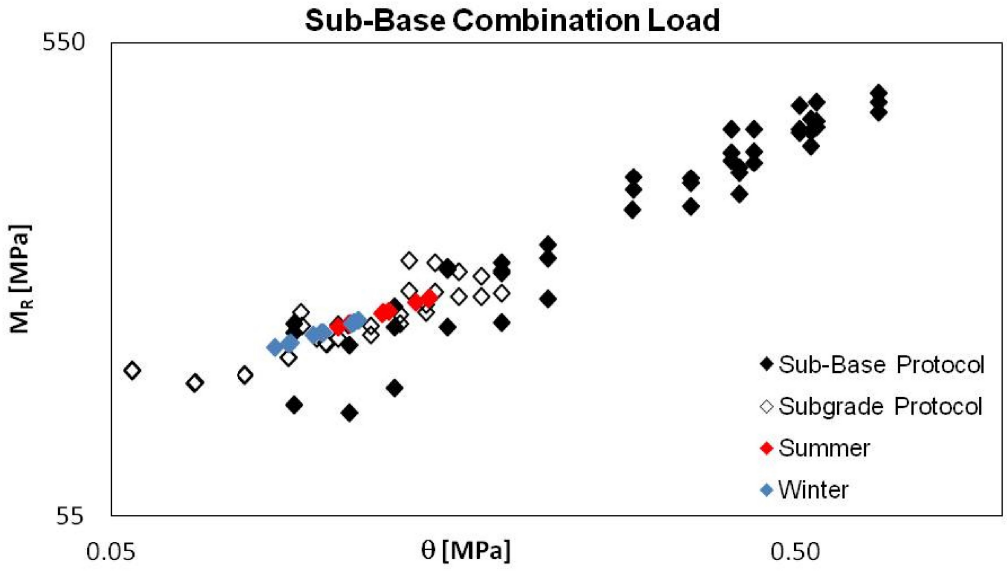

Figure 6.19: ALVA-master Results, 120kN, 10cm, With Concrete Layer, Subgrade, After Second Iteration, H-M

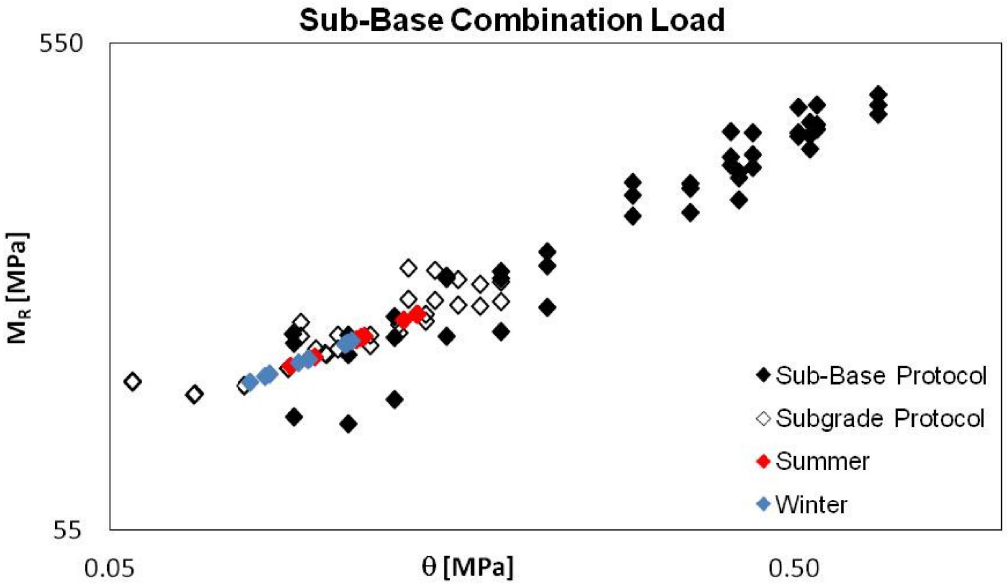

Figure 6.20: ALVA-master Results, 80kN, 10cm, Mix Protocol, After Second Iteration, H-M

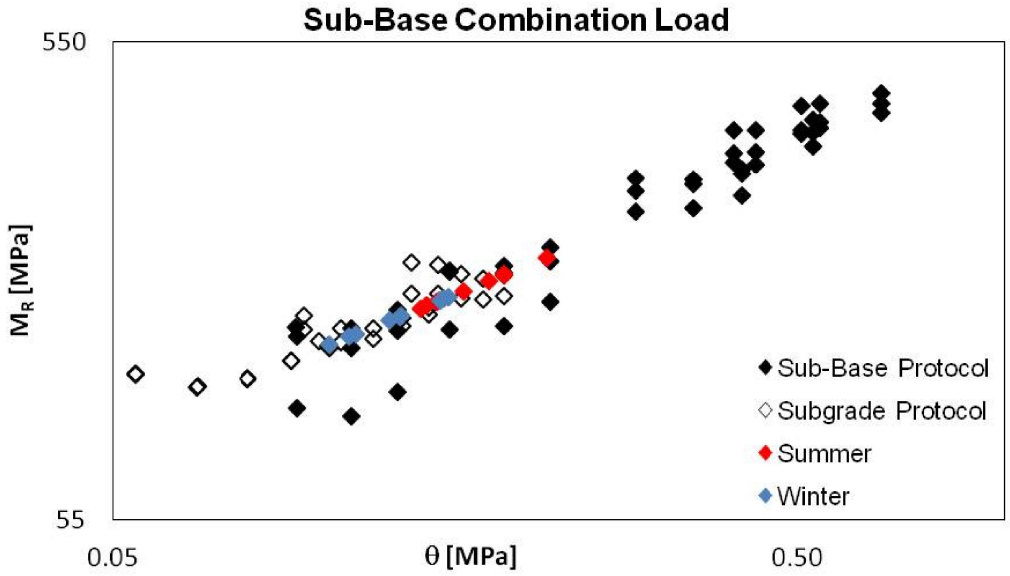

Figure 6.21: ALVA-master Results, 120kN, 10cm, Mix Protocol, After Second Iteration, H-M

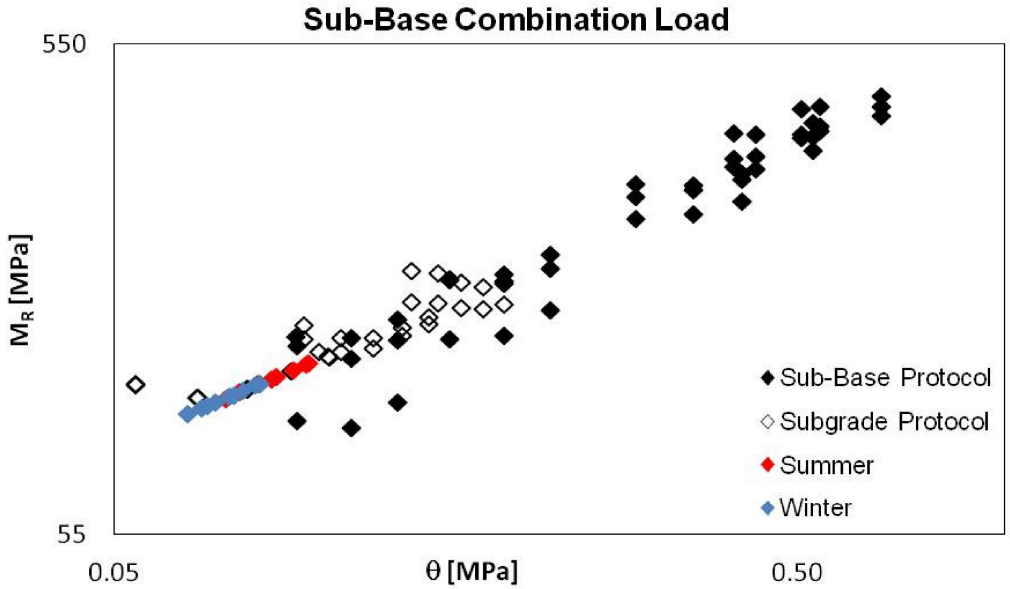

Figure 6.22: ALVA-master Results, 80kN, 10cm, With Concrete Layer, Mix Protocol, After Second Iteration, H-M

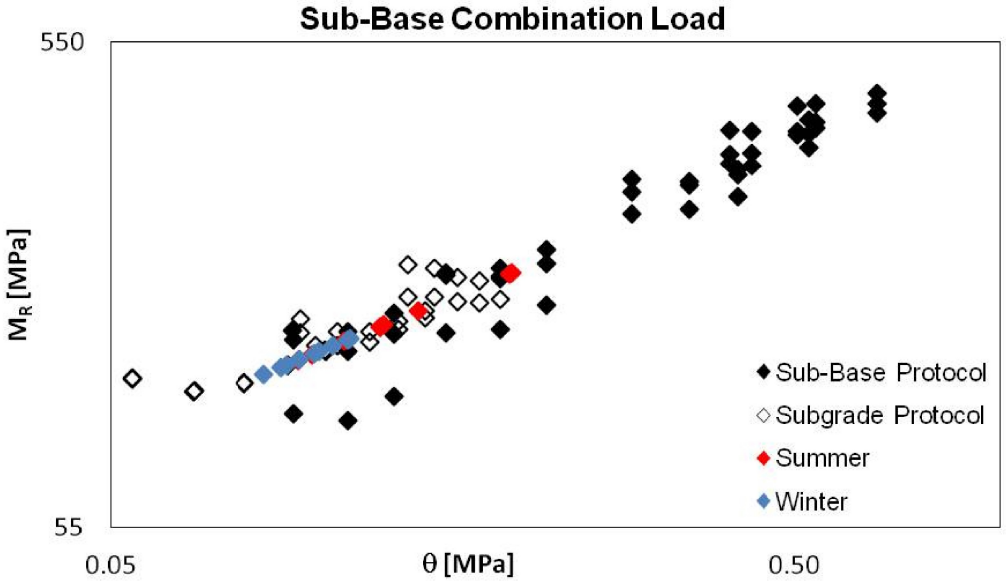

Figure 6.23: ALVA-master Results, 120kN, 10cm, With Concrete Layer, Mix Protocol, After Second Iteration, H-M

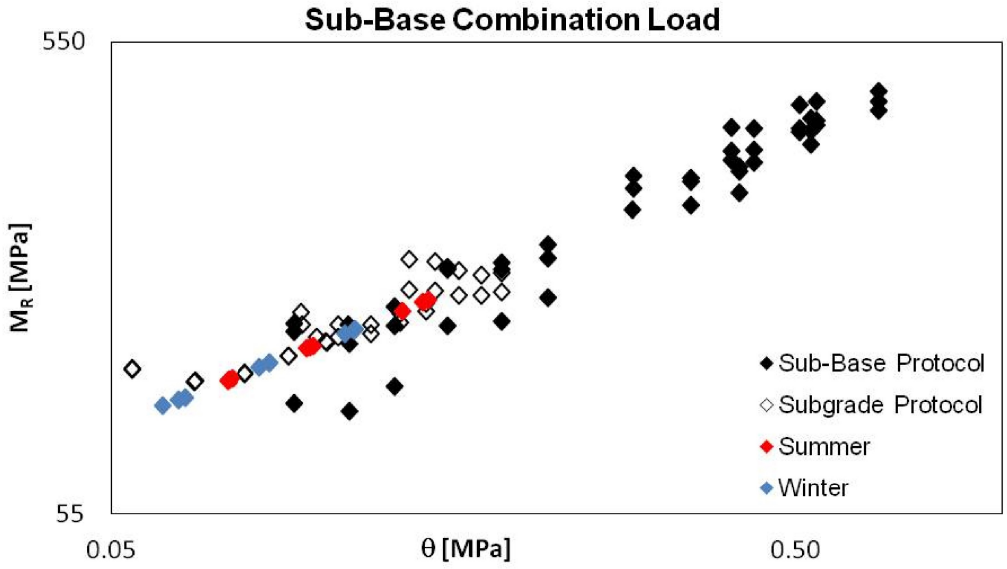

Figure 6.24: ALVA-master Results, 80kN, 20cm, Mix Protocol, After Second Iteration, H-M

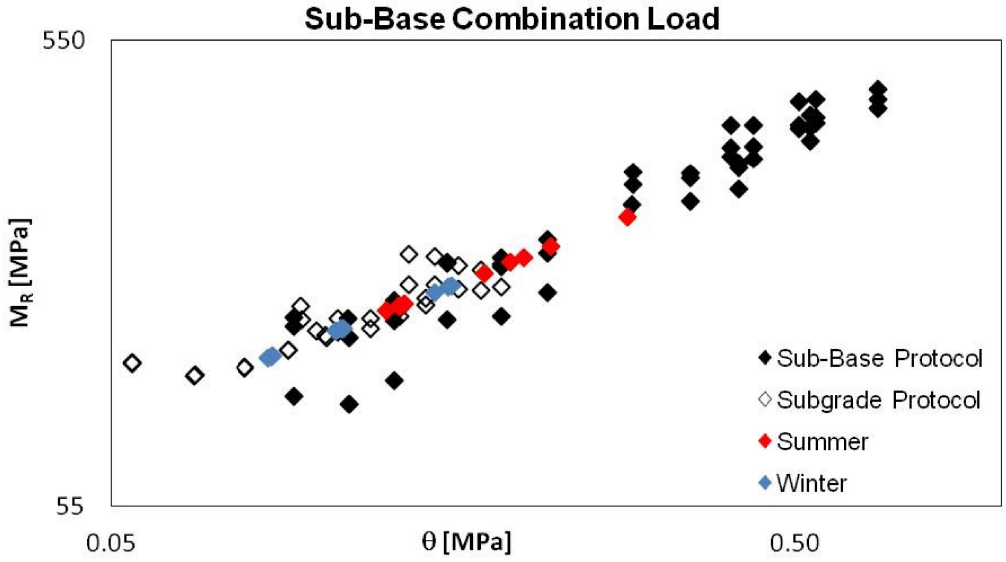

Figure 6.25: ALVA-master Results, 120kN, 20cm, Mix Protocol, After Second Iteration, H-M

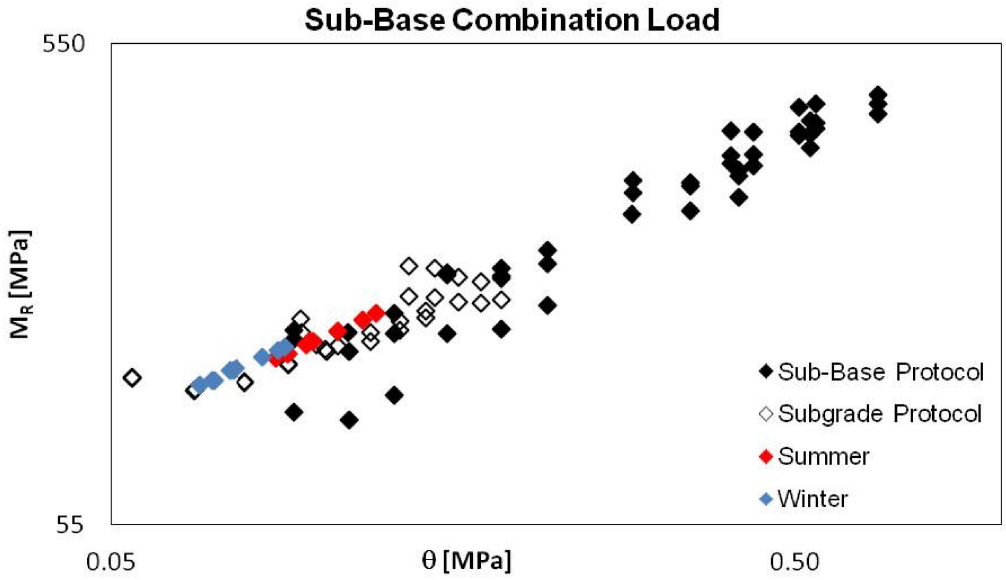

Figure 6.26: ALVA-master Results, 80kN, 20cm, With Concrete Layer, Mix Protocol, After Second Iteration, H-M

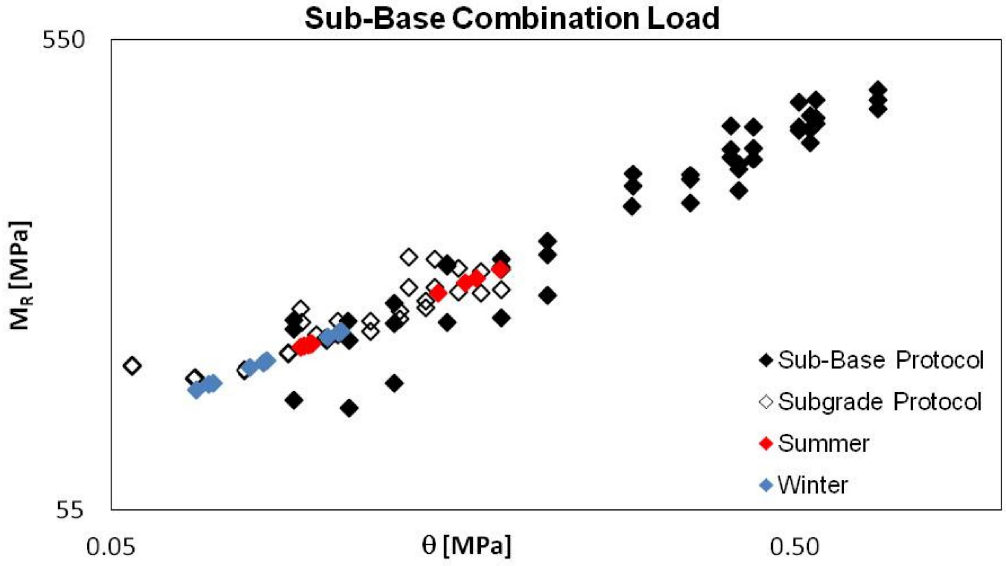

Figure 6.27: ALVA-master Results, 120kN, 20cm, With Concrete Layer, Mix Protocol, After Second Iteration, H-M

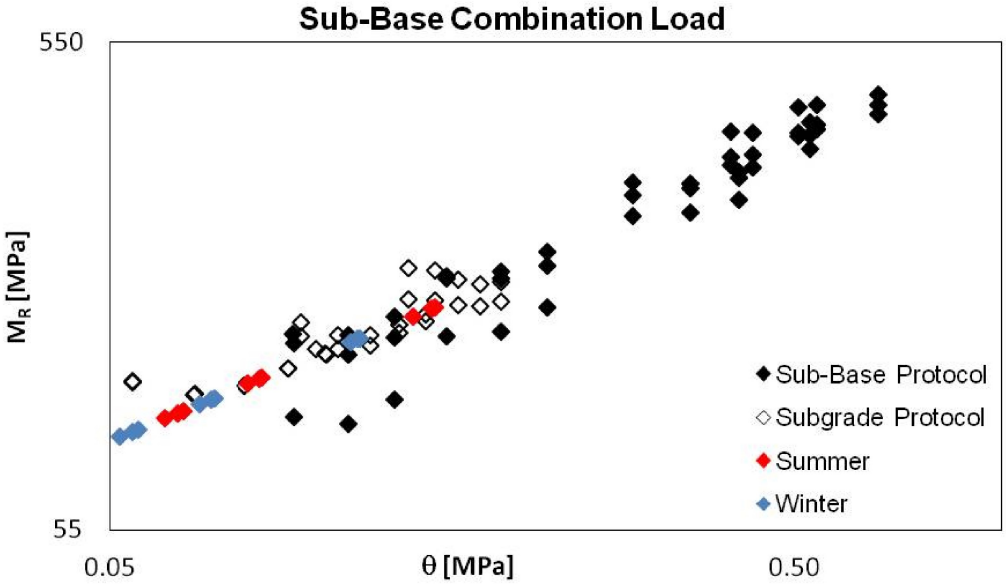

Figure 6.28: ALVA-master Results, 80kN, 30cm, Mix Protocol, After Second Iteration, H-M

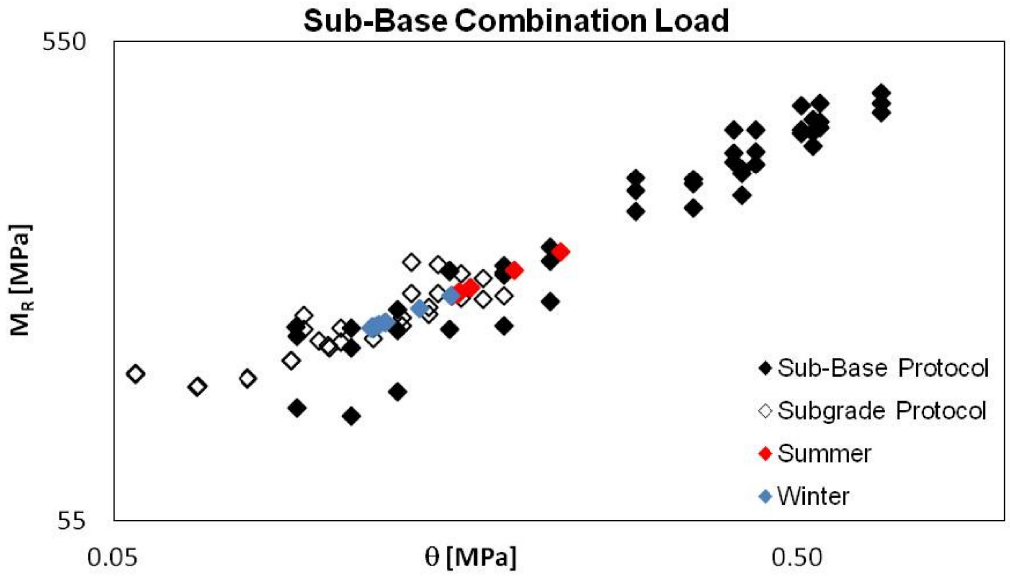

Figure 6.29: ALVA-master Results, 120kN, 30cm, Mix Protocol, After Second Iteration, H-M

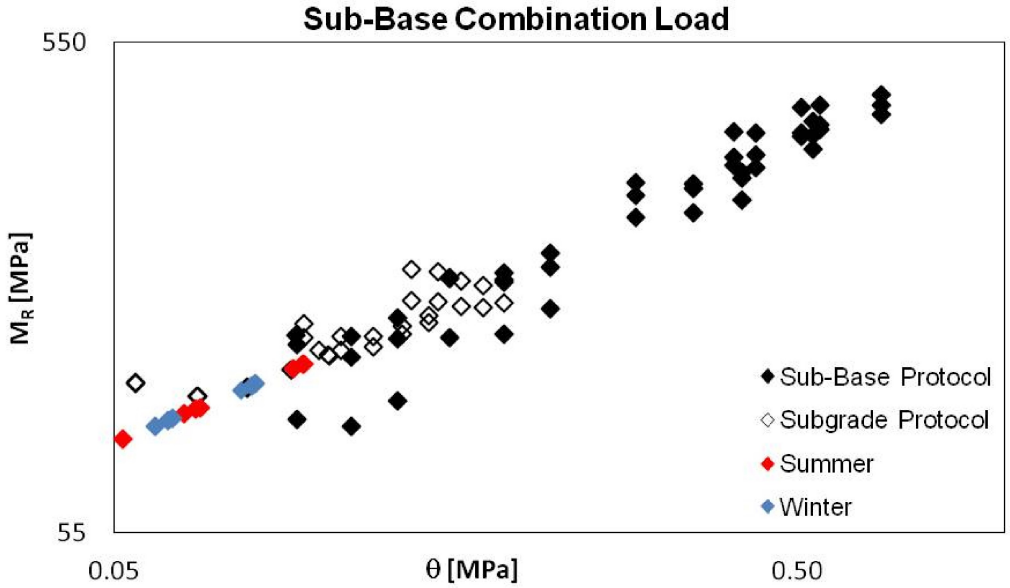

Figure 6.30: ALVA-master Results, 80kN, 30cm, With Concrete Layer, Mix Protocol, After Second Iteration, H-M

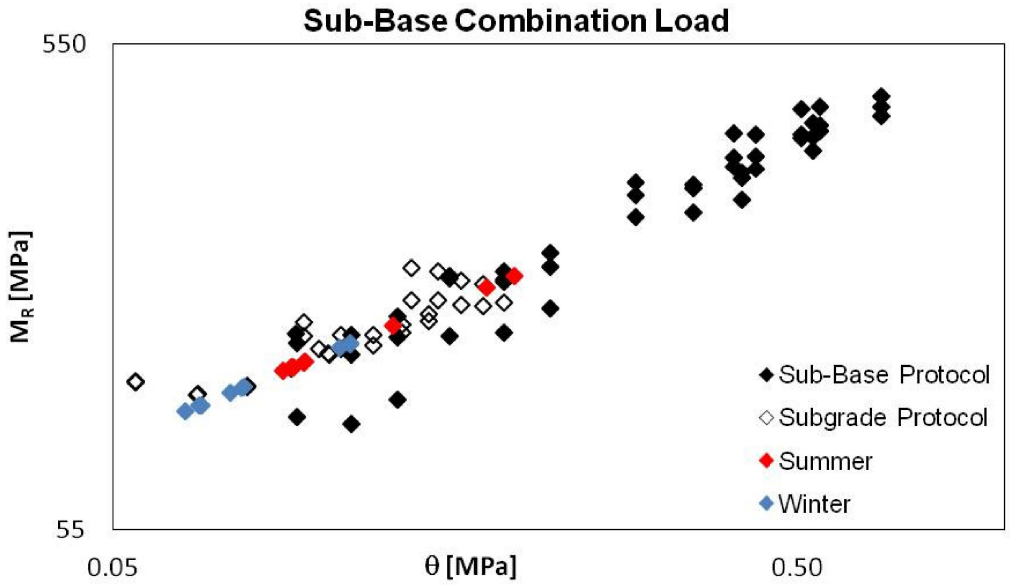

Figure 6.31: ALVA-master Results, 120kN, 30cm, With Concrete Layer, Mix Protocol, After Second Iteration, H-M

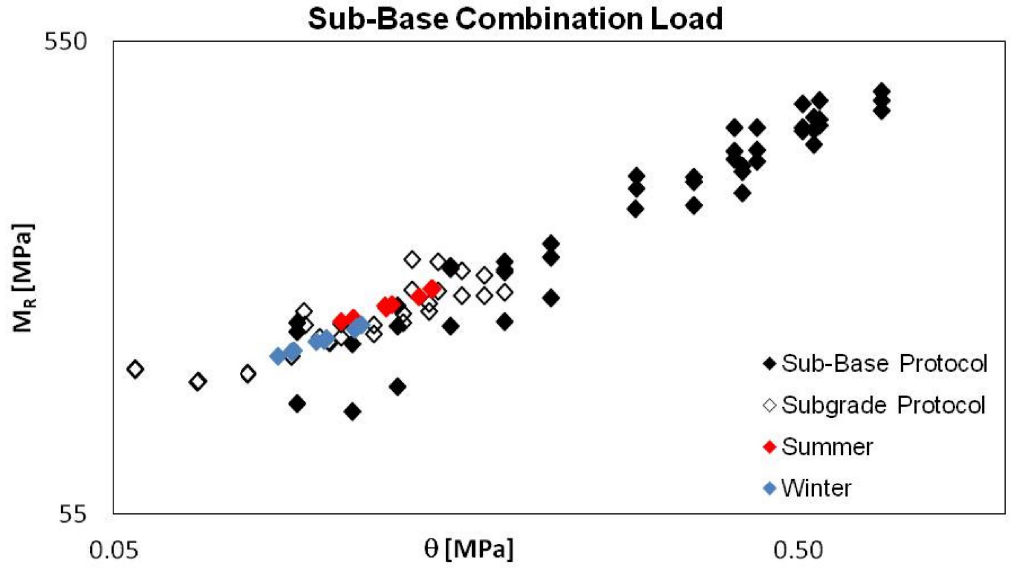

Figure 6.32: ALVA-master Results, 80kN, 10cm, Sub-Base, After Second Iteration, U

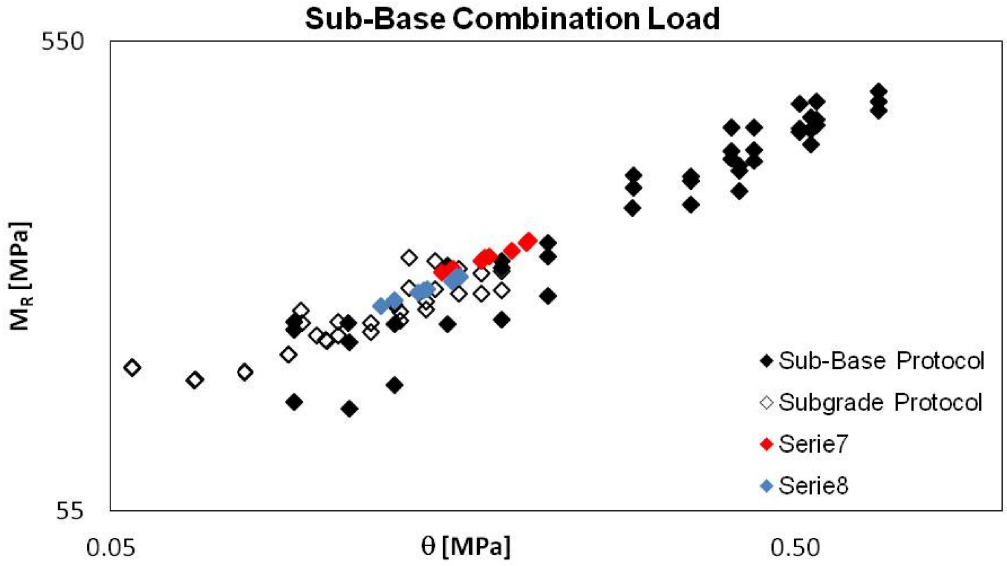

Figure 6.33: ALVA-master Results, 120kN, 10cm, Sub-Base, After Second Iteration, U

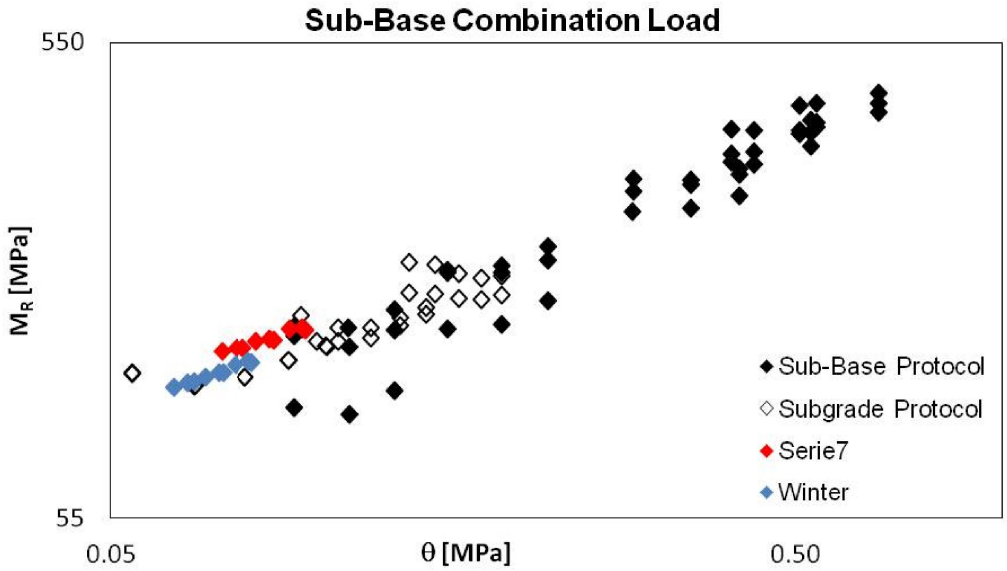

Figure 6.34: ALVA-master Results, 80kN, 10cm, With Concrete Layer, Sub-Base, After Second Iteration, U

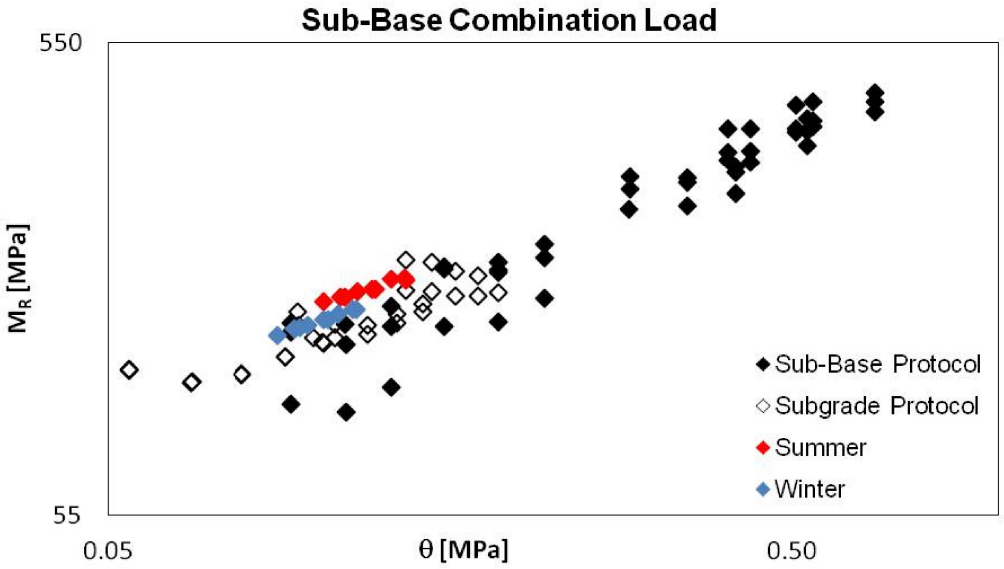

Figure 6.35: ALVA-master Results, 120kN, 10cm, With Concrete Layer, Sub-Base, After Second Iteration, U

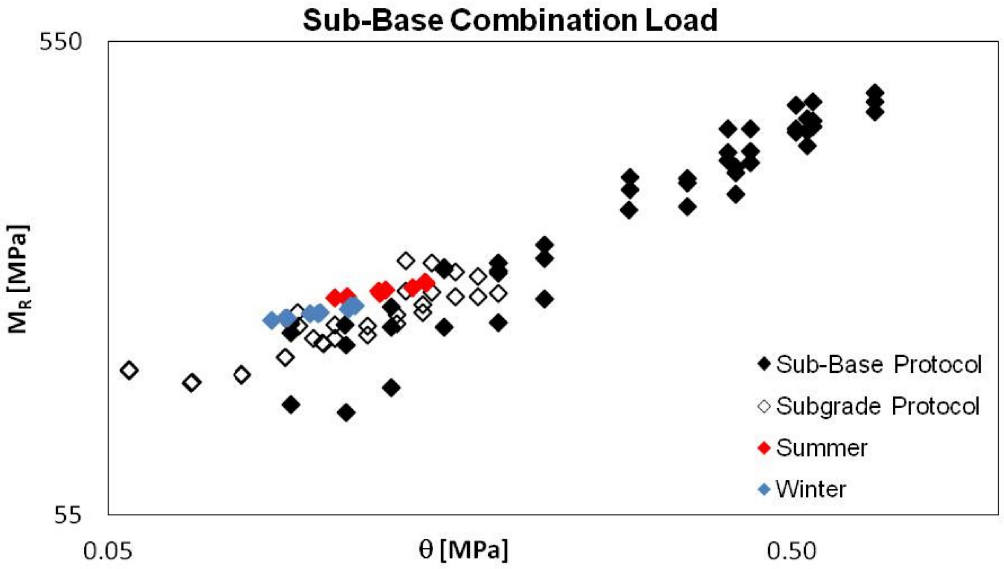

Figure 6.36: ALVA-master Results, 80kN, 10cm, Subgrade, After Second Iteration, U

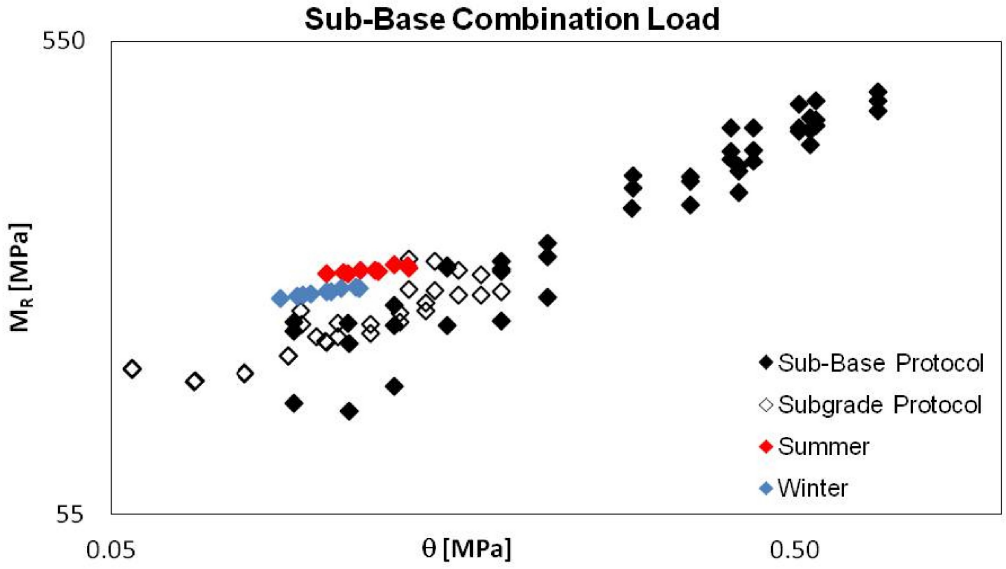

Figure 6.37: ALVA-master Results, 120kN, 10cm, Subgrade, After Second Iteration, U

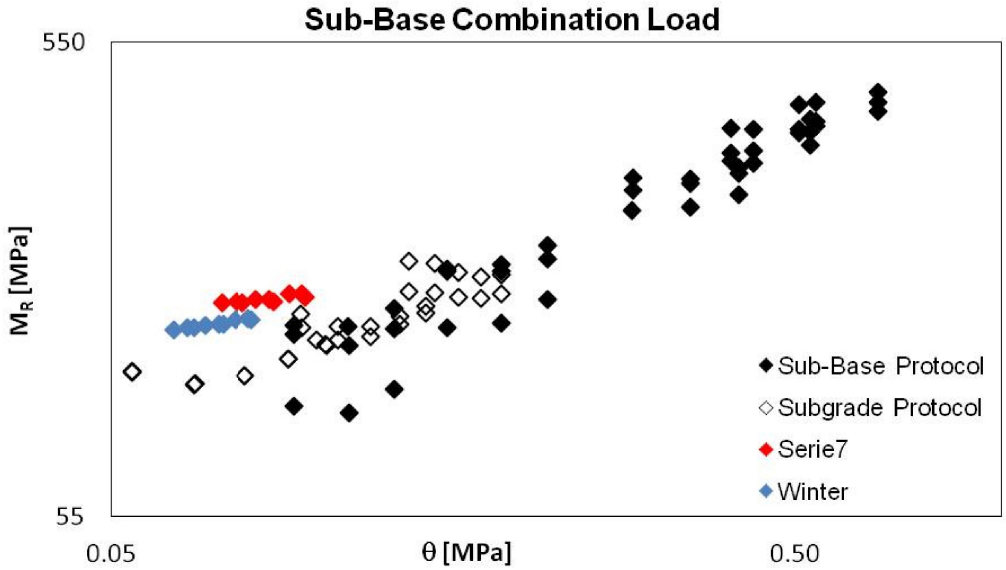

Figure 6.38: ALVA-master Results, 80kN, 10cm, With Concrete Layer, Subgrade, After Second Iteration, U

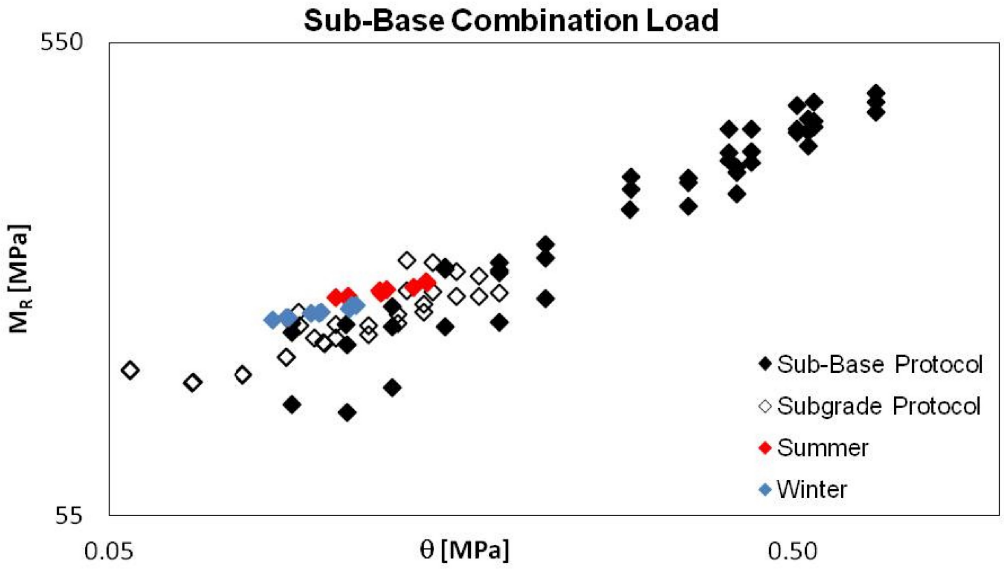

Figure 6.39: ALVA-master Results, 120kN, 10cm, With Concrete Layer, Subgrade, After Second Iteration, U

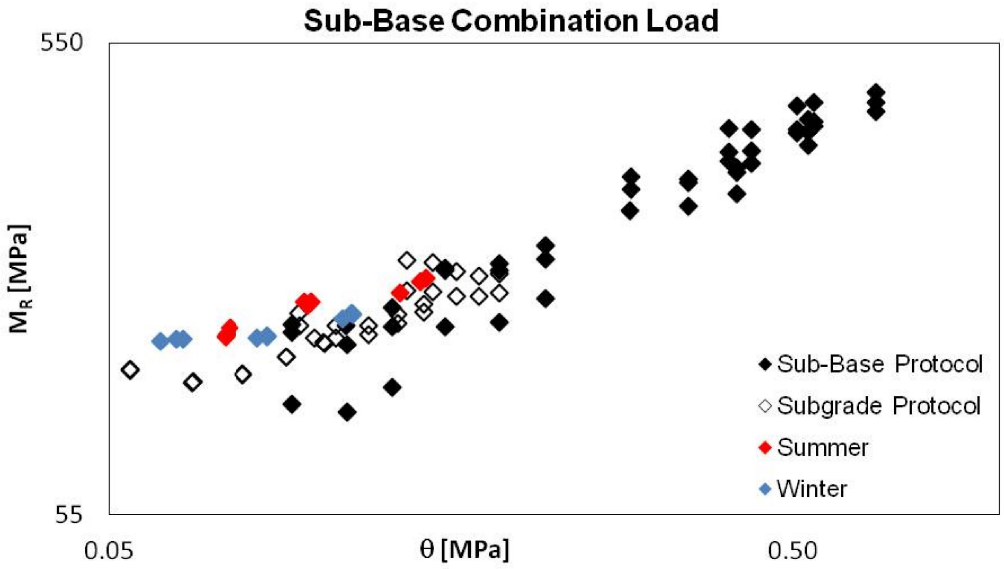

Figure 6.40: ALVA-master Results, 80kN, 20cm, Mix Protocol, After Second Iteration, U

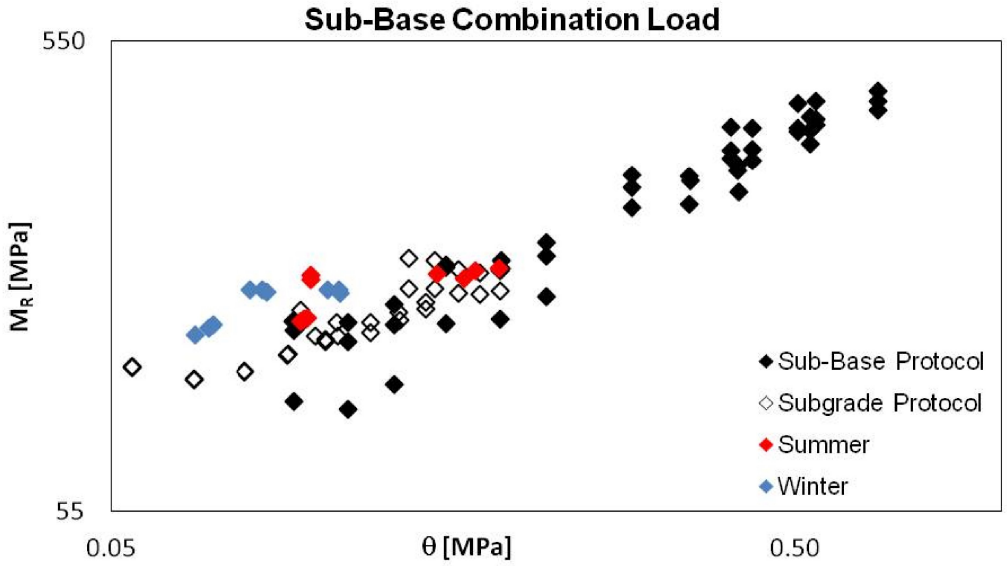

Figure 6.41: ALVA-master Results, 120kN, 20cm, Mix Protocol, After Second Iteration, U

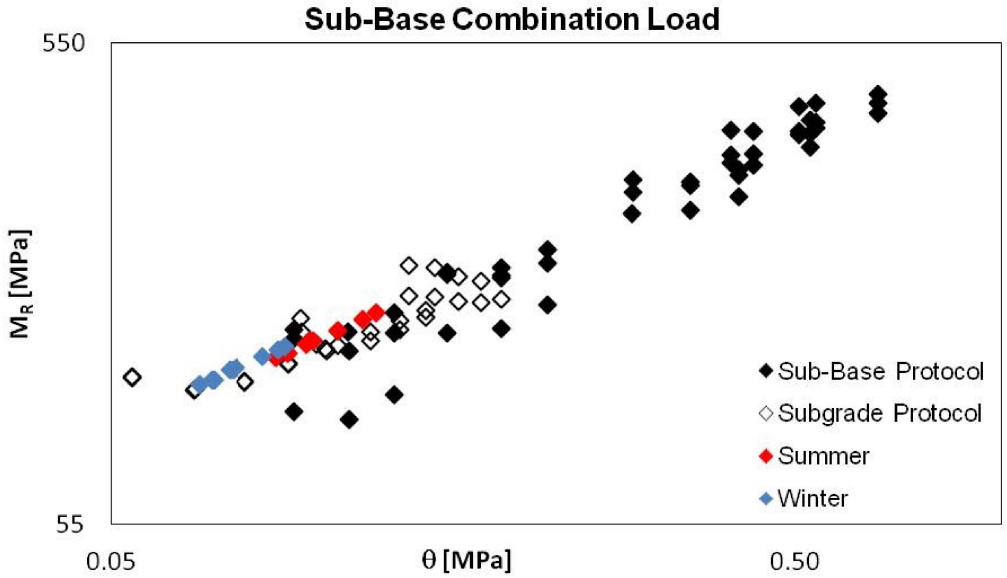

Figure 6.42: ALVA-master Results, 80kN, 20cm, With Concrete Layer, Mix Protocol, After Second Iteration, U

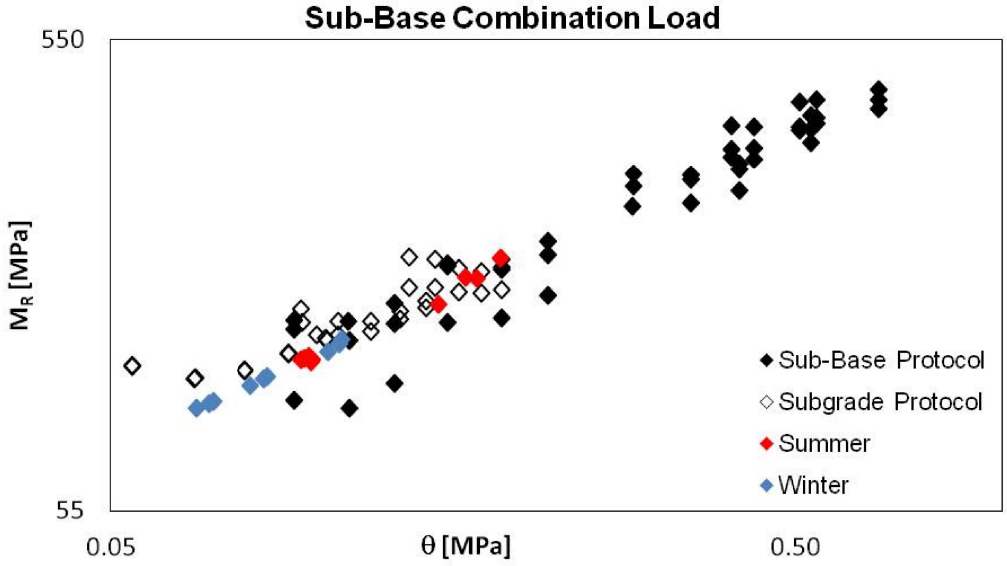

Figure 6.43: ALVA-master Results, 120kN, 20cm, With Concrete Layer, Mix Protocol, After Second Iteration, U

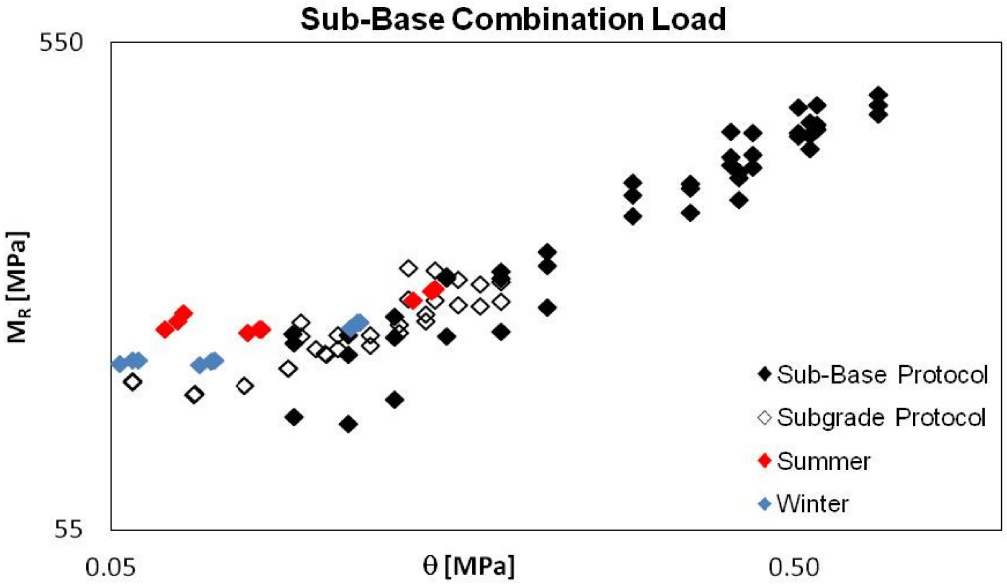

Figure 6.44: ALVA-master Results, 80kN, 30cm, Mix Protocol, After Second Iteration, U

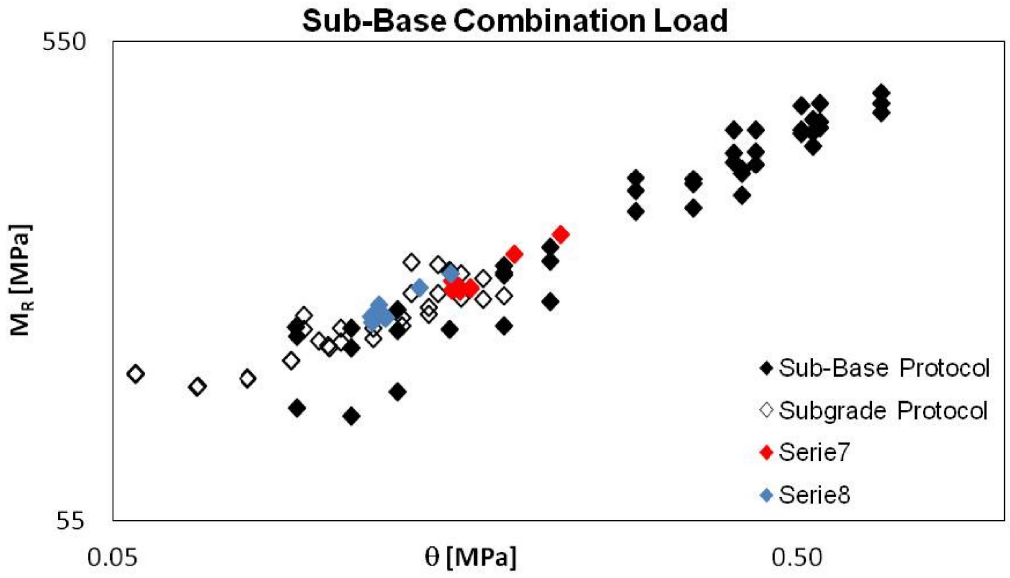

Figure 6.45: ALVA-master Results, 120kN, 30cm, Mix Protocol, After Second Iteration, U

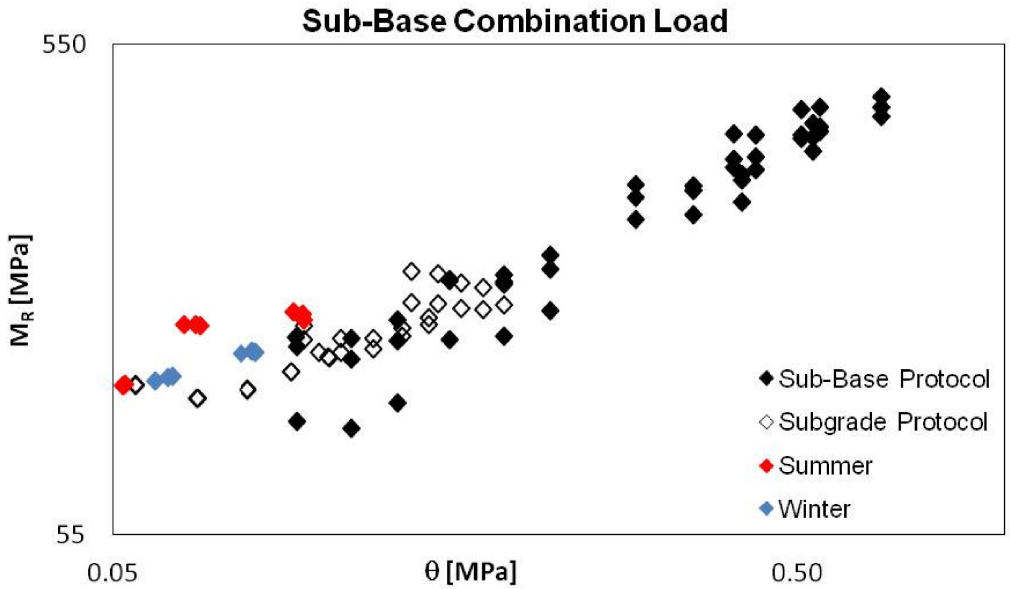

Figure 6.46: ALVA-master Results, 80kN, 30cm, With Concrete Layer, Mix Protocol, After Second Iteration, U

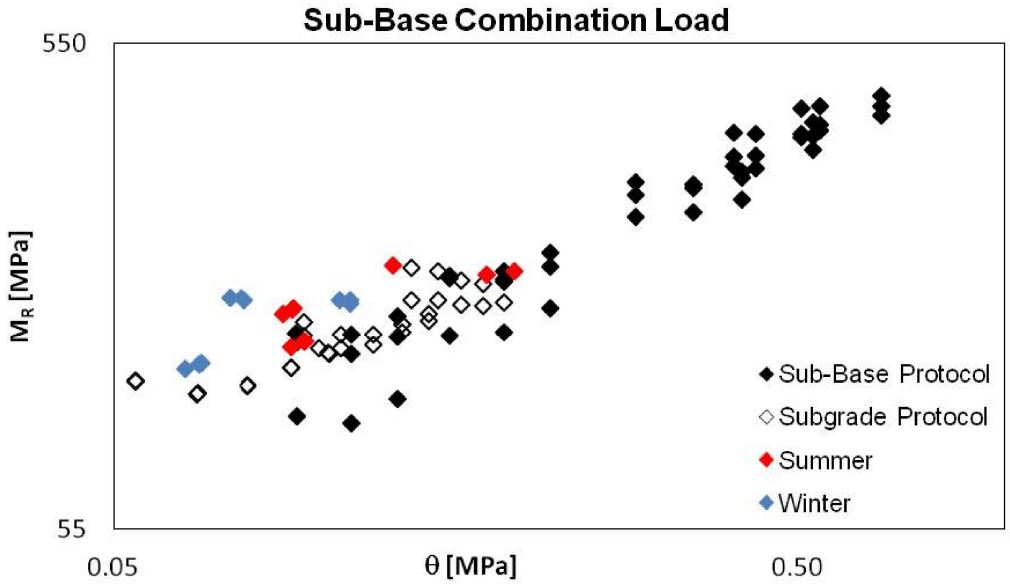

Figure 6.47: ALVA-master Results, 120kN, 30cm, With Concrete Layer, Mix Protocol, After Second Iteration, U

Bibliography

[1] Huang, Y.H..
Pavement Design and Analysis, (1993)
Prentice-Hall, Inc., Englewood Cliffs, N.J. .

[2] Fredrick Lekarp, Ulf Isacsson and Andrew Dawson.
State of the Art. I: Resilient Response of Unbound Aggregates, (2000) Jurnal of Transportation Engineering.

[3] AASHTO T292-91, Resilient Modulus of Subgrade Soil and Untreated Base-Subbase Materials.
Standard Specification for Transportation Materials and Methods of Sampling and Testing, (1998) 19th ed. American Association of state Highway and Transportation Officials, Washington, D.C., Part II, pp. 1057-1071.

[4] Rada, G., Witczak, M.W., Comprehensive Evaluation of Laboratory Resilient Moduli Result for Granular Material.
Transportation Reasearch Record No. 810, (1981) Transportation Research Board, National Research Council, Washington D.C..

[5] American Association of State Highway and Transportation Official (AASHTO).
Mechanistic-Empirical Pavement Design Guide: A Manual of Practice, (2008) Interim edition, Washington, D.C..

[6] Kolisoja, P..
Resilient Deformation Characteristics of Granular Materials, (1997) PhD thesis, Tampere University of Technology, Publ. No. 223, Tampere Finland.

[7] Mitry, F. G..
Determination of the Modulus of Resilient Deformation of Untreated base Course Material, (1964) PhD thesis, University of California, Berkeley.

[8] Monismith, C. L., Seed, H. B., Mitry, F. G., and Chan, C.K..
Prediction of Pavement Deflection From Laboratory Tests, (1967) Proc., 2nd Int. Conf. Struct. Des. of Asphalt Pavements, 109-140.

[9] Hicks, R. G., and Monismith, C. L..
Factor Influencing the Resilient Properties of Granular materials, (1971) Hwy. Res. Rec. 345, 15-31.

[10] Smith, W. S., and Nair, K..
Development of procedures for characterization of untreated granular base coarse and asphalt-treated base course materials, (1973) Rep. No. FHWA-RD-74-61, Federal Highway Administration, Washington, D.C..

[11] Uzan, J..
Characterization of Granular Material, (1985) Transp. Res. Rec. 1022, Transportation Research Board, Washington, D.C., 52–59.

[12] Sweere, G. T. H..
Unbound Granular Basis for Roads, (1990) PhD thesis, University of Delft, Delft, The Netherlands.

[13] Morgan, J. R..
The response of granular materials to repeated loading, (1966) Proc., 3rd Conf., ARRB, 1178–1192.

[14] Brown, S. F., and A. F. L. Hyde.
Significance of Cyclic Confining Stress in Repeated Load Triaxial Testing of Granular Material, (1975) Transportation Research 113 Record 537, Transportation Research Board, National Research Council, Washington, D.C., pp. 49-58.

[15] Lekarp, F., and A. R. Dawson.
Analysis of Permanent Deformation Behavior of Unbound Granular Materials, (1997) Paper presented at the International Symposium on Thin Pavements, Surface Treatments, Unbound Roads, Fredericton, New Brunswick, Canada, June 24-25.

[16] Trollope, E. H., Lee, I. K., and Morris, J..
Stresses and deformation in two-layer pavement structures under slow repeated loading, (1962) Proc., ARRB, Vol. 1, Part 2, 693–718.

[17] Hicks, R. G..
Factors influencing the resilient properties of granular materials, (1970) PhD thesis, University of California, Berkeley, Berkeley, Calif..

[18] Robinson, R. G..
Measurement of the elastic properties of granular materials using a resonance method, (1974) TRRL Supplementary Rep. No. 111UC, TRRL.

[19] Rada, G., and Witczak, M. W..
Comprehensive evaluation of laboratory resilient moduli results for granular material, (1981) Transp. Res. Rec. 810, Transportation Research Board, Washington, D.C., 23–33.

[20] Thom, N. H., and Brown, S. F..
The effect of grading and density on the mechanical properties of a crushed dolomitic limestone, (1988) Proc., 14th ARRB Conf., Vol. 14, Part 7, 94–100.

[21] Brown, S. F., and Selig, E. T..
The design of pavement and rail track foundations, (1991) Cyclic loading of soils: From theory to design, M. P. O'Reilly and S. F. Brown, eds., Blackie and Son Ltd., Glasgow, Scotland, 249–305.

[22] Barksdale, R. D., and Itani, S. Y..
Influence of aggregate shape on base behaviour, (1989) Transp. Res. Rec. 1227, Transportation Research Board, Washington, D.C., 173–182.

[23] Vuong, B.
Influence of density and moisture content on dynamic stress-strain behaviour of a low plasticity crushed rock, (1992) Rd. and Transp. Res., 1(2), 88–100.

[24] Thom, N. H., and Brown, S. F..
Effect of moisture on the structural performance of a crushed-limestone road base, (1987) Transp. Res. Rec. 1121, Transportation Research Board, Washington, D.C., 50–56.

[25] Kamal, M. A., Dawson, A. R., Farouki, O. T., Hughes, D. A. B., and Sha'at, A. A..
Field and laboratory evaluation of the mechanical behaviour of unbound granular materials in pavements, (1993) Transp. Res. Rec. 1406, Transportation Research Board, Washington, D.C., 88–97.

[26] Jorenby, B. N., and Hicks, R. G..
Base course contamination limits, (1986) Trans. Res. Rec. 1095, Transportation Research Board, Washington, D.C., 86–101.

[27] Gray, J. E..
Characteristics of graded base course aggregates determined by triaxial tests, (1962) Engrg. Res. Bull., No. 12, National Crushed Stone Association.

[28] Thom, N. H. (1988).
Design of road foundations, (1988) PhD thesis, Dept. of Civ. Engrg., University of Nottingham, Nottingham, England.

[29] Heydinger, A. G., Xie, Q. L., Randolph, B. W., and Gupta, J. D.
Analysis of resilient modulus of dense and open-graded aggregates, (1966) Transp. Res. Rec. 1547, Transportation Research Board, Washington, D.C., 1–6.

[30] Van Niekerk, A. A., Houben, L. J. M., and Molenaar, A. A. A.
Estimation of mechanical behaviour of unbound road building materials from physical material properties, (1998) Proc., 5th Int. Conf. on the Bearing Capacity of Roads and Airfields, R. S. Nordal and G. Rafsdal, eds., Vol. 3, 1221–1233.

[31] Haynes, J. G., and Yoder, E. J.
Effects of repeated loading on gravel and crushed stone base course materials used in the AASHO Road Test, (1963) Hwy. Res. Rec. 39.

[32] Dawson, A. R., Thom, N. H., and Paute, J. L.
Mechanical characteristics of unbound granular materials as a function of condition, (1996) Flexible Pavements, Proc., Eur. Symp. Euroflex 1993, A. G. Correia, ed., Balkema, Rotterdam, The Netherlands, 35–44.

[33] Seed, H. B., Mitry, F. G., Monismith, C. L., and Chan, C. K..
Prediction of flexible pavement deflections from laboratory repeated load tests, (1967) NCHRP Rep. No. 35, National Cooperative Highway Research Program.

[34] Pappin, J. W..
Characteristics of granular material for pavement analysis, (1979) PhD thesis, Dept. of Civ. Engrg., University of Nottingham, Nottingham, England.

[35] Raad, L., Minassian, G., and Gartin, S..
Characterization of saturated granular bases under repeated loads, (1992) Transp. Res. Rec. 1369, Transportation Research Board, Washington, D.C., 73–82.

[36] Dehlen, G. L..
The effect of non-linear material response on the behaviour of pavements subjected to traffic loads, (1969) PhD thesis, University of California, Berkeley, Berkeley, Calif..

[37] Boyce, J. R., Brown, S. F., and Pell, P. S..
The resilient behaviour of a granular material under repeated loading, (1976) Proc., 8th ARRB Conf. Mat. Constr. and Maintenance, Vol. 8, Part 3, 1–12.

[38] Allen, J..
The effect of non-constant lateral pressures of the resilient response of granular materials, (1973) PhD thesis, University of Illinois at Urbana-Champaign, Urbana, Ill.

[39] Moore, W. M., Britton, S. C., and Schrivner, F. H..
A laboratory study of the relation of stress to strain for a crushed limestone base material, (1970) Res. Rep. 99-5F, Study 2-8-65-99, Texas Transp. Inst., Texas A M University, College Station, Tex..

[40] Allen, J..
The effect of non-constant lateral pressures of the resilient response of granular materials, (1973) PhD thesis, University of Illinois at Urbana-Champaign, Urbana, Ill..

[41] Allen, J. J., and Thompson, M. R..
Resilient response of granular materials subjected to time dependent lateral stresses, (1974) Transp. Res. Rec. 510, Transportation Research Board, Washington, D.C., 1–13.

[42] Thom, N. H., and Brown, S. F..
The mechanical properties of unbound aggregates from various sources, (1989) Unbound aggregates in roads, R. H. Jones and A. R. Dawson, eds., 130–142.

[43] Seed, H. B., Mitry, F. G., Monismith, C. L., and Chan, C. K..
Predictions of pavement deflection from laboratory repeated load tests, (1965) Rep. No. TE-65-6, Soil Mech. and Bituminous Mat. Res. Lab., University of California, Berkeley, Berkeley, Calif..

[44] American Association of State Highway and Transportation Officials (AASHTO).
Standard Specification for Transportation Materials and Methods of Sampling and Testing, Part 2B, (2006) Washington, D.C..